Potdar, S., and Vasu, S. (2012). Large ventral lateral neurons determine the phase of evening activity peak across photoperiods in *Drosophila melanogaster*. J. Biol. Rhythms.

Rémi, J., Merrow, M., and Roenneberg, T. (2010). A circadian surface of entrainment: Varying T, τ, and Photoperiod in Neurospora crassa. J. Biol. Rhythms.

Renn, S.C.P., Park, J.H., Rosbash, M., Hall, J.C., and Taghert, P.H. (1999). A pdf neuropeptide gene mutation and ablation of PDF neurons each cause severe abnormalities of behavioral circadian rhythms in *Drosophila*. Cell.

Rieger, D., Stanewsky, R., and Helfrich-Förster, C. (2003). Cryptochrome, compound eyes, Hofbauer-Buchner eyelets, and ocelli play different roles in the entrainment and masking pathway of the locomotor activity rhythm in the fruit fly *Drosophila melanogaster*. J. Biol. Rhythms.

Rieger, D., Peschel, N., Dusik, V., Glotz, S., and Helfrich-Förster, C. (2012). The ability to entrain to long photoperiods differs between 3 *Drosophila melanogaster* wild type strains and is modified by twilight simulation. J. Biol. Rhythms.

Riemensperger, T., Fiala, A., Giraud, J., Poppinga, H., Birman, S., Sun, J., and Xu, A.Q. (2018). Neural Control of Startle-Induced Locomotion by the Mushroom Bodies and Associated Neurons in *Drosophila*. Front. Syst. Neurosci.

Roenneberg, T., Daan, S., and Merrow, M. (2003). The art of entrainment. J. Biol. Rhythms.

Rosato, E., and Kyriacou, C.P. (2006). Analysis of locomotor activity rhythms in *Drosophila*. Nat. Protoc.

Rutila, J.E., Suri, V., Le, M., So, W.V., Rosbash, M., and Hall, J.C. (1998). Cycle is a second bHLH-PAS clock protein essential for circadian rhythmicity and transcription of *Drosophila* period and timeless. Cell.

Schlichting, M., and Helfrich-Förster, C. (2015). Photic entrainment in *Drosophila* assessed by locomotor activity recordings. In Methods in Enzymology.

Schlichting, M., Menegazzi, P., Lelito, K.R., Yao, Z., Buhl, E., Dalla Benetta, E., Bahle, A., Denike, J., Hodge, J.J., Helfrich-Forster, C., et al. (2016). A Neural Network Underlying Circadian Entrainment and Photoperiodic Adjustment of Sleep and Activity in *Drosophila*. J. Neurosci.

Schmid, B., Helfrich-Förster, C., and Yoshii, T. (2011). J Biol Rhythms. A New ImageJ Plug-in "ActogramJ" Chronobiol. Anal.

Sehadova, H., Glaser, F.T., Gentile, C., Simoni, A., Giesecke, A., Albert, J.T., and Stanewsky, R. (2009). Temperature Entrainment of *Drosophila*'s Circadian Clock Involves the Gene nocte and Signaling from Peripheral Sensory Tissues to the Brain. Neuron 64, 251–266.

Stoleru, D., Peng, Y., Nawathean, P., and Rosbash, M. (2005). A resetting signal between *Drosophila* pacemakers synchronizes morning and evening activity. Nature.

Tang, C.H.A., Hinteregger, E., Shang, Y., and Rosbash, M. (2010). Light-mediated TIM degradation within *Drosophila* pacemaker neurons (s-LNvs) is neither necessary nor sufficient for delay zone phase shifts. Neuron.

Tataroglu, O., and Emery, P. (2014). Studying circadian rhythms in *Drosophila melanogaster*. Methods.

Tomioka, K., Miyasako, Y., and Umezaki, Y. (2008). PDF as a coupling mediator between the light-entrainable and temperature-entrainable clocks in *Drosophila*

melanogaster . Acta Biol. Hung.
Vaccaro, A., Birman, S., and Klarsfeld, A. (2016). Chronic jet lag impairs startle-induced locomotion in *Drosophila*. Exp. Gerontol.
Vansteensel, M.J., Michel, S., and Meijer, J.H. (2008). Organization of cell and tissue circadian pacemakers: A comparison among species. Brain Res. Rev. 58, 18–47.
Walbeek, T.J., and Gorman, M.R. (2017). Simple Lighting Manipulations Facilitate Behavioral Entrainment of Mice to 18-h Days. J. Biol. Rhythms.
Yadlapalli, S., Jiang, C., Bahle, A., Reddy, P., Meyhofer, E., and Shafer, O.T. (2018). Circadian clock neurons constantly monitor environmental temperature to set sleep timing. Nature.
Yang, Z., and Sehgal, A. (2001). Role of molecular oscillations in generating behavioral rhythms in *Drosophila*. Neuron.
Yao, Z., Bennett, A.J., Clem, J.L., and Shafer, O.T. (2016). The *Drosophila* Clock Neuron Network Features Diverse Coupling Modes and Requires Network-wide Coherence for Robust Circadian Rhythms. Cell Rep.
Yoshii, T., Wulbeck, C., Sehadova, H., Veleri, S., Bichler, D., Stanewsky, R., and Helfrich Forster, C. (2009). The Neuropeptide Pigment-Dispersing Factor Adjusts Period and Phase of *Drosophila*'s Clock. J. Neurosci. 29, 2597–2610.
Yoshii, T., Rieger, D., and Förster, C.H. (2012). Two clocks in the brain: An update of the morning and evening oscillator model in *Drosophila*. Prog. Brain Res.
Yoshii, T., Hermann-Luibl, C., and Helfrich-Föorster, C. (2016). Circadian light-input pathways in *Drosophila*. Commun. Integr. Biol.

Chapter 4. Ionotropic GABA and Acetylcholine Signaling to *Drosophila* Clock Neurons Controls Circadian and Sleep-Wake Behavior.

Jenna L Persons[1], TJ Waller[1], Deepika Pandian[1], Alyssa Kalsbeek[1], and Orie T Shafer[1]

[1]Department of Molecular, Cellular and Developmental Biology, University of Michigan, Ann Arbor, MI 48109,

Author Contributions

JLP, conception and design, data acquisition, analysis and interpretation of data, drafting and revising the manuscript; TJW, AK, DP, data acquisition, analysis and interpretation of data; OTS, conception and design, analysis and interpretation of data, drafting and revising the manuscript.

Abstract

Sleep-wake behavior in mammals emerges from the interplay between neurons of the circadian network, sleep-wake centers and sensory pathways. The so-called “clock neurons” of the circadian network are essential to time sleep and wakefulness with daily rhythms in the environment. Interestingly, clock neurons are more excitable during wakefulness, and more inhibited during sleep suggesting that their activity may physiologically represent distinct environmental and behavioral states. However, the

meaning of these physiological rhythms in excitability are largely unknown due to the complexity of many model systems. *Drosophila melanogaster* is a tractable circadian model organism to tease apart the mechanisms controlling clock neurons' physiological rhythms and their importance to circadian, and sleep-wake behavior. Using electrophysiology, live-imaging studies and the advantages of the fly system, we previously found that two conserved neurotransmitters, GABA and acetylcholine, physiologically represent day and night in a critical clock neuron population (Chapter 2). We determined that these physiological rhythms are variably coupled to extrinsic light cycles and intrinsic molecular clock elements. Herein, we show that GABAergic and acetylcholinergic signals are received in part through ionotropic receptors. Finally, we combine genetic manipulations with behavioral studies to demonstrate that the identified rhythms in ionotropic neurotransmission function in the fly clock network to coordinate circadian and sleep-wake rhythms.

Introduction

Circadian rhythms help terrestrial organisms anticipate light and temperature rhythms in the environment to properly time daily activities like sleep and wake (Vansteensel et al., 2008). Circadian rhythms are often centrally controlled by dedicated circuits in the brain (Herzog, 2007). In humans and mammalian model organisms, the so-called clock neuron network in the suprachiasmatic nuclei (SCN) of the hypothalamus coordinates daily bouts of sleep and activity with input and output centers (Welsh et al., 2010). Consequently, sleep-wake states in mammals are the result of a complex interplay between neurons of clock network in the SCN, sleep and wake centers, and sensory pathways (Scammell et al., 2017). The SCN is the neural interface where information from

the environment and vigilance-state information from sleep-wake centers is integrated with endogenous molecular rhythms to adjust the *timing* of daily behaviors (Scammell et al., 2017). Accordingly, the neurons of the SCN are more excitable during the day during wakefulness, and more inhibited at night during sleep (Colwell, 2011; DeWoskin et al., 2015; Wang et al., 2012). This finding suggests that the physiological state of the SCN network might directly signal distinct environment and behavior states.

The precise causes and relevance of the SCN's physiological rhythms remain an active area of research. A recent study suggests that neurotransmission, along with cell intrinsic methods underlie the SCN's synchronous voltage rhythms (Enoki et al., 2017; Herzog et al., 2017). Neurotransmission within the clock network itself, primarily via the neurotransmitter GABA and peptide vasoactive intestinal polypeptide (VIP), is essential to coordinate SCN neurons' endogenous molecular clock rhythms and network communication (Aton et al., 2005, 2006; Freeman et al., 2013). Outside of the SCN proper, sleep-wake centers and neurons of the retinohypothalamic tract make functional physiological connections with the SCN (Golombek and Rosenstein, 2010; Welsh et al., 2010). These pathways provide critical feedback to the SCN about the environment and vigilance state via neuropeptides and transmitters including acetylcholine and glutamate (Bina et al., 1993; S.M. et al., 2013; Yang et al., 2010). It is likely that many parallel pathways generate the rhythms of the SCN, ultimately fine-tuning sleep-wake cycles to match rhythms in the environment. But to date the meaning of the SCN's physiological rhythms in excitability, their molecular basis and behavioral importance are unknown. The majority of our physiological understanding of the SCN may be attributed to work in rodent model systems. However, the network's size and genetic scale make it difficult to causally

tie small populations of neurons or single transmitter systems to features of daily sleep-wake behavior.

Drosophila melanogaster is an ideal circadian model organism to identify the contributors to clock network physiology and interrogate their consequences for sleep-wake behavior. With less than 1% the neurons of SCN networks, the fly clock network nevertheless produces an endogenous rhythm in sleep and activity and, through a sensitivity to environmental cues, times behavior with daily environmental rhythms (Herzog, 2007; Stoleru et al., 2007). The network's 150 neurons are subdivided into anatomically, and genetically distinct classes, whose distributed actions coordinate the fly's bimodal sleep-wake profile (Yoshii et al., 2012). While the ventral lateral neurons (l- and s-LNvs) and dorsal neurons (DN1s) drive peaks in morning wakefulness, dorsal lateral neurons (LNds) and the 5th s-LNV promote evening wakefulness (Helfrich-Förster et al., 2007). A recent study provided evidence that each populations' increased neural activity (as inferred by Ca^{2+} transients) is causal to these bouts of wakefulness, and therefore asynchronous (Liang et al., 2016). Electrophysiological studies of the s- and l-LNvs and DN1s show that they also exhibit physiological changes in membrane excitability as a function of time of day in 12:12 light:dark conditions (LD) (Cao and Nitabach, 2008; Flourakis et al., 2015). Coherent with their roles in coordinating morning wakefulness, these populations are more electrically active during the morning, and less active during the night (Cao and Nitabach, 2008; Flourakis et al., 2015). It remains unknown whether all neurons of the fly clock network exhibit physiological rhythms in excitability like the SCN, if they are synchronous, or how they may be regulated. However, our intricate knowledge of the network's individual contributions when leveraged with the

fly's reduced genomic scale, and tools to manipulate defined neuron populations' neural activity, potentially allows us to directly link clock neuron physiology to sleep-wake behavior.

Neurotransmission provides critical communication to the fly clock network that patterns sleep-wake behavior and creates endogenous rhythms (Nitabach, 2006; Nitabach et al., 2002, 2005). Neuropeptides released by the network, including PDF, the functional analog of mammalian VIP, underlie the asynchronous Ca^{2+} transients that properly time sleep-wake cycles (Liang et al., 2016; Yao and Shafer, 2014; Yoshii et al., 2009). In addition to the network's peptidergic actions, extensive arborizations suggest that direct, synaptic communication mediates communication between clock neuron populations and to sleep and sensory centers (Helfrich-Förster, 2003; Schubert et al., 2018). The functionality of these direct synaptic connections, the transmitter types released, and the physiological or behavioral relevance of these messages remain largely unexplored. Cell type specific sequencing reveals that the clock neuron networks may be broadly receptive to fast-neurotransmission from GABA, glutamate, and acetylcholine conducted through ionotropic receptors (Abruzzi et al., 2017). We were struck by the possible conservation between mammals and flies of these transmitter types in communicating between the environment, circadian clock and sleep-wake centers. Our previous studies sought to determine the physiological states that two classic neurotransmitters, GABA and acetylcholine, might represent in the fly clock network. Towards this aim, we characterized GABAergic and cholinergic signaling across the circadian day using electrophysiology and ASAP2f live-imaging in the evening-wake promoting cells, the LNds (Yang et al., 2016; Yao, 2016; Chapter 2). We found that GABA

receptivity is stronger in the middle of the night, while cholinergic receptivity is stronger in the middle of the day (Chapter 2). Interestingly, while GABAergic signal strength is strongly controlled by the molecular clock, cholinergic signal strength is tied to light inputs that themselves are controlled by the molecular clock (Chapter 2).

Our initial findings defined the physiological functions of classic neurotransmitters GABA and acetylcholine in a critical clock neuron population, the “evening cells” or LNds. They suggest that these conserved neurotransmitters represent distinct “day” and “night” (or wakefulness and sleep) physiological states, variably coupled to extrinsic (light sensitive-inputs) and cell-intrinsic (molecular clock) elements. Together, we identified a rhythm in fast-neurotransmitter receptivity and their potential regulators in the evening cells. We did not address the relevance of these physiological rhythms in fast-neurotransmitter inputs to fly behavior. The LNds’ neural increased excitation is causal to the fly’s evening bout of wakefulness (Grima et al., 2004; Liang et al., 2016; Stoleru et al., 2004, 2005). Therefore, we speculated that GABA and acetylcholine would modulate the ability of the LNds to time and promote wakefulness at night, and consequently influence patterns of sleep. Using live-imaging and behavioral studies, we test the simple model that GABA inhibition to the LNds decrease evening activity and promotes sleep, while cholinergic excitation promotes evening wakefulness and decreases sleep. We combined the genetically-encoded voltage sensor (GEVI) ASAP2f with RNAi to specifically target and decrease the expression of GABAergic and cholinergic receptor subunits in the LNds (Yang et al., 2016). Relative to existing methods to assess neural activity, ASAP2f records changes in membrane voltage across many cells *in vivo,* with greater resolution for inhibitory, hyperpolarizing events (Yang et al., 2016). Prior to our studies, GEVIs had not

been used successfully to record changes in excitability outside of sensory networks in the *Drosophila* brain, in the clock network specifically, or to bath applied neurotransmitters (Chapter 2). Voltage sensors like ASAP2f have many advantages over electrophysiology that might afford us the opportunity to understand the mechanistic determinates of neural physiology and their consequences for behavior. Therefore, a major part of this work is to determine the degree to which our available tools and analysis techniques are able to confidently, quantitatively link LNd physiology to sleep-wake behavior. We anticipate that our insight on the capabilities and limitations of existing methodology will inform future studies. Herein, using ASAP2f we confirm that GABA and acetylcholine signals to the LNds are received in part through ionotropic receptors (Yang et al., 2016). Finally, we use these RNAi tools to demonstrate that ionotropic neurotransmission functions in the clock network and the LNds specifically to control critical aspects of circadian timing and sleep-wake rhythms.

Results

Nicotinic acetylcholine receptors mediate acute, cholinergic inputs onto the LNds. Acetylcholine, the major excitatory neurotransmitter in the fly brain, is thought to provide critical light information from the environment to the clock network at least in part through the PDF+ lateral clock neurons (Kolodziejczyk et al., 2008; Lelito and Shafer, 2012; Muraro and Ceriani, 2015; Restifo and White, 1990). Acetylcholine therefore, may be a resetting signal that maintains proper timing of the clock network's behavioral outputs with relevant environmental cues. However, the physiological mechanisms that underlie its actions in the clock network at large remained largely unexplored. We previously characterized acetylcholine's physiological role in the network's evening-activity

promoting cells, the LNds, to address this gap. The neural activity of the LNds coordinates the fly's activity in anticipation of dusk and facilities light entrainment of endogenous rhythms (Cusumano et al., 2009; Grima et al., 2004; Stoleru et al., 2004; Yao and Shafer, 2014). Our characterization of the responsiveness of LNds to acute application of acetylcholine using whole-cell patch-clamp and ASAP2f recordings confirmed that it provides direct, excitatory inputs to the LNds (Yao, 2016; Chapter 2). Nicotinic ionotropic receptors (nAChRs) are the primary conductors of acute cholinergic signals to the LNds (Yao, 2016). We also demonstrated that the LNds are more depolarized by acetylcholine during the day in standard entrainment conditions (12:12LD) (Chapter 2). These time-of-day dependent responses are in part light mediated as they fail to persist in constant darkness but interestingly, we found that the effect of light on cholinergic receptivity in entrained conditions is controlled by the molecular clock (Chapter 2). Taken together, we determined that the physiology of the evening cells is affected by fast ionotropic neurotransmission via acetylcholine.

The behavioral relevance of cholinergic signaling in the clock network remains unknown. As a first step towards addressing this question, we sought to identify functional tools in the clock network to knock down the expression of nAChRs using clock network specific GAL4s and monitor sleep-wake behavior in entrained conditions (12:12LD) and endogenous rhythms in constant conditions (DD). Mammalian nAChRs are homopentamers of alpha subunits or heteropentamers of alpha and beta subunits. The fly genome has 10 total genes encoding nAChR subunits- 3 beta subunits and 7 alpha subunits (Jones et al., 2007). All but one subunit is enriched in the fly brain relative to the body, however the composition of functional receptor subunits is unknown (Jones et al.,

2007; Wu et al., 2014). We performed a RNAi screen to identify subunits potentially mediating clock network excitability and behavioral rhythmicity. We expressed RNAis to each of the 10 *nAChR* subunit genes using the network-wide driver *CLK856-GAL4*, entrained flies to 12:12LD cycles for 5 days and then released flies in to constant darkness for 14 days (Gummadova et al., 2009). Only RNAi elements targeting to the -α3 subunit decreased rhythmicity in constant conditions below 50% (33.33% rhythmicity averaged across 3 independent behavior runs). The -β3 subunit was a close second, averaging 56% rhythmicity across 3 independent runs (summarized in Table 1). Interestingly, -α3 and -β3 subunits, though the latter to a lesser degree, have documented roles in sleep-wake behavior. The subunits' genetic interaction with the SLEEPLESS (SSS) protein suppresses nAChR-mediated excitation to promote sleep (Wu et al., 2014). For the remainder of our studies, we used the -α3 subunit RNAi as a tool to examine the physiological and behavioral roles of nicotinic transmission in the LNds and clock network.

To confirm that our behavioral results were linked to reduced receptivity to cholinergic signaling, we directly examined sensitivity of the LNds to nicotine with knockdown of *nAChRα3*. We used the genetically encoded voltage indicator, ASAP2f, for these studies (see Materials and Methods for detailed procedure). ASAP2f reflects changes in voltage by movement of a charged membrane helix linked to GFP wherein decreased and increased fluorescence represent depolarization and hyperpolarization, respectively (Yang et al., 2016). At our acquisition rate (2Hz) and without an independent measurement of baseline membrane potential or imaging fast enough to capture single action potentials in the LNds, we cannot interpret the changes we observe in terms of "inhibition", a prevention of firing, or "excitation", an increase in firing. However, we can

confidently determine increases in “hyperpolarization” (negative charge) or “depolarization” (positive charge) using our methodology. We knocked down the -α3 subunit with the strongest RNAi line identified in our behavior screen using *CLK856-GAL4, UAS-ASAP2f* flies. We reasoned that excitation would be greatest during the peak of LNd neuronal activity as determined by GCaMP6f Ca^{2+} transients and our previous physiological studies, and performed imaging sessions in the daytime between ZT4-8 (Liang et al., 2016; Chapter 2). Studies were performed in the presence of 2uM tetrodotoxin (TTX) to examine effects of nicotine, a nAChR agonist, directly on LNds. We’ve previously demonstrated that TTX application alone has no effect on the LNds in the mid-day and mid-night windows assessed with co-application of transmitter for the remainder of physiological experiments in this manuscript (Chapter 2). We also used a post-hoc data processing method that fits each LNds’ response a 6^{th}-order polynomial in order to accurately quantify and compare results. Our fitting method minimizes ASAP2f sensor noise due to movement of live brains in the perfusion system that is intensified by imaging at high magnification. We previously confirmed that 6^{th}-order polynomial fitting reduced high-frequency noise of the original response data while preserving the traces’ total response area (Chapter 2).

We initially noticed that while wildtype neurons’ ASAP2f fluorescence traces remain close to baseline during and after vehicle application, *nAChRa3* knockdown LNds exhibit spontaneous voltage changes (Figure 1A, C). Specifically, RNAi increases the amount of apparent hyperpolarization in recorded LNds (Figure 1C). We are imaging too slowly (2Hz) to capture single action potentials, but it is likely that these represent relevant changes in membrane potential due to a decrease in cholinergic signaling to LNds

expressing *nAChRa3* RNAi. We found that a 30-second perfusion of 0.5mM nicotine over wildtype and RNAi-expressing brains induces depolarization in the majority of LNds by the end of the 200-second imaging session (Figure 1B, D). Qualitatively it appears that RNAi LNds depolarize more slowly to nicotine application (Figure 1D). We quantified the total response area, and net response area, and minimum fluorescence of responses for the duration of the imaging session (Figure 2). When compared to wildtype, *nAChRa3* knockdown significantly increases the total response area during vehicle application, suggesting that LNds may exhibit more basal hyperpolarization without excitatory, nicotinic inputs (Figure 2A). Nicotine application in both wildtype and RNAi LNds causes significantly depolarization relative to vehicle application: increasing total and negative response area (Figure 2A, B), and mean minimum fluorescence change (Figure 2C). When these calculations are performed using the entire imaging session, we observe no difference between wildtype and RNAi LNd responses to nicotine. We believed that there we qualitative differences in the response time (Figure 1), therefore we performed the same quantification using the frames during, and up to the offset of vehicle or nicotine application (Figure 3). There are no significant differences between any group in total response area or net response area, though wildtype LNds trend towards greater depolarization to nicotine during this shortened analysis window (Figure 3A, B). However, wildtype LNds, but not *nAChRa3* RNAi LNds are significantly depolarized relative to their respective vehicle controls as assessed by mean maximum fluorescence change (Figure 3C). This suggests that wildtype LNds begin to respond and reach a maximum depolarization with more rapidity than those expressing *nAChRa3* RNAi. We also sorted LNd responses into three categories based on their maximum or minimum fluorescence

relative to vehicle controls (Figure 4). Non-responders (grey) are those cells whose maximum or minimum fluorescence falls between 2X the vehicle controls' mean fluorescence. Responders with maximums greater than 2X vehicle average mean are considered hyperpolarized (red) and those with minimums less than 2X vehicle average mean are depolarized (blue) (Figure 4A, B). There were no qualitative or quantitative differences between wildtype and RNAi LNd responses to nicotine (Figure 4A-D). We believe that our genetic manipulations do have an effect on the receptivity of LNds to nicotinic signaling by delaying the response time to maximum depolarization (Figure 3C). This suggests that there may be fewer functional receptors available on LNds as a consequence of RNAi knockdown. We also noticed that RNAi-expressing LNds often displayed increases in ASAP2f fluorescence during control perfusions of vehicle, suggesting that excitatory cholinergic inputs normally keep the LNds depolarized (Figure 1C, 2A). Taken together, we feel comfortable asserting that effects we observe in behavioral experiments may be attributed at least in part to a direct disruption of nicotinic cholinergic signaling.

GABA-A receptors contribute to the acute GABAergic receptivity of the LNds. As in mammals, GABA is the major fast inhibitory neurotransmitter in the fly brain (Restifo and White, 1990). GABA inhibition in *Drosophila* promotes proper timing and maintenance of sleep-wake behavior (Agosto et al., 2008; Chung et al., 2009; Parisky et al., 2008). Though GABA signals may be received through metabotropic and ionotropic mechanisms in flies, ionotropic signals from GABA-ARs promote nighttime sleep by inhibiting the neural activity of the clock networks' morning wake-promoting PDF+ LNvs (Agosto et al., 2008; Chung et al., 2009; Parisky et al., 2008). Ionotropic currents may presumably be

conducted through any one of the fly's three GABA-AR subunit encoding genes (*Rdl*, *Grd*, *Lcch3*), though to date RDL is the only subunit with documented functionality and roles in sleep (Agosto et al., 2008; Chung et al., 2009; Parisky et al., 2008). The physiological role of GABA signaling to the clock networks' other wake-promoting populations (like the evening wake promoting LNds) and consequently, GABA's roles in shaping the timing of wakefulness and sleep remain largely unknown (Stoleru et al., 2004, 2005). To address the first part of this gap, we previously tested the LNds' receptivity to GABA using electrophysiological and ASAP2f live-imaging studies. Our studies found that acute GABA application causes inhibitory, hyperpolarizing responses primarily through GABA-ARs in the LNds (Yao, 2016; Chapter 2). These hyperpolarizing responses to GABA are greater during the nighttime, persist independently of light:dark cycles, and are controlled by the molecular clock (Chapter 2). We also found that the molecular clock controls the polarity of responses to GABA signaling: while we only observed depolarization to 0.75mM GABA during the daytime in wildtype cells, in per^{01} LNds we observed a considerable percentage of depolarizing cells in subjective day and nighttime (Chapter 2).

Our electrophysiological experiments using picrotoxin confirm that GABA-ARs mediate acute, inhibitory responses in the LNds (Yao, 2016). In order to determine the behavioral functions of ionotropic GABA signaling to the clock network and LNds, we first sought to establish the physiological effects of genetic manipulations to decrease signaling in GAL4 defined clock network populations. We expressed RNAi to *Rdl* using *CLK856-GAL4* combined with a *UAS-ASAP2f* element that simultaneously drives the expression of RNAi and the genetically-encoded voltage sensor ASAP2f across the clock

network (Gummadova et al., 2009; Liu et al., 2007; Yang et al., 2016). Hyperpolarization causes ASAP2f fluorescence increases, while depolarization causes fluorescence decreases (Yang et al., 2016). We previously demonstrated that ASAPf fluorescence increases robustly in response to acute GABA application, with increased response magnitudes at nighttime, in LNds (Chapter 2). To vet the usefulness of our genetic tool, we measured changes in ASAP2f fluorescence to the application of 0.75mM GABA in the presence of 2uM TTX in LNds expressing *Rdl* RNAi (Liu et al., 2007). We chose 0.75mM GABA because it is slightly below the apparent saturation concentration (1mM) and performed all experiments during the middle of the night (ZT14-18) when the strength of GABA's hyperpolarizing effects peaks in the LNds (Chapter 2). We fitted LNd responses with a 6th-order polynomial post-hoc and derived quantifications from these fitted traces.

We observed no qualitative differences between spontaneous voltage responses of wildtype or *Rdl* RNAi LNds during vehicle application (Figure 5A, C). As we have previously observed at this concentration of GABA, there is a mix of both hyperpolarization and depolarization in both wildtype and *Rdl* knockdown LNds (Figure 6B, D; Chapter 2). We quantified total response area, net area and mean minimum and maximum fluorescence change for each group (Figure 6). There are no quantitative differences between ASAP2f fluorescence time courses in the presence of vehicle perfusion for any of these analyses (Figure 6A-D). In response to GABA application, wildtype and knockdown LNds exhibit total response areas significantly greater than their respective vehicle controls (Figure 6A). We found that the majority of LNd responses to GABA are depolarized relative to controls (Figure 6B). The total response area of depolarizations near significance only in the knockdown relative to vehicle control and

between knockdown and wildtype suggesting that the LNds may be more depolarized to GABA with *Rdl* RNAi (GABA KD vs. vehicle KD p = 0.1174; GABA KD vs. GABA WT p= 0.1671) (Figure 6B). Indeed, in response to GABA application *Rdl* RNAi is the only group with significantly greater minimum response fluorescence relative to its vehicle control (Figure 6C). Though there appear to be trends towards increased hyperpolarization to GABA relative to vehicle in wildtype LNds, these values are not significant between any groups included in the analysis (GABA WT vs. vehicle WT p = 0.1924). We wondered whether the marginal differences between wildtype and knockdown LNd responses to GABA were due to non-responsive cells. We sorted LNd responses to GABA using the same procedure as used in our physiological studies with nicotine (Figure 7). We labeled non-responders in grey, hyperpolarized responders in blue, and depolarized responders in red (Figure 7A, B). We eliminated nearly 60% of LNds as non-responsive from wildtype and *Rdl* RNAi GABA experiments (Figure 7C). There were marginally more hyperpolarized cells by population in wildtype experiments, and approximately the same number of depolarized cells between wildtype and RNAi LNds (Figure 7C). After sorting, we quantified and compared the mean maximum and minimum fluorescence change of wildtype and *Rdl* knockdown LNd responses to GABA (Figure 7D). Wildtype cells approach significantly greater maximum hyperpolarization to GABA relative to knockdown cells (p = 0.0858) (Figure 7D). Knockdown LNds, on the other hand approach significantly greater maximum depolarization to GABA relative to wildtype cells (p = 0.0902) (Figure 7D).

Together, these results demonstrate that *Rdl* RNAi significantly increases the levels of depolarization, and non-significantly minimizes the hyperpolarizing effects of

GABA application. We only expected to observe decreases in hyperpolarization with reduced *Rdl* expression, so the latter effect was rather surprising but not physiologically unfeasible. The increases in depolarization we observe in LNds with *Rdl* knockdown could be a direct or indirect result of fewer functional receptors. In the former, direct mechanism, GABA itself may be depolarizing when there are reduced levels of GABA-ARs. In the latter, indirect mechanism, excitation from other neurochemical modalities dominates simply as a consequence of less GABA-mediated inhibition. Given that we are performing our studies in the presence of TTX to block neurotransmission, it seems likely that GABA itself is exerting an excitatory action when there are fewer RDL receptors. However, we cannot exclude the possibility that intrinsic, spontaneous firing we've previously observed in LNds may be more likely without GABA inhibition and contribute to our present observations (Yao, 2016). Nevertheless, our results suggest that the LNds' physiological responses to GABA are perturbed by *Rdl* RNAi, but are not sufficient to completely eliminate responses. We posit that there are redundant mechanisms that compensate for the reduction of RDL levels. For example, through the other potential GABA-AR subunits, metabotropic GABA-BRs, or inhibition from neurochemicals like glutamate (Gmeiner et al., 2013; Guo et al., 2016; Hamasaka et al., 2005, 2007). An alternative explanation for all of our observations is that our genetic manipulations to decrease *Rdl* levels may have been incomplete. We do not have confirmation that our GAL4 driver is driving RNAi expression sufficient enough to eliminate all GABA-ARs. Perhaps, if we increased RNAi expression, we would see the expected decreases in hyperpolarization as well as increases in depolarization with GABA application.

Fast-neurotransmitter receptivity across CCNN, and in LNds specifically facilitates behavioral rhythmicity and periodicity, sleep and activity. Male flies exhibit a characteristic bimodal distribution of activity and sleep under a 12:12 light:dark cycle (Tataroglu and Emery, 2014). Their activity anticipates the transitions of light around dawn and dusk, while they sleep during the day and throughout the night (Rosato and Kyriacou, 2006). The daily morning and evening activity peaks are controlled by the PDF+ LNvs and the LNds, respectively (Grima et al., 2004; Stoleru et al., 2004). The neural activity of the LNds (as inferred by Ca^{2+} transients) peaks just hours before the evening activity peak they promote in anticipation of lights-off (Liang et al., 2016). Therefore, the neuronal activity of the LNds must be temporally modulated to properly coordinate and time activity and sleep with daily environmental rhythms. Our live-imaging and previous electrophysiological characterization show that GABA inhibits, and acetylcholine excites LNds via GABA-ARs and nAChRs, respectively (Yao, 2016). We previously demonstrated that these transmitters dominate during different times of day (Chapter 2). While GABA's hyperpolarizing effects peak during the night, acetylcholine's depolarizing effects peak during the day. Their distinct physiological distributions suggests GABAergic and cholinergic signaling may have disparate behavioral roles across the day within the LNds, and perhaps across the clock network at large. Therefore, we decided to examine the fly's endogenous rhythms, and entrained activity and sleep profiles when these fast-neurotransmitter inputs are disrupted. Given that the LNds coordinate the evening bout of wakefulness, we speculated that disrupting GABA inhibition would increase evening activity and decrease sleep, while disrupting cholinergic excitation would decrease evening activity and increase sleep.

Our ASAP2f experiments demonstrate that *nAChRa3* RNAi physiologically reduces depolarizing responses to the cholinergic agonist nicotine, and promotes hyperpolarization in the LNds. This suggests that cholinergic excitation normally increases neural activity and depolarizes the LNds. Following our behavioral model, we anticipated that disrupting cholinergic excitation of the LNds with RNAi would decrease evening behavior in light:dark cycles. Given cholinergic signaling's correlation with environmental light cycles, we also predicted that in the absence of cholinergic excitatory signals, the LNds may not properly entrain to light cycles and exhibit desynchrony in constant darkness and temperature (DD). We examined the consequences of *nAChRa3* RNAi expression for circadian behavior, sleep and activity in 12:12LD and constant conditions (DD) in male flies expressing RNAi using a network-wide driver *CLK856-GAL4* and a highly specific split-GAL4, *MB122B-GAL4* that expresses in the three CRY+ LNds and the 5th-small LNv, the so-called "evening-oscillators" (Pfeiffer et al., 2010). We note that there are no known drivers that are specific for the LNds. Though we cannot exclude the possibility that expression in the PDF negative 5^{th}-small is contributing to our observations, this subpopulation was recently shown to be more anatomically related to the LNds, suggesting it's classification as an LNv may be a misnomer (Schubert et al., 2018).

Knocking down the expression of *nAChRa3* subunits across the entire network using *CLK856-GAL4* causes visibly less rhythmic behavior in DD than flies from relevant control lines (Figure 8A). We quantified the overall percent rhythmicity for each genotype (Figure 8B-D, bolded percentages superimposed on bars, summarized in Table 2). *nAChRa3* RNAi causes a dramatic decrease in the proportion of flies displaying

significant periodicity in their locomotor activity relative to controls in the first 4-days after the transition to constant darkness, and in the last 4-days of the 14-day DD experiment (Figure 8B, C). Rhythmicity over the entire 14-days of DD is only marginally decreased relative to controls (Figure 8D). These findings suggest that *nAChRa3* RNAi expression decreases the consistency of rhythmicity in constant conditions, particularly after environment transitions, and as these new conditions persist. They are however, on average exhibiting some rhythmicity over the course of the experiment. We also quantified the periodicity of rhythmic flies across genotypes. We observe that *nAChRa3* RNAi flies are significantly lengthened in periodicity in constant conditions relative to controls in the first 4-days and across the entire 14-days of DD (Figure 8B, D). The single fly that remained rhythmic in the last 4-days of DD exhibited regular periodicity (Figure 8C). Together our data suggest that nicotinic signaling to the clock network maintains behavior rhythmicity particularly by shortening the fly's endogenous rhythms to match light:dark entrainment conditions.

We examined the circadian rhythms of flies expressing RNAi to *nAChRa3* in the LNds under the control of the split-GAL4 *MB122B-GAL4* (Figure 9). We observed very few RNAi-expressing flies with lengthened periodicity relative to flies in control genotypes (Figure 9A). The population rhythmicity for each genotype was not noticeably different between groups (Figure 9B-D, bolded percentages). The periodicity of flies from all genotypes in constant conditions was between 23 to 24-hrs and not significantly different in any portion of the experiment (Figure 9B-D). We conclude that nicotinic signaling's role in endogenous timekeeping we observed using the *CLK856-GAL4* in constant conditions does not appear to be mediated through the LNds exclusively, though we observed a

small number of flies with lengthened periods in DD (summarized in Table 2). It is possible that diminished nicotinic signaling to another population- perhaps the PDF+ l- or s-LNvs is the source of our observations. Alternatively, it is possible that a physiological loss of cholinergic signaling in any single clock-network population can be compensated by the actions of another. Thus, only when nicotinic signaling is decreased network-wide would be observe severe consequences to behavior, though this “emergent” network property remains to be tested. Finally, our results might also be explained by a technical failure to express RNAi comparably between the two GAL4 drivers.

We wondered if nicotinic signaling to the clock network at large contributed to sleep and activity behavior under standard entrainment conditions (12:12LD cycles). We quantified the average total activity in the first 3-entrained LD days for *nAChRa3* RNAi and control flies in the lights-on (henceforth, “day”) or lights-off (hereafter, “night”) portions of the LD experiment (Figure 10A). Though there were not quantitative differences in the day or night (Figure 10B), we noticed qualitatively that many *nAChRa3* RNAi-expressing flies exhibited reduced evening anticipation to the day-night transition. We quantified the activity levels between ZT8 and ZT12 and found that RNAi flies had significantly reduced activity (as a percentage of total activity in the 24-hr period) in the 4-hours before lights-off relative to RNAi control flies only (Figure 10C). We quantified the levels of evening anticipation by determining the slope of a linear regression projected through the hours preceding Zeitgeber transitions, in this case ZT8-12 prior to lights-off, for each fly (10E, individual fly linear regressions in light grey, genotype average linear regression in dark grey). The average evening anticipation slope was significantly decreased in RNAi flies relative to the RNAi control but not the GAL4 control, suggesting that nicotinic input to the

clock network at large plays a role but is not causal to proper evening anticipation in 12:12LD cycles (Figure 10D).

The fly's evening peak of activity is attributed to the neural activity of the LNds (Stoleru et al., 2004, 2005). According to our model, the decrease in evening anticipation we observed as a consequence of decreased cholinergic signaling to the clock network might be mediated by the LNds. Using results from two independent behavioral experiments, we calculated the total activity in the day and night portions of the day where *nAChRa3* knockdown was limited to the 3 CRY+ LNds under the control of *MB122B-GAL4* (Figure 11A). Relative to control genotypes, *nAChRa3* RNAi significantly increases overall day activity and decreases night activity (Figure 11B). We observed qualitative differences in evening activity and anticipation in RNAi-expressing flies in the hours surrounding the lights-off transition that were similar, but more pronounced than in *CLK856-GAL4* experiments (Figure 11A). Particularly, we noticed that evening activity appears to start earlier than that of the controls, suggesting that the LNds are less synchronized, and therefore produce a lower amplitude evening activity peak. We quantified the percentage of the total 24-hour period activity occurring between ZT8 and ZT12 and found that it was significantly greater in RNAi-expressing flies relative to both controls (Figure 11C). Coherent with our visual assessment, *nAChRa3* RNAi in the LNds significantly reduces evening anticipation slope by more than half relative to control genotypes (11D, E). These data confirm that the nicotinic signaling to the LNds specifically helps coordinate evening peak activity and anticipation of the day-night transition.

Cholinergic signaling to the LNds predominates during the day in our physiological experiments (Chapter 2). In *Drosophila* like in mammals, acetylcholine may strongly promote wakefulness in relevant neuronal populations (Bina et al., 1993; Yang et al., 2010). One possible explanation for decreases in evening activity we observe with decreased cholinergic excitation is increases in sleep. We quantified, and averaged fly sleep for the first 3 entrained days of 12:12LD (Figure 12A, 13A). Sleep is any period of inactivity (no IR-beam crosses) greater than 5-minutes as previously described (Andretic and Shaw, 2005; Hendricks et al., 2000). Relative to the RNAi control genotype, there are marginal but significant increases in night sleep in *nAChRa3* RNAi flies when either *CLK856-GAL4 or MB122B-GAL4* drivers are used (Figure 12B, 13B). Qualitatively we also observed decreases in morning sleep when RNAi was expressed across the clock network (Figure 12A, C). In contrast, RNAi limited to the CRY+ LNds and 5th-small increases early morning sleep though the spread of data points in this window indicates that the trend is not unidirectional and represents a mix of increases and decreases relative to controls (Figure 13A, B). Taken together our analyses suggest that cholinergic excitation through *nAChRa3* to the clock network, specifically through the CRY+ LNds promotes evening activity without significantly, directionally influencing sleep quantity or timing. This finding supports our model and is coherent with published observations that the increased neural activity of the LNds is causal to evening wakefulness (Liang et al., 2016). It is also the first study to identify a role for cholinergic signaling in synchronizing the behavioral efforts of the LNds.

Our physiological experiments demonstrated that *Rdl* RNAi disturbs the acute responses of the LNds to GABA application. With *Rdl* RNAi expressed in the LNds we

observed qualitative, but non-significant decreases in hyperpolarization, and significant increases in depolarization relative to wildtype controls. This latter finding suggests that GABAergic signaling through *Rdl* promotes hyperpolarization at baseline in the LNds. We certainly expected more dramatic results on acute hyperpolarization to GABA with *Rdl* RNAi, rather than increased depolarization. It is possible that our knockdown was incomplete or alternatively, that the physiological consequences of perturbed GABA-AR signaling are compensated by network actions, intracellular mechanisms that may increase GABA-BR and glutamatergic inhibition, or reduce excitatory signal receptivity. Perhaps unsurprisingly given our physiological findings, inhibitory GABA-AR signaling through subunit RDL has no profound contributions to circadian rhythmicity or periodicity in DD when expressed in the clock network as a whole with *CLK856-GAL4*, or the LNds specifically with *MB122B-GAL4* (Figure 14A-H, summarized in Table 3). This is in stark contrast to the dramatic effects on endogenous timekeeping with reduced excitatory nicotinic signaling.

Given our present knowledge it is impossible to discern whether *Rdl*'s apparent disconnection to endogenous rhythmicity is due to incomplete knockdown, compensatory mechanisms or true biological irrelevance. It does not, however, preclude the possibility of ionotropic GABAergic signals' relevance in entrained, light:dark conditions. According to our model, we predicted that decreasing GABAergic signaling to the LNds by expressing *Rdl* RNAi would increase evening activity and decrease sleep. Thus, we quantified the average activity and sleep for the first 3 entrained days of 12:12LD. We find that GABA-AR/*Rdl* knockdown relative to the GAL4 control significantly reduces overall day activity quantity, and increases night quantity when expressed across the clock

network (Figure 15A, B). We noticed that qualitatively there were decreases in morning anticipation in *CLK856-GAL4* flies expressing RNAi (Figure 15A), however the levels of activity or morning anticipation were unchanged relative to controls (Figure 15C-E). When expression is limited to the LNds and 5th-small under the control of *MB122B-GAL4*, there are no differences in the day or night total activity (Figure 16B). However, we noticed an even more pronounced decrease in morning anticipation to lights-on in RNAi flies than in *CLK856-GAL4* experiments (Figure 16A). Compared to both controls, *Rdl* RNAi flies display significantly reduced morning activity quantity between ZT 22 and ZT2 (Figure 16C). Further, the slope of stereotypical activity increases preceding and anticipating lights-on is significantly reduced in *Rdl* knockdown flies relative to both controls (Figure 16D,E). The reduction in daytime activity is accompanied by increased daytime sleep relative to the GAL4 control only when expressed clock-wide (compare Figure 17A,B to 17C,D). This suggests that in this particular case activity decreases are not explained by coincident increases in sleep.

Our findings support that ionotropic GABAergic signaling to the LNds facilities the coordination of morning wakefulness. These results are surprising given that the LNds' activity is causal to the fly's evening bout of wakefulness (Liang et al., 2016; Stoleru et al., 2004, 2005). In contrast to our model's predictions inhibiting the LNds' activity, rather than promoting sleep or controlling evening activity, actually facilitates bouts of morning wakefulness promoted by other neuron classes- namely the s- and l-LNvs. Our behavioral findings with *nAChRa3* and *Rdl* RNAi make sense if viewed in the light of precisely timed reciprocal inhibition. In short, we propose that the morning peak of wakefulness coordinated by the PDF+ wake-promoting cells is *indirectly* gated by GABAergic inhibition

of the LNds, while the evening peak of activity is *directly* gated by cholinergic excitation of the LNds. It is also possible that evening wakefulness coordinated by the LNds is *indirectly* gated by the inhibition of the LNvs though this prediction was not tested in our experiments (Helfrich-Förster et al., 2007). The clock neuron network expresses many neuropeptides and neurotransmitters that potentially serve behavioral functions. Our physiological and behavioral studies do not paint the entire picture in terms of neuronal populations, or relevant peptides and transmitters. Nevertheless, our findings that the LNds' excitation via acetylcholine promotes evening wakefulness and inhibition via GABA promotes morning wakefulness hint that rhythms in fast-neurotransmitter receptivity play a functional role in patterning sleep-wake and circadian behavior through direct and indirect mechanisms.

Discussion

Acetylcholine and GABA make physiologically relevant ionotropic inputs to the LNds. In principle, the tools available in the *Drosophila* circadian model system make it possible to determine the molecular and neurophysiological correlates of sleep-wake behavior. Genetically encoded voltage sensors (GEVIs) that assess membrane voltage changes in vivo had not been used to assess the receptivity of neurons in the *Drosophila* central brain to applied neurotransmitters (Chapter 2). GEVIs like ASAP2f have many advantages additional to existing *in vivo* methodology like Ca^{2+} and cAMP live-imaging (Tian et al., 2009; Yang et al., 2016; Yao et al., 2012). ASAP2f reflects voltage changes across populations of cells without invasive single-cell techniques of electrophysiology, and has greater resolution for potentially inhibitory, hyperpolarizing events (Yang et al., 2016). The extent to which ASAP2f would be useful to draw a direct link between clock neuron

physiology controlled by neurochemicals and circadian behavior was unknown prior to our studies (Chapter 2). Thus, we characterized the responsiveness of LNds to classical fast neurotransmitters acetylcholine and GABA (Yao, 2016, Chapter 2). Acute application of GABA hyperpolarizes, while acetylcholine depolarizes the LNds (Yao, 2016, Chapter 2). These studies confirm our electrophysiological findings and suggest that ASAP is a feasible tool to assess acute physiological receptivity of neurons in the clock neuron network to bath-applied neurotransmitters.

Herein, we combined GAL4-specific RNAi with ASAP2f membrane voltage analysis to assess the limitations of the *Drosophila* models' available tools in addressing our central aim: understanding how neurotransmitters control clock neuron physiology and sleep-wake behavior. Acetylcholine excites the LNds, thus we suspected that directing RNAi to *nAChRa3* would lead to decreased depolarization, excitation to cholinergic agonists (Yao, 2016, Chapter 2). Indeed, we observed decreases in the physiological receptivity of the LNds to nicotine as assessed by ASAP2f imaging, confirming Z. Yao's electrophysiological findings that suggested acetylcholine provides excitatory synaptic inputs to the LNds via ionotropic nAChRs (Yao, 2016). *nAChRa3* RNAi also increase the levels of hyperpolarization LNds experience at baseline suggesting that nicotinic inputs normally keep the LNds depolarized. This remains to be tested through more sensitive methodology like electrophysiology or higher-speed ASAP2f imaging to capture single action potentials. Finally, our results do not preclude the physiological relevance of metabotropic mAChRs in the LNds, as it appears the LNds express both cholinergic receptor types (Abruzzi et al., 2017).

Our previous electrophysiological studies with picrotoxin found that GABA provides acute, fast inhibitory synaptic inputs onto the LNds via the ligand-gated chloride channel subunit, RDL/GABA-AR (Yao, 2016). Our ASAP2f studies sought to independently confirm these findings and to establish the functionality of *Rdl* RNAi to genetically decrease receptivity to GABA. We expected that RNAi would decrease hyperpolarization in the LNds to bath-applied GABA as inferred by ASAP2f imaging. However, we found that expressing *Rdl* RNAi in the LNds decreased hyperpolarizing responses to GABA with p-values that only approached significance. Instead, *Rdl* RNAi significantly increased the levels of depolarization to GABA. We conclude that our RNA is sufficient to decrease, but not entirely eliminate cellular responses to GABA and further, that GABA normally keeps the LNds in hyperpolarized. There are two challenges that might explain the lack of significantly decreased hyperpolarization with *Rdl* RNAi. First, the RNAi efficiency may not be great enough to completely eliminate hyperpolarizing responses. Given that there are trends towards significance, and there are significant increases in depolarization in knockdown LNds it also seems likely that we have reached the resolution threshold of our imaging technique or analysis methods. Perhaps, imaging faster or with better quantitative means of extracting signal from noise we would see significant results. Barring these technical hurdles, there are also biological reasons for our observations. Compensatory mechanisms may substitute for the loss of RDL subunits, including formation of GABA-ARs composed predominately of other possible subunits, increases in inhibition through GABA-BRs, or glutamatergic receptors, and intrinsic methods to decrease cellular excitability. Alternatively, there may be little turnover in *Rdl* mRNA that is reducing RNAi efficiency. However, it seems unlikely given that RDL

is expressed at consistent levels in the LNds as inferred from clock-network population specific RNA-sequencing (Abruzzi et al., 2017). In the future, it will be useful to knockdown GABA-BRs and ARs in combination, utilize multiple RNAi constructs targeting *Rdl* simultaneously to increase efficacy, co-express Dicer2, and use adult-specific knock down to avoid compensation that may occur during development.

GABAergic and cholinergic receptivity control distinct aspects of circadian timekeeping, daily activity and sleep. The bimodal activity of male flies in entrained conditions is primarily attributed to two dominate clock network populations. The neural activity of the PDF+ s- and l- LNvs coordinate morning wakefulness, while the LNds coordinate evening wakefulness (Grima et al., 2004; Liang et al., 2016; Stoleru et al., 2004, 2005). Having determined the consequences of our RNAi tools for LNd physiology, we used the same genetic manipulations from our physiological studies to determine the contributions of nicotinic and GABAergic signaling to circadian timekeeping, sleep and activity in 12:12 LD entrained and constant conditions (DD). The physiological receptivity to GABAergic and cholinergic signals are timed across the day in the LNds. Thus, we predicted rather simple-mindedly that decreasing cholinergic excitation with *nAChRa3* RNAi would decrease evening wakefulness and increase sleep, and decreasing GABAergic inhibition with *Rdl* RNA might increase evening wakefulness and decrease sleep. We found that expressing RNAi to *nAChRa3* across the clock network dramatically decreased rhythmicity, while the few flies that remained rhythmic exhibited lengthened periodicity in DD. When we expressed *nAChRa3* RNAi using *MB122B-GAL4*, we determined that cholinergic signaling's rhythm-promoting effects were not maintained by the CRY+ LNds and 5th-small. Barring the possibility that our RNAi is not driven

successfully with *MB122B-GAL4*, we suspect that other populations in the network contribute to these effects, for example the PDF+ s- and l-LNvs. Entraining light information received by cholinergic cells in the optic lobes may feed in to the clock network through the s- and l-LNvs to coordinate the disparate endogenous rhythms of clock network populations and facilitate rhythmicity in constant conditions (Liang et al., 2016; Muraro and Ceriani, 2015; Yao and Shafer, 2014). We did not find dramatic effects on circadian rhythmicity or periodicity with *Rdl* RNAi expressed throughout the clock network or in the CRY+ LNds. However, given that the network is in theory widely receptive to acute, GABAergic signaling and that *Rdl* RNAi changes the GABA receptivity of recorded LNds, we cannot exclude the possibility that GABA has a timekeeping role in other populations in the network (Chapter 2, Abruzzi et al., 2017). For the reasons argued in our physiological discussion, it is formally possible that our *Rdl* manipulations in the LNds may not be strong enough to decrease RDL levels enough to effect endogenous circadian timing. We note that our knockdowns persist throughout development and nervous systems are plastic. Thus, we may not be able to overcome compensation by the actions of other cells in the network or increased inhibition to the LNds through other pathways including metabotropic GABA-BRs or glutamate.

We were also interested in the effects of these neurotransmitters on sleep-wake behavior in 12:12 light:dark (LD) entrained conditions. Our behavioral experiments suggest that nicotinic excitation in the clock network, specifically via the CRY+ LNds contributes to evening activity in 12:12 LD. The LNds' increased neural activity is causal to evening wakefulness (Grima et al., 2004; Liang et al., 2016; Stoleru et al., 2004, 2005). We found that flies expressing *nAChR* RNAi in the LNds have less evening anticipation

amplitude and more evening activity, as a consequence of starting their behavior peak earlier in the day. This confirm our model's expectations that decreasing cholinergic inputs, the LNds' neural activity and perhaps the population's synchrony, would perturb their evening behavior peak. It remains unknown whether increases in the LNds' neural activity (Ca^{2+} transients) are set cell-intrinsically or through the actions of precisely timed neurochemical inputs. Our findings do not exclude intrinsic regulation of cellular excitability to acetylcholine or other relevant neurochemicals. However, they do identify a new role for cholinergic signaling and nAChRs in coordinating the behavioral outputs of the LNds and suggest that their activity is not exclusively guided by intrinsic mechanisms. Interestingly, we found that *nAChRa3* RNAi limited to the CRY+ LNds and 5th-small quantitatively increased sleep during the first half of the day, though the qualitative data trends show a mix of increases and decreases relative to controls. This data suggests that the cholinergic excitation of LNds may be, rather surprisingly, sleep promoting in mid-morning after the PDF+ cells coordinate morning wakefulness. In contrast to our model's expectations that decreased GABA inhibition would increase evening behavior and decrease sleep, we observed negligible effects on total, or evening wakefulness and sleep when *Rdl* RNAi was expressed in the clock network or in the LNds specifically. Instead, we found significant decreases in morning wakefulness with RNAi expressed in the LNds, and trends towards significant decreases when RNAi was expressed across the clock network. These data suggest that GABAergic signals conducted by GABA-AR subunit RDL in the LNds promotes daytime activity in the morning hours surrounding lights-on. This was unusual given that 1) in the literature GABA-AR expression in the s- and l-LNvs primarily promotes sleep, not activity and 2) the neuronal activity of the LNds

is causal to evening activity, while that of the LNvs is causal to morning activity (Chung et al., 2009; Gmeiner et al., 2013; Grima et al., 2004; Liang et al., 2016; Parisky et al., 2008; Stoleru et al., 2004, 2005). These data suggest at the very least that the roles of particular neurotransmitters may be heterogenous across the clock network. Further, that our assumptions that clock neuron populations and neurochemicals are exclusively "wake" or "sleep" promoting may be incorrect.

The presence of precisely timed reciprocal inhibition between the evening LNds and morning PDF+ cells may explain our findings with both *Rdl* and *nAChRa3* knockdown. Cholinergic excitation of the LNds in the evening increases their activity and directly promotes evening activity. GABAergic inhibition of the LNds in the morning decreases their activity and indirectly activates the LNvs to promote morning activity. Though it remains to be tested, we speculate that a similar arrangement exists to promote evening wakefulness, wherein the timed inhibition of the LNvs may relieve LNd inhibition, gating their excitation and indirectly promoting evening activity. Though the neuronal sources of GABAergic and cholinergic inputs to the LNvs and LNds remain mysterious, it seems likely receive timed inhibitory and excitatory signals from out-of-clock network inputs. The strength and meaning of these inputs could be regulated by environmental and molecular clock-mediated rhythms in receptor turnover or neuronal excitability. This is suggested by our previous ASAP2f physiological studies wherein increases in GABA and acetylcholine transmitter receptivity in the LNds occur at distinct times during the day and are to differing degrees coupled to light-inputs and the molecular clock (Chapter 2). Together, our studies demonstrate that our available tools and methodology are sufficient in most cases to directly link neural physiology to behavior. ASAP2f functions in vivo in

the clock network and when coupled with RNAi to assess the receptivity of clock neurons to bath-applied neurotransmitters. In the future, coupling ASAP2f with a functional analysis of RNAi efficiency will make these physiological studies more compelling. Our behavioral studies also paint a more complex view of the evening cells, the LNds, and their neurotransmitter modulators. Not only do the LNds promote evening wakefulness but also morning wakefulness. Interestingly, the “sleep” neurotransmitter GABA, facilitates the LNds’ promotion of morning wakefulness. These studies suggest that clock neuron populations and neurochemicals are perhaps not unimodal, mediating a single aspect of behavior. We anticipate that as the roles of the clock networks’ rich neurochemical machinery are explored, multi-functionality may be the norm rather than the exception.

Materials and Methods

Drosophila Strains. Flies were reared on cornmeal-sucrose-yeast media under a 12:12 light: dark cycle at 25°C. The following fly lines were used: w^{1118}, y,v; attp40 (Bloomington stock: 36304), y,v;;attp2 (Bloomington stock: 36303), *w;CLK856-GAL4;* (Gummadova et al., 2009), *w; MB122B-AD; MB122B-DBD* (Pfeiffer et al., 2010), *w;;UAS-Rdl 8-10J RNAi* (Liu et al., 2007), *y,v;UAS-nAChR3a RNAi* (Bloomington stock: 61225), *w;UAS-ASAP2f;* (Bloomington stock: 65414), (Yang et al., 2016), and *w;CLK856-GAL4, UAS-ASAP2f;* (stably recombined for the purposes of these studies).

ASAP2f Live Imaging. Male flies expressing the ASAP2f construct under the control of the *CLK856-GAL4* were entrained to 12:12 LD cycles and aged 5-7 days. Flies were anesthetized on ice in daytime or nighttime as specified in text and figure legends. Daytime dissections were performed in the presence of ambient environmental light. Flies

dissected for nighttime applications were in kept under aluminum foil in complete darkness until dissection and all environmental light in, or to the room was off. For experiments in constant darkness, constant temperature flies were removed from incubators on the first full day of DD and kept in foiled vials until dissection. Fresh HL3 was prepared to the following specifications in 1mL of milliQ water: 70mM NaCl, 5mM KCl, 1.5mM $CaCl_2$, 20mM $MgCl_2$ hexhydrate, 10mM $NaHCO_3$, 5mM trehalose dihydrate, 115mM sucrose, 5mM HEPES (Yao et al., 2012). The solution was titrated to pH 7.1 and vacuum filtered. All solutions for imaging experiments herein were prepared in HL3, pH 7.1. Brains were dissected in room temperature HL3, placed in the bottom of a 35mm petri dish with a perfusion insert and adhesive layer (PDI, Bioscience Tools) and allowed to equilibrate for 2min prior to imaging with constant flow of room temperature HL3 with 2uM tetrodotoxin with the exception of experiments in Figures 2, 3 with *acute* application of 2uM tetrodotoxin. Preparations were visualized using an Olympus Fluoview FV1000 confocal equipped with an Olympus LUMPlanFI 40×/0.8 W water-immersion objective (Olympus, Center Valley, PA). The LNds were identified by their anatomical locations and expression of fluorescent ASAP2f proteins (Yang et al., 2016). We used a magnetic microscope adapter appropriate for the Olympus Fluoview confocal microscope to hold the petri dish in place on the stage (MA-110, Bioscience Tools). We used an 8-channel pinch-value perfusion system calibrated to deliver each solution at the same flow rate, without cross talk between solutions and manually controlled the delivery of each solution for the appropriate duration of the imaging session (PS-8H, Bioscience Tools). An 8-channel perfusion manifold delivered solutions to the Petri dish from the pinch-valve system, while a magnetic holder equipped with suction tubing controlled the liquid outflow

(MTH-P and MTH-S, Bioscience Tools). Each brain was imaged for 90sec total with a 488nm laser between 5-10% power and a frame rate of 2 frames/second (2Hz). Sessions were structured as follows: 15-second pre-stimulus, 30-sec stimulus with vehicle (HL3) containing 2uM tetrodotoxin, XmM nicotine with 2uM TTX, or XmM GABA with 2uM TTX, followed by 45-second HL3 wash out. Brains were imaged only once, and received only one stimulus or vehicle application.

ASAP2f Imaging Analysis. ROIs were drawn around the cell bodies of LNds using Olympus Fluoview software. Each ROI per brain represents a single LNd in either hemisphere identified by anatomical position and expression of the ASAP2f fluorescent construct. Raw intensities were exported for duration of imaging session and then normalized to percent fluorescence changes or deltaF/F_0 where F_0 is calculated as the average of raw intensity values in the frames before stimulus or vehicle application. Brains that moved significantly due to poor mounting were excluded from further analyses. We used the statistical analysis software, Prism to transform percent fluorescence values for each ROI using a centered, 6^{th}-order polynomial (GraphPad, Prism version 8.0.2 for Mac, GraphPad Software, San Diego, California USA). Centering converts each X-value collection bin to XC = X - MeanX. X therefore is a constant and only the fluorescence values are fitted to the 6^{th}-order polynomial. Individual ROIs best-fit curves (light grey lines on trace plots), the mean of all fitted curves (black solid lines), and 95% prediction bands (black dashed lines surrounding the solid line) that enclose the area representing 95% of "future" data points interpolated from the curve were calculated. Prediction bands represent the uncertainty in the true position of the curve (enclosed by the confidence bands), and the scatter of data around the curve. We automatically removed outliers from

trace data using ROUT method with FDR less than 1% (GraphPad, Prism version 8.0.2 for Mac, GraphPad Software, San Diego, California USA). We tested each experimental group for normality with a D'Agostino-Pearson normality test that assumes that the spread of points for each X-value collection bin is normally distributed between replicates (GraphPad, Prism version 8.0.2 for Mac, GraphPad Software, San Diego, California USA). R^2 values were calculated for all experiments and included on graph title as an indicator of the fit of the 6^{th}-order polynomial to the original, un-fitted traces. Maximum (inhibition) and Minimum (excitation) Fluorescence values were calculated by selecting the maximum or minimum intensities in 6^{th}-order fitted frames following vehicle stimulus and represented in histograms with the mean and SEM for each stimulus. The Total Response Area and Net Response Area were quantified using Prism software's AUC analysis over the fitted data (GraphPad, Prism version 8.0.2 for Mac, GraphPad Software, San Diego, California USA). Outliers were identified by Prism using the ROUT method with Q (False-discovery rate) = 1% and excluded from analysis (GraphPad, Prism version 8.0.2 for Mac, GraphPad Software, San Diego, California USA). Significance between maximum or minimum fluorescence values (delta F/F0) and total or net response areas of traces ($P<0.05$) was calculated using One-way ANOVA with Sidak correction for multiple comparisons between all groups (GraphPad, Prism version 8.0.2 for Mac, GraphPad Software, San Diego, California USA). Where fewer than three groups were being analyzed, we determined significance using an unpaired t-test with Welch's correction between each pair (GraphPad, Prism version 8.0.2 for Mac, GraphPad Software, San Diego, California USA). Significance ($p<0.05$) is reported with actual values when P-value is <0.05. Significant values are bolded.

*Sleep and Activity Behavio*r. Individual flies aged 5-7 days were placed in glass recording tubes containing 2% agar-4% sucrose food. Tubes were loaded into DAM2 *Drosophila* Activity Monitors (TriKinetics, Waltham, MA) for locomotor activity recording. Flies were maintained at a constant temperature of 25°C throughout recording and activity counts were collected in 1-minute bin during 6 days of entrained 12:12 LD cycle and two weeks of constant darkness.

Sleep and Activity Analyses. Rhythmicity and periodicity of individual flies were determined by χ–square analysis with a confidence level of 0.01 using ClockLab software from Actimetrics (ClockLab, Wilmette, IL, USA). Rhythmic Power, a measure of the strength of the free-running rhythm, was calculated by subtracting the periodogram amplitude from the χ–square value at a significance of 0.01. Rhythmic flies were those with Power values greater than 10. Results from ClockLab analysis are included in Tables 1, 2 and 3. Activity and sleep quantities were calculated using the PHASE software for MATLAB (Chapter 3). Activity data from the DAM-system was gathered in total beam crosses per 1-minute bin, binned into 30-minute intervals and normalized to the average total activity for each individual fly. When multiple flies were averaged from a single genotype, the averaging was first done by individual flies and then, in a separate step, averaged by days. We excluded dead and inactive flies from our analysis. Sleep is defined as uninterrupted inactivity lasting for five minutes or more, as previously described (Andretic and Shaw, 2005; Hendricks and Sehgal, 2004; Huber et al., 2004). We used PHASE to quantify sleep from DAM-acquired activity data (Chapter 3). PHASE marks any 1-minute data collection bins that were part of a 5-minute (or more) series of bins without activity (IR beam crosses) as sleep bins. Sleep bins are subsequently marked with a 1,

and all other non-sleep bins are marked with a zero. Normalized activity or sleep features across the entire 24-hour LD period, or in Zeitgeber-on or –off portions of the day were compared between genotypes using One-way ANOVA with a Tukey correction for multiple comparisons. Activity anticipation intensities (slopes) were compared between genotypes using One-way ANOVA with a Tukey correction for multiple comparisons.

Genotype	Runs	Rhythmic	Rhythmic N	Period (of Rhythmic flies)
nAChR α1 UAS RNAi (28688)/Clk 856-Gal4	3	91.67%	55	23.79 ± 0.34
nAChR α1 UAS RNAi (28688)/W1118	3	92.59%	50	23.58 ± 0.21
nAChR α2 UAS RNAi (27493)/Clk 856-Gal4	3	77.97%	46	23.71 ± 1.8
nAChR α2 UAS RNAi (27493)/W1118	3	87.72%	50	23.72 ± 1.65
nAChR α3 UAS RNAi (27671)/Clk 856-Gal4	3	74.58%	44	23.65 ± 0.3
nAChR α3 UAS RNAi (27671)/W1118	2	97.73%	43	23.64 ± 0.23
nAChR α3 UAS RNAi (61225)/Clk 856-Gal4	**3**	**33.33%**	**21**	**26.43 ± 1.74**
nAChR α3 UAS RNAi (61225)/W1118	**3**	**95.52%**	**64**	**24.13 ± 0.35**
nAChR α4 UAS RNAi (31985)/Clk 856-Gal4	3	40.98%	25	23.72 ± 1.83
nAChR α4 UAS RNAi (31985)/W1118	3	76.19%	48	23.79 ± 1.74
nAChR α5 UAS RNAi (25943)/Clk 856-Gal4	3	85.00%	51	23.56 ± 0.56
nAChR α5 UAS RNAi (25943)/W1118	3	81.67%	49	23.62 ± 0.24
nAChR α6 UAS RNAi (25835)/Clk 856-Gal4	3	75.00%	48	23.47 ± 0.38
nAChR α6 UAS RNAi (25835)/W1118	3	89.06%	57	23.35 ± 0.6
nAChR α6 UAS RNAi (52885)/Clk 856-Gal4	3	93.33%	56	23.4 ± 0.49
nAChR α6 UAS RNAi (52885)/W1118	3	89.83%	53	23.43 ± 0.29
nAChR α6 UAS RNAi (57818)/Clk 856-Gal4	3	82.26%	51	23.83 ± 0.34
nAChR α6 UAS RNAi (57818)/W1118	3	96.83%	61	23.65 ± 0.31
nAChR α7 UAS RNAi (27251)/Clk 856-Gal4	3	65.52%	38	23.93 ± 1.96
nAChR α7 UAS RNAi (27251)/W1118	3	85.00%	51	23.7 ± 1.62
nAChR α7 UAS RNAi (51049)/Clk 856-Gal4	3	96.72%	59	23.97 ± 2.2
nAChR α7 UAS RNAi (51049)/W1118	3	98.33%	59	23.78 ± 0.31
nAChR β1 UAS RNAi (31883)/Clk 856-Gal4	3	98.31%	58	24.01 ± 1.56
nAChR β1 UAS RNAi (31883)/W1118	3	94.92%	56	23.63 ± 0.28
nAChR β2 UAS RNAi (28038)/Clk 856-Gal4	3	64.41%	38	23.68 ± 0.29
nAChR β2 UAS RNAi (28038)/W1118	3	88.14%	52	23.64 ± 0.32
nAChR β3 UAS RNAi (25927)/Clk 856-Gal4	**3**	**56.36%**	**31**	23.39 ± 0.21
nAChR β3 UAS RNAi (25927)/W1118	**3**	**80.00%**	**48**	23.48 ± 0.21
Clk 856-Gal4/W1118	5	97.17%	103	23.94 ± 1.67

Table 4.1. Summary results from RNAi screen for nAChRs with relevance in circadian behavior.

5-7 day old *CLK856-GAL4* male flies expressing RNAi for *nAChR* subunits or crossed to control line w^{1118} in 12:12 LD entrained conditions for 5 days were released into constant darkness for 14-days. The average rhythmicity, number of rhythmic flies, and periods of rhythmic flies was calculated from three independent behavior experiments. See Materials and Methods for detailed analysis procedure using ClockLab. In **bold**, the alpha3 subunit RNAi selected for physiology and behavior experiments, the beta3 subunit RNAi, and relevant controls.

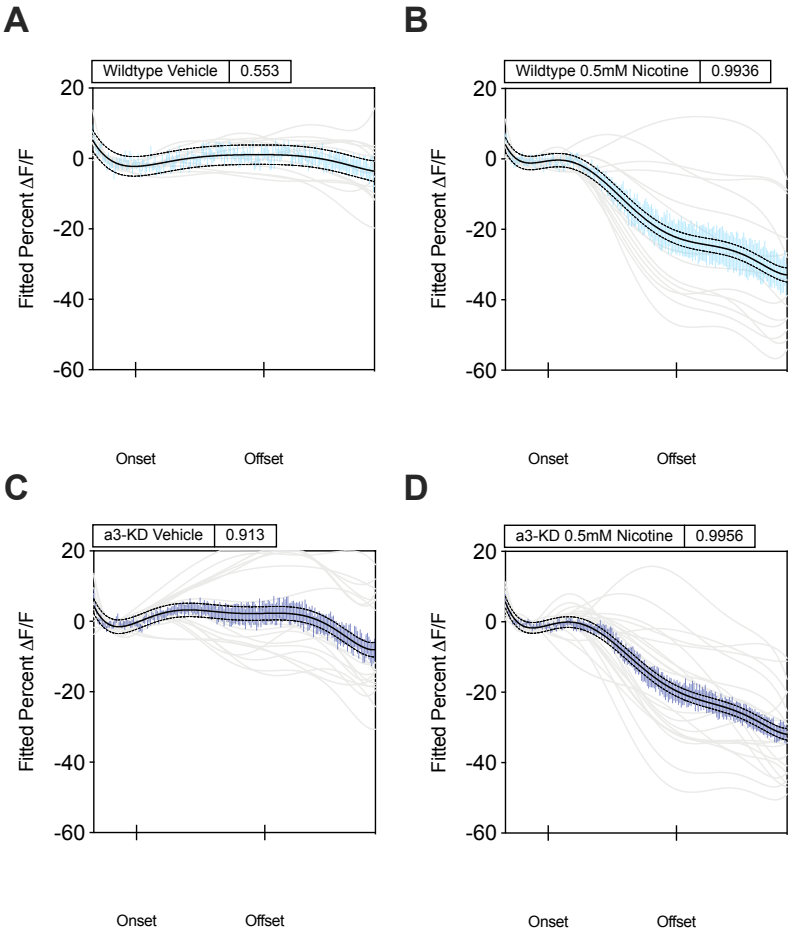

Figure 4.1. Wildtype and nAChRa3 RNAi-expressing LNd ASAP2f fluorescence responses to vehicle or 0.5mM nicotine, 2uM TTX.

Brains were dissected and imaged during ZT4-8 during the day of LD. Data was collected from a minimum of 2 independent crosses on two days of experimentation. Each light grey line represents one LNd with polynomial fitting. The SEM of raw traces (blue) with fitted mean (solid black) and 95% confidence prediction bands (dashed black) is superimposed on each plot. The R^2 for the fitted mean is included on the title of each plot. A, C. Percent deltaF/F LNd responses to vehicle (HL3) with 2uM TTX in wildtype (A) or *nAChRa3* RNAi (C). B, D. Percent deltaF/F LNd responses to 0.5mM nicotine with 2uM TTX in wildtype (B) or n*AChRa3* RNAi (D). Brains, LNds for each plot: A. 5, 15, B. 5, 14, C. 7, 24, D. 7, 23.

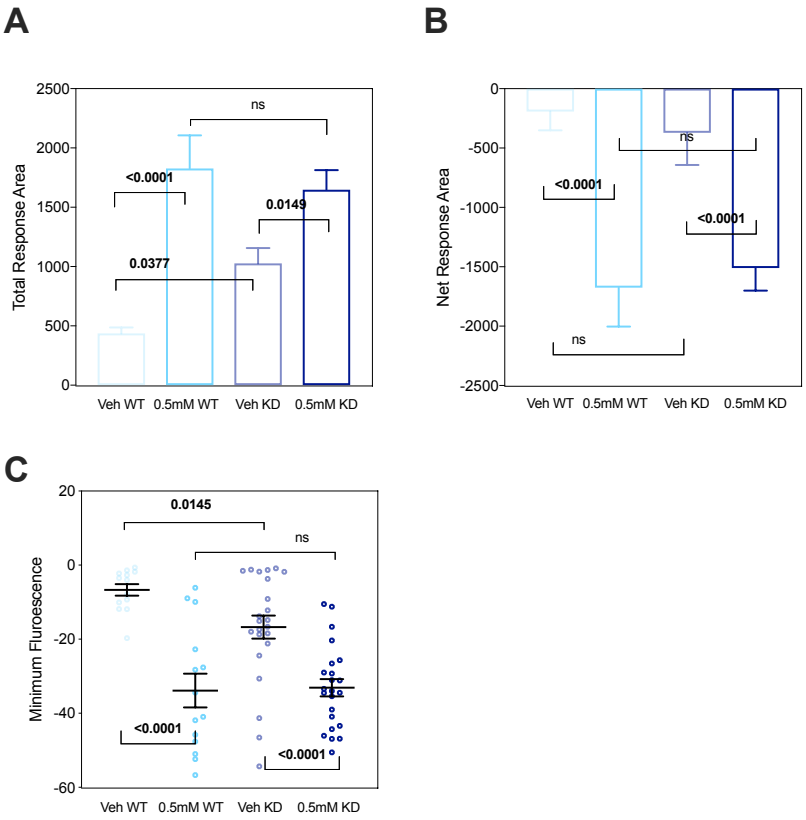

Figure 4.2. Quantification of LNd responses to vehicle or 0.5mM nicotine with 2uM TTX in wildtype (light blue) and nAChRa3 RNAi LNds (dark blue) between ZT4-8 in 12:12LD. All data is quantified from traces in Figure 2 *using the frames during, and after vehicle or nicotine application*. A. Total response area. B. Net area of LNd responses. C. Mean minimum fluorescence of fitted traces. Each dot represents a single LNd's minimum fluorescence. All statistics are calculated using One-way ANOVA with Sidak correction for multiple comparisons between all groups. Significance ($p<0.05$) is reported with actual values when P-value is <0.05. Significant values are bolded.

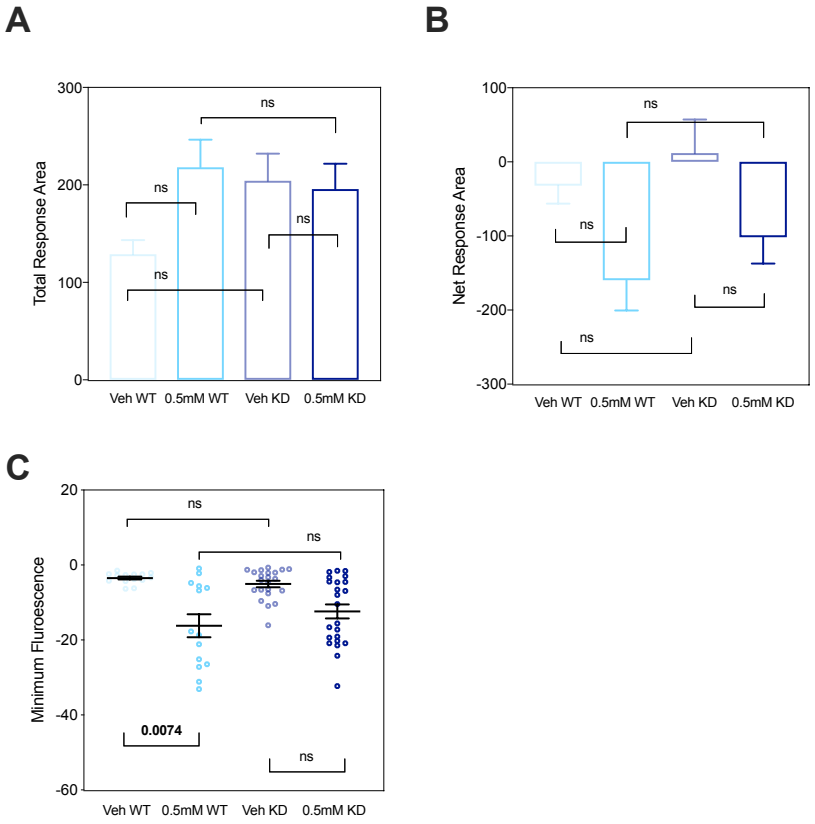

Figure 4.3. Quantification of LNd responses to vehicle or 0.5mM nicotine with 2uM TTX in wildtype (light blue) and nAChRa3 RNAi LNds (dark blue) between ZT4-8 in 12:12LD. All data is quantified from traces in Figure 2 *using only the frames during stimulus*. A. Total response area of traces from LNds during vehicle and nicotine application. B. Net area of LNd responses during application window. C. Minimum fluorescence of fitted traces during application window. Each dot represents a single LNd's minimum fluorescence. All statistics are calculated using One-way ANOVA with Sidak correction for multiple comparisons between all groups. Significance ($p<0.05$) is reported with actual values when P-value is <0.05. Significant values are bolded.

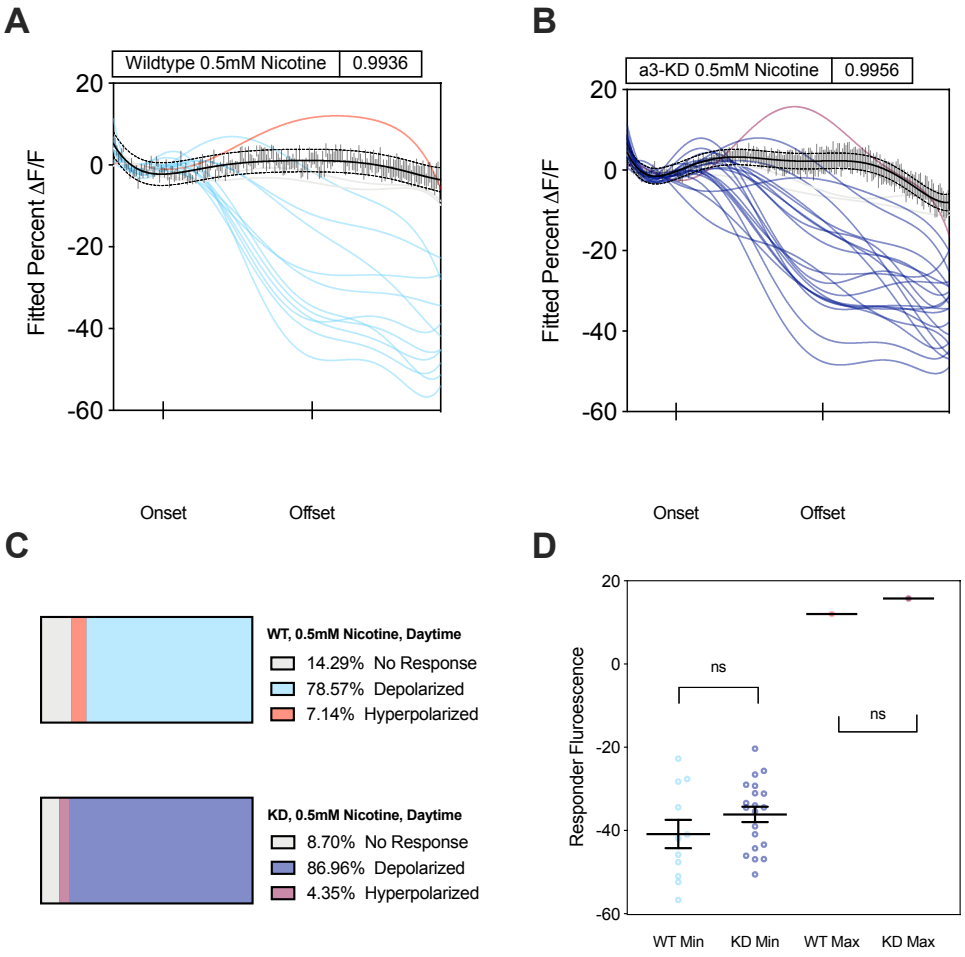

Figure 4.4. Sorting of wildtype and nAChRa3 RNAi-expressing LNd responses to 0.5mM nicotine and vehicle.

See Materials and Methods for sorting methodology. A, B. Visual depiction of sorted responses to 0.5mM nicotine in wildtype (light blue, A) and knockdown (dark blue, B). Non-responding cells are in grey, depolarized cells are in blue, and hyperpolarized cells in red. The relevant day or night vehicle control fitted mean and SEM is superimposed with the LNd traces. C. The percentages of cells in each category and the number of LNds, and brains used in each quantification for each experiment. D. Quantification of maximum and minimum fluorescence values of LNd responses excluding non-responding cells (grey, “no response”). All statistics are calculated using an unpaired t-test with Welch’s correction between each pair. P-values are reported with actual values. Significant P-values (<0.05) are bolded.

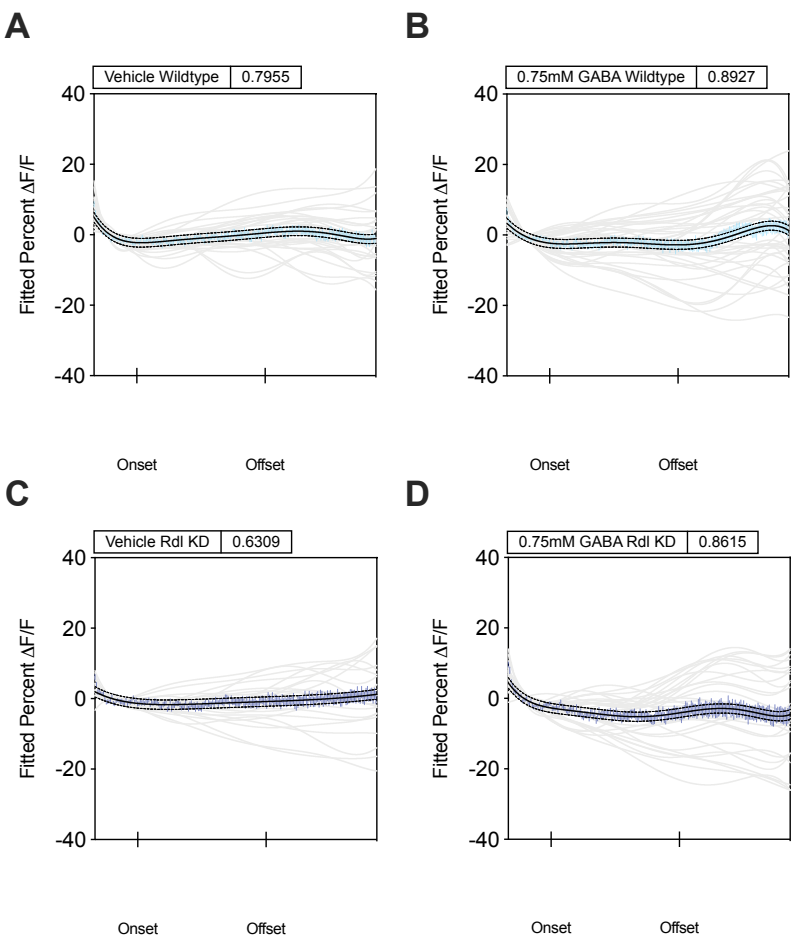

Figure 4.5. Wildtype and Rdl RNAi-expressing LNd responses to vehicle or 0.75mM GABA with 2uM TTX.

Brains were dissected and imaged during ZT14-18 during the night of LD. Data was collected from a minimum of 2 independent crosses on two days of experimentation. Each light grey line represents one LNd with polynomial fitting. The SEM of raw traces (blue) with fitted mean (solid black) and 95% confidence prediction bands (dashed black) is superimposed on each plot. The R^2 for the fitted mean is included on the title of each plot. A, C. Percent deltaF/F LNd responses to vehicle (HL3) with 2uM TTX in wildtype (A) or *Rdl* RNAi (C). B, D. Percent deltaF/F LNd responses to 0.75mM GABA with 2uM TTX in wildtype (B) or *Rdl* RNAi (D). Brains, LNds for each plot: A. 11, 3, B. 11, 40, C. 9, 31, D. 9, 31.

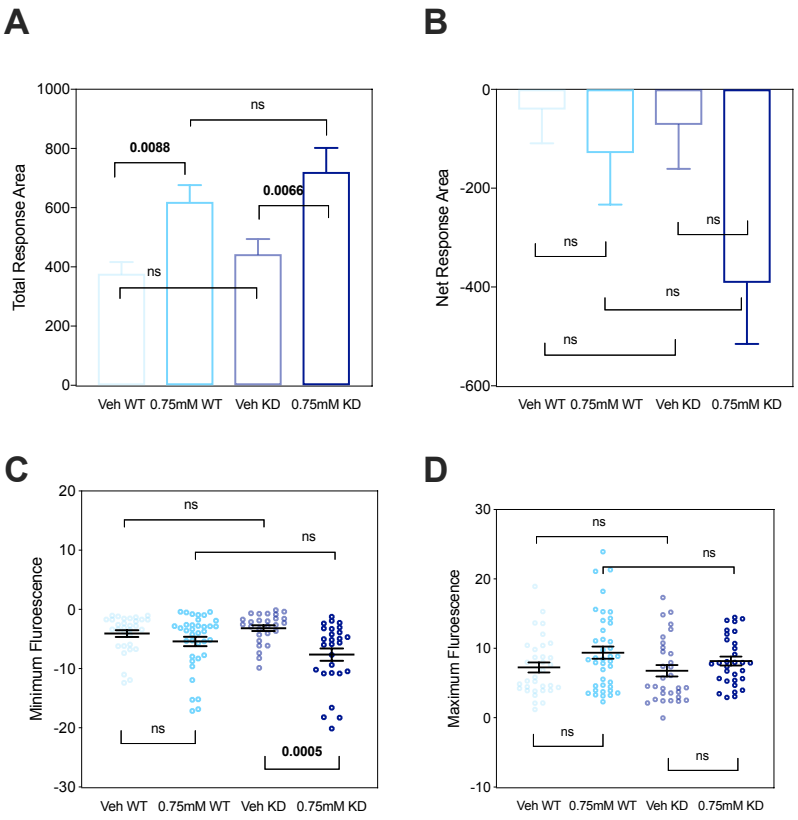

Figure 4.6. Quantification of LNd responses to vehicle or 0.75mM nicotine with 2uM TTX in wildtype (light blue) and Rdl RNAi LNds (dark blue) between ZT14-18 in 12:12LD.
All data is quantified from traces in Figure 6 using the frames during, and after vehicle or GABA application. A. Total response area. B. Net area of LNd responses. C. Minimum fluorescence of fitted traces. Each dot represents a single LNd's minimum fluorescence. D. Maximum fluorescence of fitted traces. Each dot represents a single LNd's maximum fluorescence. All statistics are calculated using One-way ANOVA with Sidak correction for multiple comparisons between all groups. Significance ($p<0.05$) is reported with actual values when P-value is <0.05. Significant values are bolded.

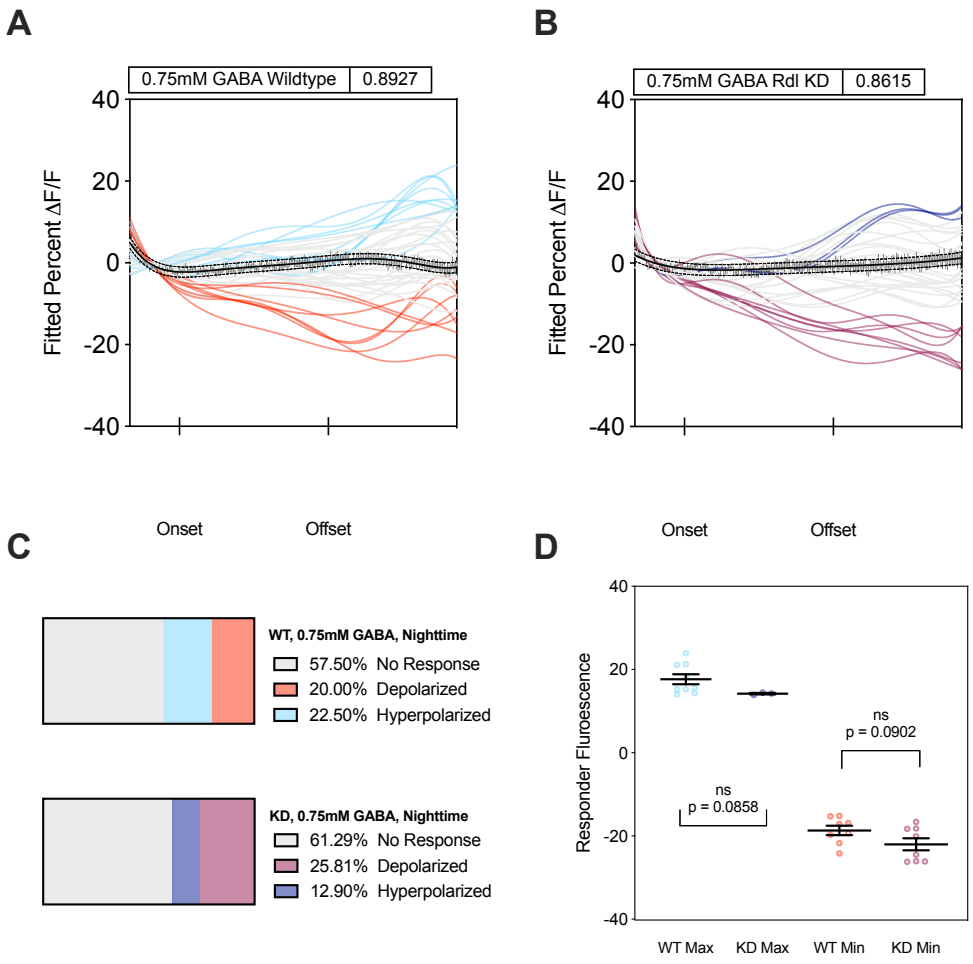

Figure 4.7. Sorted wildtype and Rdl RNAi-expressing LNd responses to 0.75mM GABA and vehicle.

See Materials and Methods for sorting methodology. A, B. Visual depiction of sorted responses to 0.75mM GABA in wildtype (light blue, A) and *Rdl* knockdown LNds (dark blue, B). Non-responding cells are in grey, depolarized cells are in red, and hyperpolarized cells in blue. The relevant day or night vehicle control fitted mean and SEM is superimposed with the LNd traces. C. The percentages of cells in each category and the number of LNds, and brains used in each quantification for each experiment. D. Quantification of maximum and minimum fluorescence values of LNd responses excluding non-responding cells (grey, “no response”). All statistics are calculated using an unpaired t-test with Welch’s correction between each pair. P-values are reported with actual values. Significant P-values (<0.05) are bolded.

First 4 Days				
Genotype	Runs	Rhythmic	Rhythmic N	Period (of Rhythmic flies)
MB122B>nAChRa3 RNAi	2	80.65%	25	24.30 ± 0.11
MB122B-GAL4/+	2	87.50%	49	24.64 ± 0.09
nAChRa3 RNAi (61225)/+	2	97.56%	40	24.03 ± 0.03
Clk856-GAL4>nAChRa3 RNAi	1	15.38%	2	27.17 ± 0.42
Clk856-GAL4/+	1	87.10%	27	23.95 ± 0.09
nACHRa3-RNAi (61225)/+	1	51.61%	16	23.97 ± 0.04
Last 4 Days				
Genotype	Runs	Rhythmic	Rhythmic N	Period (of Rhythmic flies)
MB122B>nAChRa3 RNAi	2	42.86%	12	23.25 ± 0.49
MB122B-GAL4/+	2	70.27%	26	24.06 ± 0.11
nAChRa3 RNAi (61225)/+	2	66.67%	24	23.76 ± 0.19
Clk856-GAL4>nAChRa3 RNAi	1	9.10%	1	24.00 ± 0.00
Clk856-GAL4/+	1	48.28%	14	23.61 ± 0.09
nACHRa3-RNAi (61225)/+	1	46.43%	13	23.62 ± 0.13
All 14 Days				
Genotype	Runs	Rhythmic	Rhythmic N	Period (of Rhythmic flies)
MB122B>nAChRa3 RNAi	2	100%	28	24.09 ± 0.04
MB122B-GAL4/+	2	97.30%	36	24.39 ± 0.08
nAChRa3 RNAi (61225)/+	2	100%	36	23.88 ± 0.05
Clk856-GAL4>nAChRa3 RNAi	1	72.73%	8	28.50 ± 1.00
Clk856-GAL4/+	1	100%	29	23.83 ± 0.08
nACHRa3-RNAi (61225)/+	1	100%	28	23.77 ± 0.05

Table 4.2. Summary of the average rhythmicity, number of rhythmic flies, and periods of rhythmic flies in behavioral experiments with GAL4-driven nAChRa3 RNAi.
See Materials and Methods for detailed analysis procedure using ClockLab.

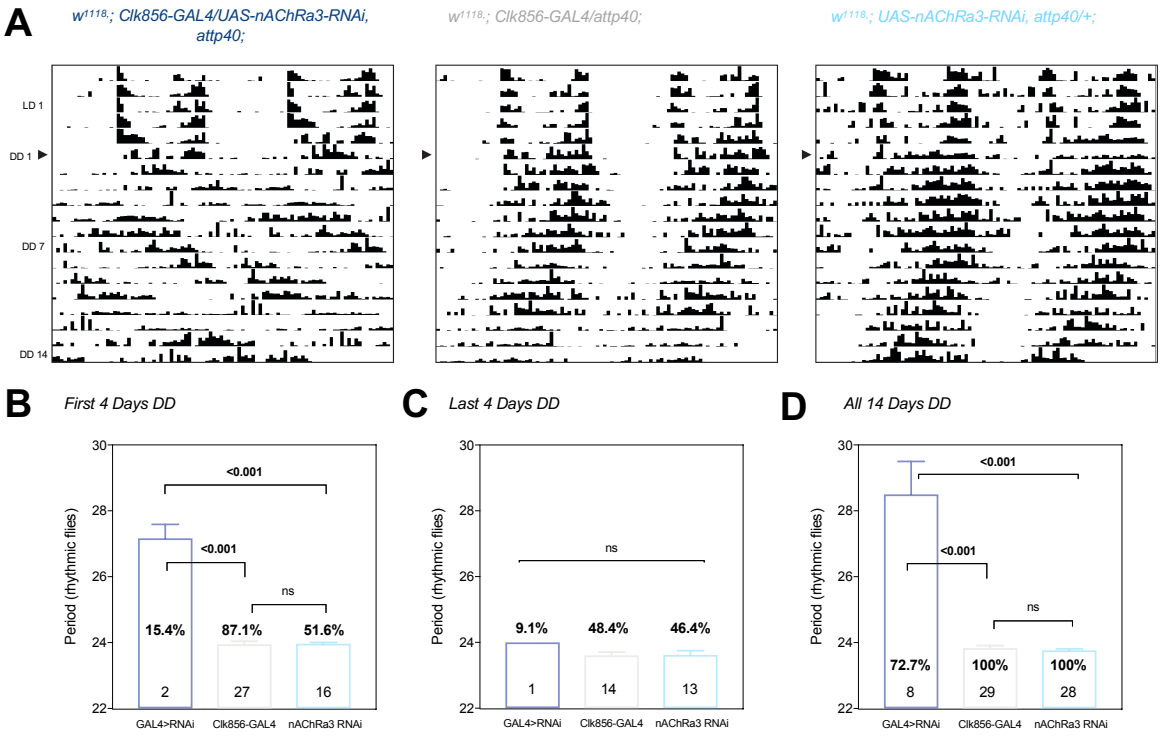

Figure 4.8. Nicotinic receptivity in the entire clock neuron network contributes to endogenous timekeeping periodicity and rhythmicity in constant conditions.
A-D. 2-5 day old male flies expressing RNAi under control of *CLK856-GAL4* (dark blue), or control lines (grey and light blue) crossed to appropriate background were entrained for two days to 12:12 LD cycles in constant temperature. After 6 days of LD, flies were released in to constant darkness and temperature (DD) for 14 days. A. Representative actograms spanning the entire behavior run for each genotype. B-D. Periodicity of rhythmic flies for the first 4 days (B), last 4 days (C) or all days (D) of DD. Percent rhythmicity for each genotype is reported at the bottom of each bar. A summary of the number, and rhythmic power of flies in each calculation is included in Supplemental Table 2. Data represents one experimental replicate. Error bars on histograms represent SEM between flies. All statistics are calculated using One-way ANOVA with Tukey's correction for multiple comparisons between all groups. Actual P-values are reported and bolded for values with significance less than 0.05. Values greater than 0.05 are reported as "ns" or non-significant.

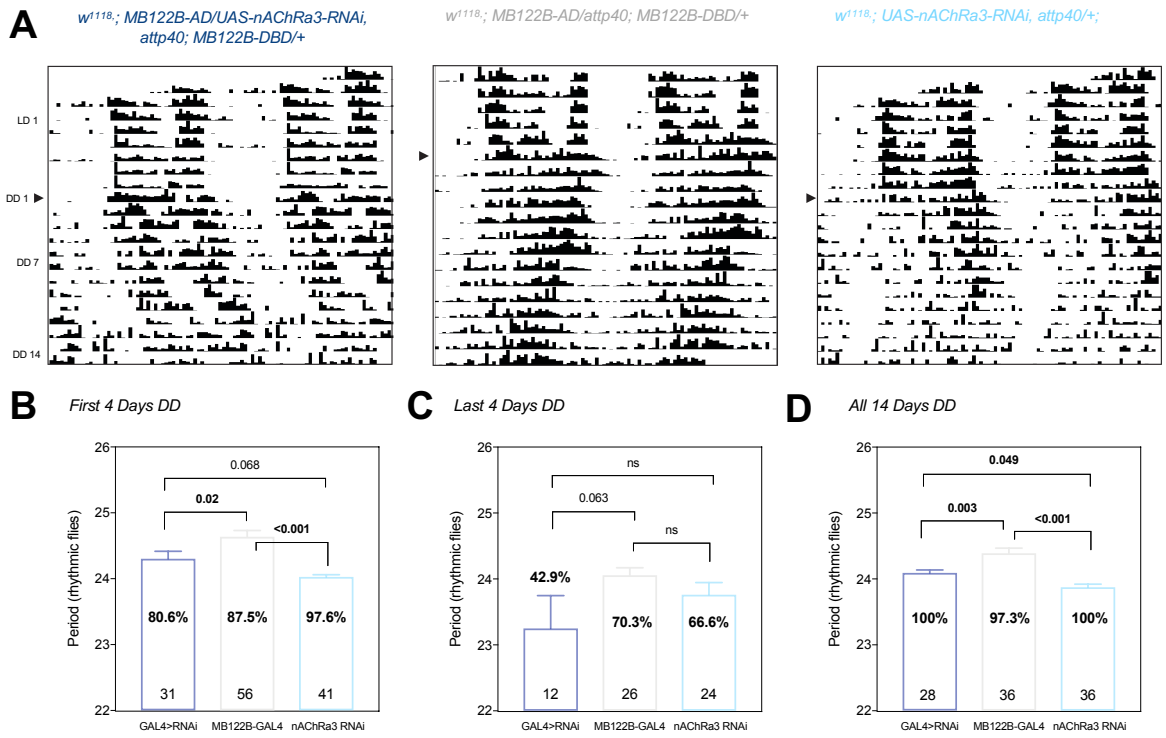

Figure 4.9. Cholinergic signaling to the CRY+ LNds contributes marginally to the clock network's endogenous timekeeping periodicity and rhythmicity in constant conditions.
A-D. 2-5 day old male flies expressing RNAi under control of *MB122B-GAL4* (dark blue), or control lines (grey and light blue) crossed to appropriate background were entrained for two days to 12:12 LD cycles in constant temperature. After 6 days of LD, flies were released in to constant darkness and temperature (DD) for 14 days. A. Representative actograms spanning the entire behavior run for each genotype. B-D. Periodicity of rhythmic flies for the first 4 days (B), last 4 days (C) or all days (D) of DD. Percent rhythmicity for each genotype is reported at the bottom of each bar. A summary of the number, and rhythmic power of flies in each calculation is included in Supplemental Table 2. Data represents one experimental replicate. Error bars on histograms represent SEM between flies. All statistics are calculated using One-way ANOVA with Tukey's correction for multiple comparisons between all groups. Actual P-values are reported and bolded for values with significance less than 0.05. Values greater than 0.05 are reported as "ns" or non-significant.

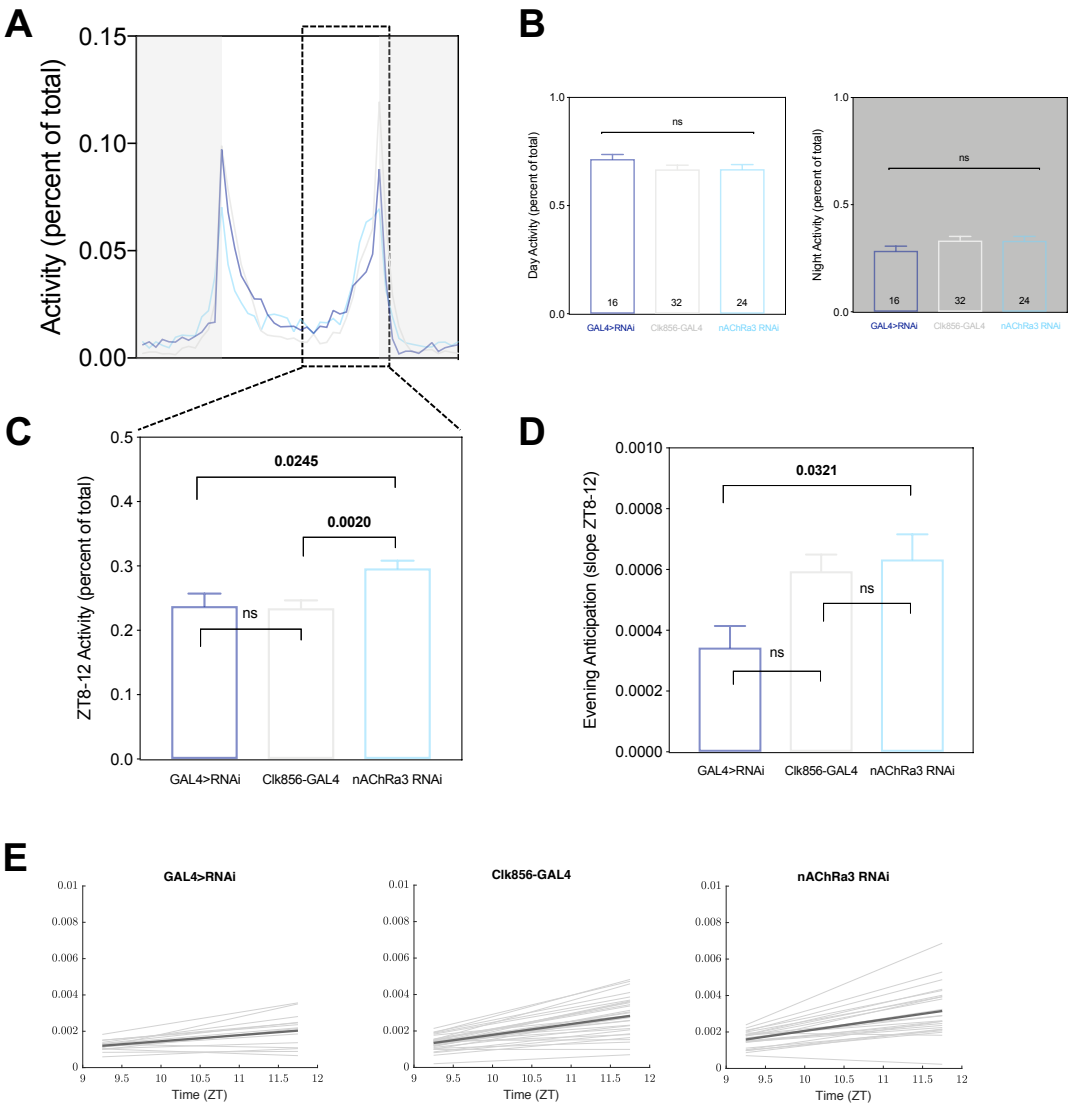

Figure 4.10. Nicotinic signaling to the clock neuron network promotes evening anticipatory activity, and acute sensory "startle" responses to lights-off transitions.

A-D. 2-5 day old male flies were entrained for two days to 12:12 LD cycles in constant temperature. All data in figure is sourced from the first 3 entrained days of 12:12 LD. A. Average normalized (IR beam crosses per bin/total beam crosses in period) daily activity for the first 3 entrained days of 12:12 LD of flies expressing *nAChRa3* RNAi under the control of *CLK856-GAL4* (dark blue), GAL4 control (grey) and RNAi control (light blue). Solid line represents activity mean averaged first by days, then by flies. SEM between experimental replicates is shaded above and below each mean line. B. Average normalized IR beam crosses (raw counts) in each 30min bin during the day (left) or night (right) portions of 3 days in 12:12 LD cycle. C. Average of 3 LD days' IR normalized beam crosses in each 30min bin between ZT8 and ZT12. D. The mean of each genotypes' morning anticipation slope. Slopes are determined by projecting a best-fit line through each flies' 3 days average 1-min activity data in the 4 hours leading up to lights off (ZT8 to ZT 12). E. Visual representation of evening anticipation slope (ZT8 to ZT12, X-axis) . Light grey lines are individual fly slopes and dark lines are the mean slope for each genotype. Data in figure represents one experimental replicate. Error bars on histograms represent SEM between individual flies. All statistics are calculated using One-way ANOVA with Tukey's correction for multiple comparisons between all groups. Actual P-values are reported for values with significance less than 0.05. Values greater than 0.05 are reported as "ns" or non-significant. N for each group is reported in (B) : 16, GAL4>RNAi, 32, GAL4, 24, RNAi.

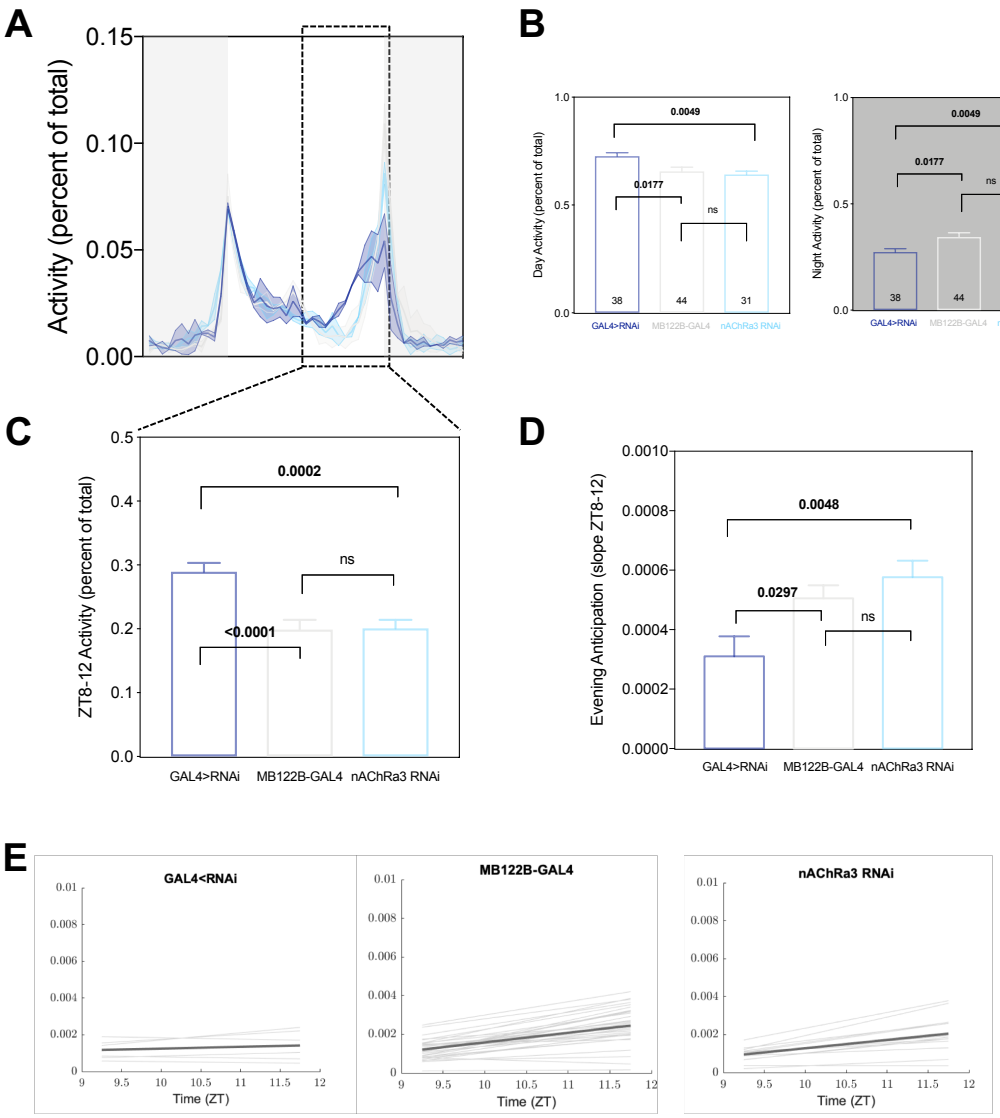

Figure 4.11. Nicotinic signaling to the CRY+ LNds contributes to overall activity levels during the day, but does not solely direct, evening anticipatory activity, and acute sensory "startle" responses to lights-off transitions.

A-D. 2-5 day old male flies were entrained for two days to 12:12 LD cycles in constant temperature. All data in figure is sourced from the first 3 entrained days of 12:12 LD. A. Average normalized (IR beam crosses per bin/total beam crosses in period) daily activity for the first 3 entrained days of 12:12 LD of flies expressing *nAChRa3* RNAi under the control of *MB122B-GAL4* (dark blue), GAL4 control (grey) and RNAi control (light blue). Solid line represents activity mean averaged first by days, then by flies. SEM between experimental replicates is shaded above and below each mean line. B. Average normalized IR beam crosses (raw counts) in each 30min bin during the day (left) or night (right) portions of 3 days in 12:12 LD cycle. C. Average of 3 LD days' IR normalized beam crosses in each 30min bin between ZT8 and ZT12. D. The mean of each genotypes' morning anticipation slope. Slopes are determined by projecting a best-fit line through each flies' 3 days average 1-min activity data in the 4 hours leading up to lights off (ZT8 to ZT12). E. Visual representation of evening anticipation slope (ZT8 to ZT12, X-axis) . Light grey lines are individual fly slopes and dark lines are the mean slope for each genotype. Data in figure represents two experimental replicates. Error bars on histograms represent SEM between individual flies. All statistics are calculated using One-way ANOVA with Tukey's correction for multiple comparisons between all groups. Actual P-values are reported for values with significance less than 0.05. Values greater than 0.05 are reported as "ns" or non-significant. N for each group is reported in (B) : 38, GAL4>RNAi, 44, GAL4, 31, RNAi.

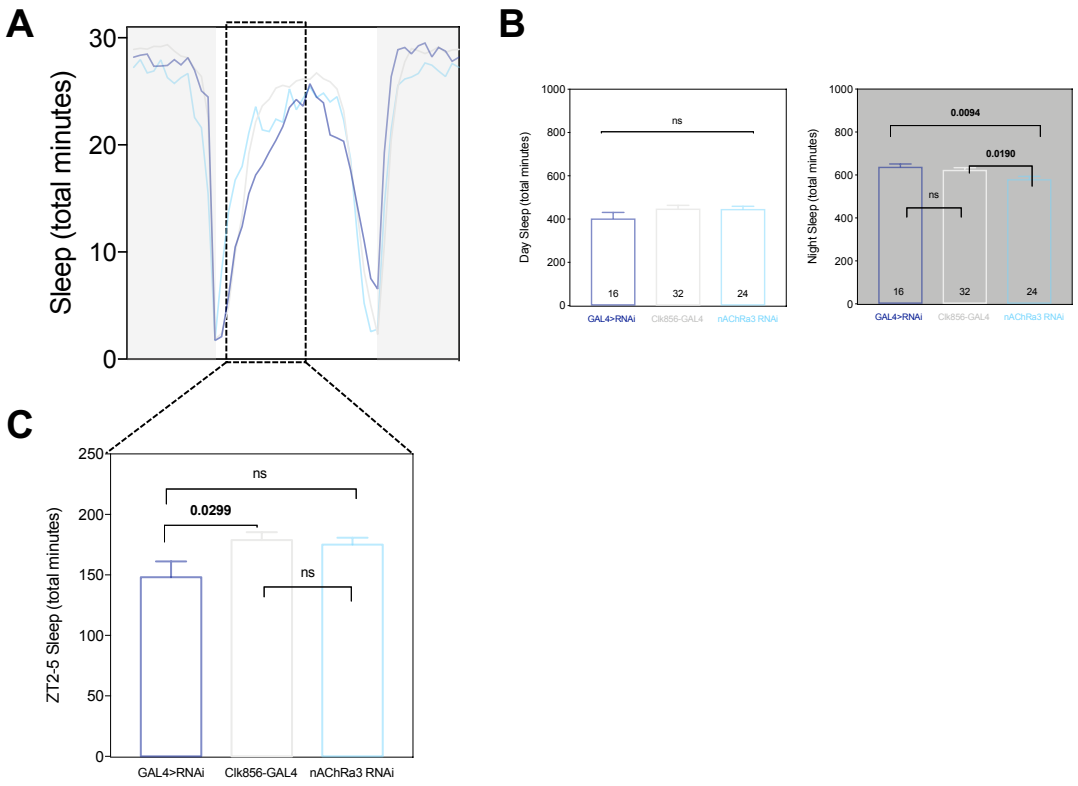

Figure 4.12. Nicotinic signaling to the clock network does not contribute to sleep coordination.

A-C. 2-5 day old male flies were entrained for two days to 12:12 LD cycles in constant temperature. All data in figure is sourced from the first 3 entrained days of 12:12 LD. A. Average sleep per 30-min bin for the first 3 entrained days of 12:12 LD of flies expressing *nAChRa3* RNAi under the control of *Clk856-GAL4* (blue), GAL4 control (grey) and RNAi control (light blue). Solid line represents sleep mean averaged first by days, then by flies. SEM is shaded above and below each mean line. B. The average of 3 days sleep during the day or night portions of the 12:12 LD cycle. The effective maximum for each 12 hour portion for a single day is 720 minutes. C. The average of 3 days sleep in each 30min bin between ZT2 and ZT5. Figure data is sourced from one experimental replicate. Error bars on histograms represent SEM between individual flies. All statistics are calculated using One-way ANOVA with Tukey's correction for multiple comparisons between all groups. Actual P-values are reported for values with significance less than 0.05. Values greater than 0.05 are reported as "ns" or non-significant. N for each group is reported in (B) : 16, GAL4>RNAi, 32, GAL4, 24, RNAi.

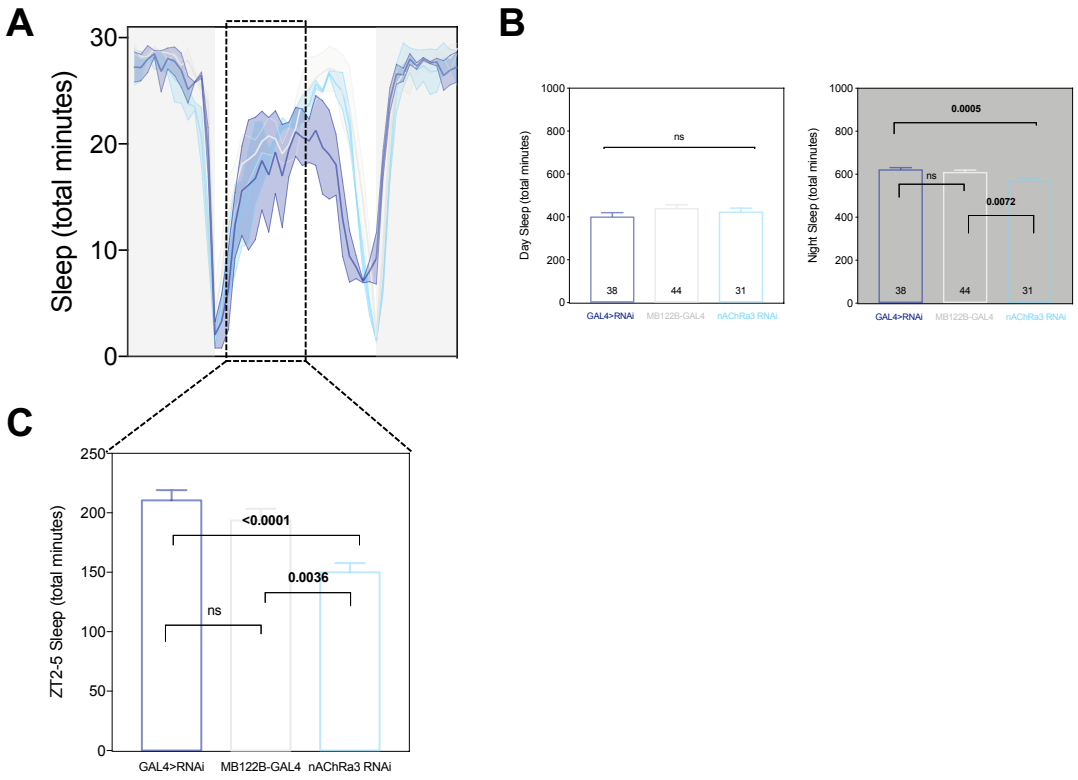

Figure 4.13. Nicotinic signaling to the CRY+ LNds does not significantly contribute to sleep behavior.

A-C. 2-5 day old male flies were entrained for two days to 12:12 LD cycles in constant temperature. All data in figure is sourced from the first 3 entrained days of 12:12 LD. A. Average sleep per 30-min bin for the first 3 entrained days of 12:12 LD of flies expressing *nAChRa3* RNAi under the control of *MB122B-GAL4* (blue), GAL4 control (grey) and RNAi control (light blue). Solid line represents sleep mean averaged first by days, then by flies. SEM is shaded above and below each mean line. B. The average of 3 days sleep during the day or night portions of the 12:12 LD cycle. The effective maximum for each 12 hour portion for a single day is 720 minutes. C. The average of 3 days sleep in each 30min bin between ZT2 and ZT5. Figure data is sourced from two experimental replicates. Error bars on histograms represent SEM between individual flies. All statistics are calculated using One-way ANOVA with Tukey's correction for multiple comparisons between all groups. Actual P-values are reported for values with significance less than 0.05. Values greater than 0.05 are reported as "ns" or non-significant. N for each group is reported in (B) : 38, GAL4>RNAi, 44, GAL4, 31, RNAi.

First 4 Days				
Genotype	Runs	Rhythmic	Rhythmic N	Period (of Rhythmic flies)
MB122B>Rdl RNAi	2	77.14%	27	23.76 ± 0.08
MB122B-GAL4/+	2	95.12%	39	23.60 ± 0.05
Rdl(8-10J) RNAi/+	2	91.53%	54	23.82 ± 0.06
Clk856-GAL4>Rdl RNAi	2	95.56%	86	23.81 ± 0.07
Clk856-GAL4/+	2	90.48%	76	23.84 ± 0.04
Rdl(8-10J) RNAi/+	2	96.10%	74	23.73 ± 0.05
Last 4 Days				
Genotype	Runs	Rhythmic	Rhythmic N	Period (of Rhythmic flies)
MB122B>Rdl RNAi	2	77.42%	24	23.25 ± 0.13
MB122B-GAL4/+	2	14.29%	4	23.32 ± 0.11
Rdl(8-10J) RNAi/+	2	74.47%	35	23.41 ± 0.12
Clk856-GAL4>Rdl RNAi	2	77.78%	63	23.26 ± 0.06
Clk856-GAL4/+	2	80%	56	23.37 ± 0.06
Rdl(8-10J) RNAi/+	2	64.52%	40	23.51 ± 0.15
All 14 Days				
Genotype	Runs	Rhythmic	Rhythmic N	Period (of Rhythmic flies)
MB122B>Rdl RNAi	2	90.32%	28	23.43 ± 0.04
MB122B-GAL4/+	2	100%	4	23.37 ± 0.04
Rdl(8-10J) RNAi/+	2	95.83%	45	23.54 ± 0.48
Clk856-GAL4>Rdl RNAi	2	98.77%	80	23.36 ± 0.16
Clk856-GAL4/+	2	88.57%	62	23.62 ± 0.04
Rdl(8-10J) RNAi/+	2	100%	62	23.58 ± 0.06

Table 4.3. Summary of the average rhythmicity, number of rhythmic flies, and periods of rhythmic flies in behavioral experiments with GAL4-driven Rdl RNAi.
See Materials and Methods for detailed analysis procedure using ClockLab.

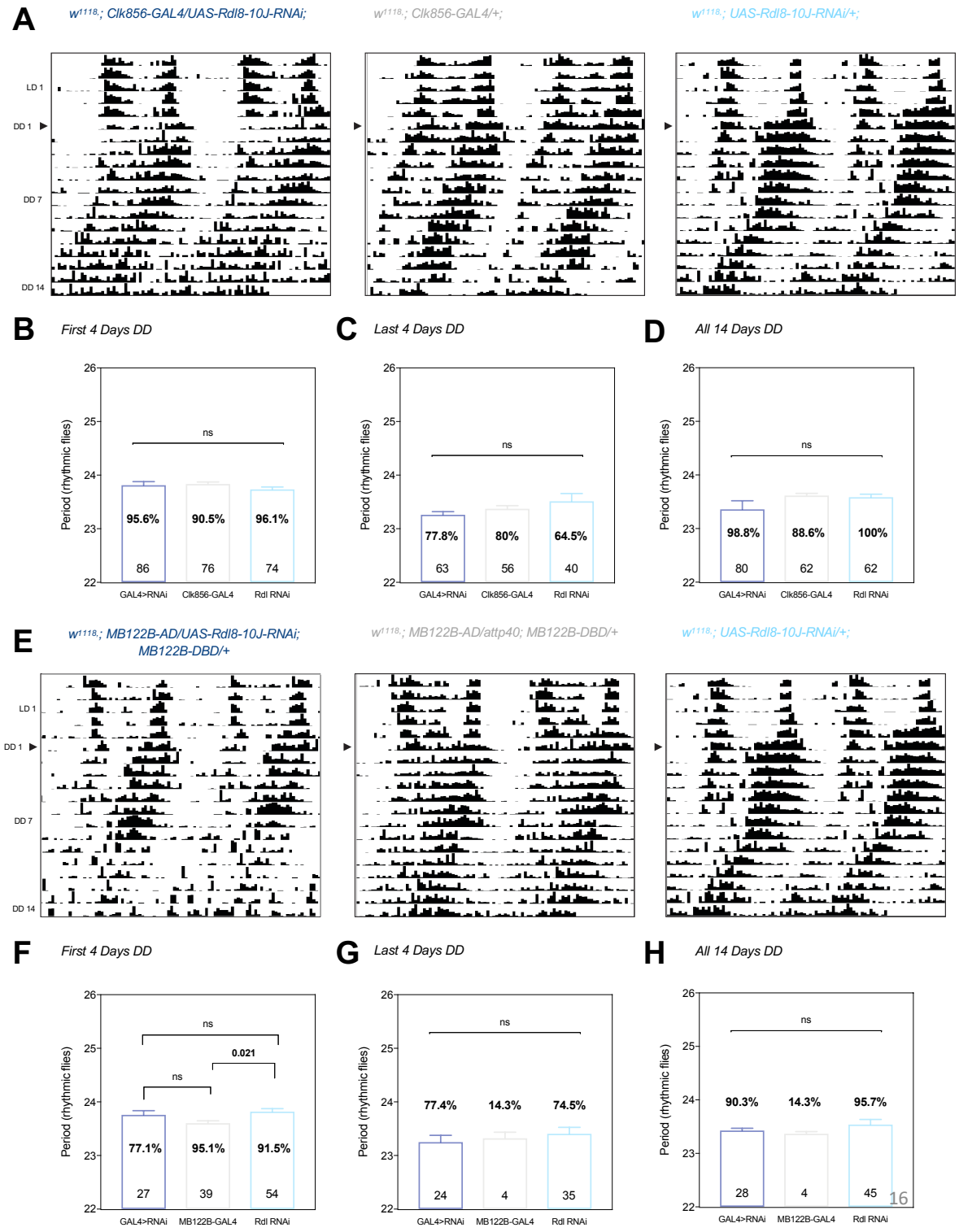

Figure 4.14. GABAergic signaling through receptor subunit Rdl is not essential in the clock network, or CRY+ LNds to maintain behavioral periodicity and rhythmicity in constant conditions.

A-H. 2-5 day old male flies expressing *Rdl* RNAi under control of *Clk856-GAL4* or *MB122B-GAL4* (dark blue), or control lines (grey and light blue) crossed to appropriate background were entrained for two days to 12:12 LD cycles in constant temperature. After 6 days of LD, flies were released in to constant darkness and temperature (DD) for 14 days. A, E. Representative actograms spanning the entire behavior run for each genotype. B-D, F-H. Periodicity of rhythmic flies for the first 4 days (B, F), last 4 days (C, G) or all days (D, H) of DD. Percent rhythmicity for each genotype is reported at the bottom of each bar. A summary of the number, and rhythmic power of flies in each calculation is included in Supplemental Table 2. Data represents one experimental replicate. Error bars on histograms represent SEM. All statistics are calculated using One-way ANOVA with Tukey's correction for multiple comparisons between all groups. Actual P-values are reported and bolded for values with significance less than 0.05. Values greater than 0.05 are reported as "ns" or non-significant.

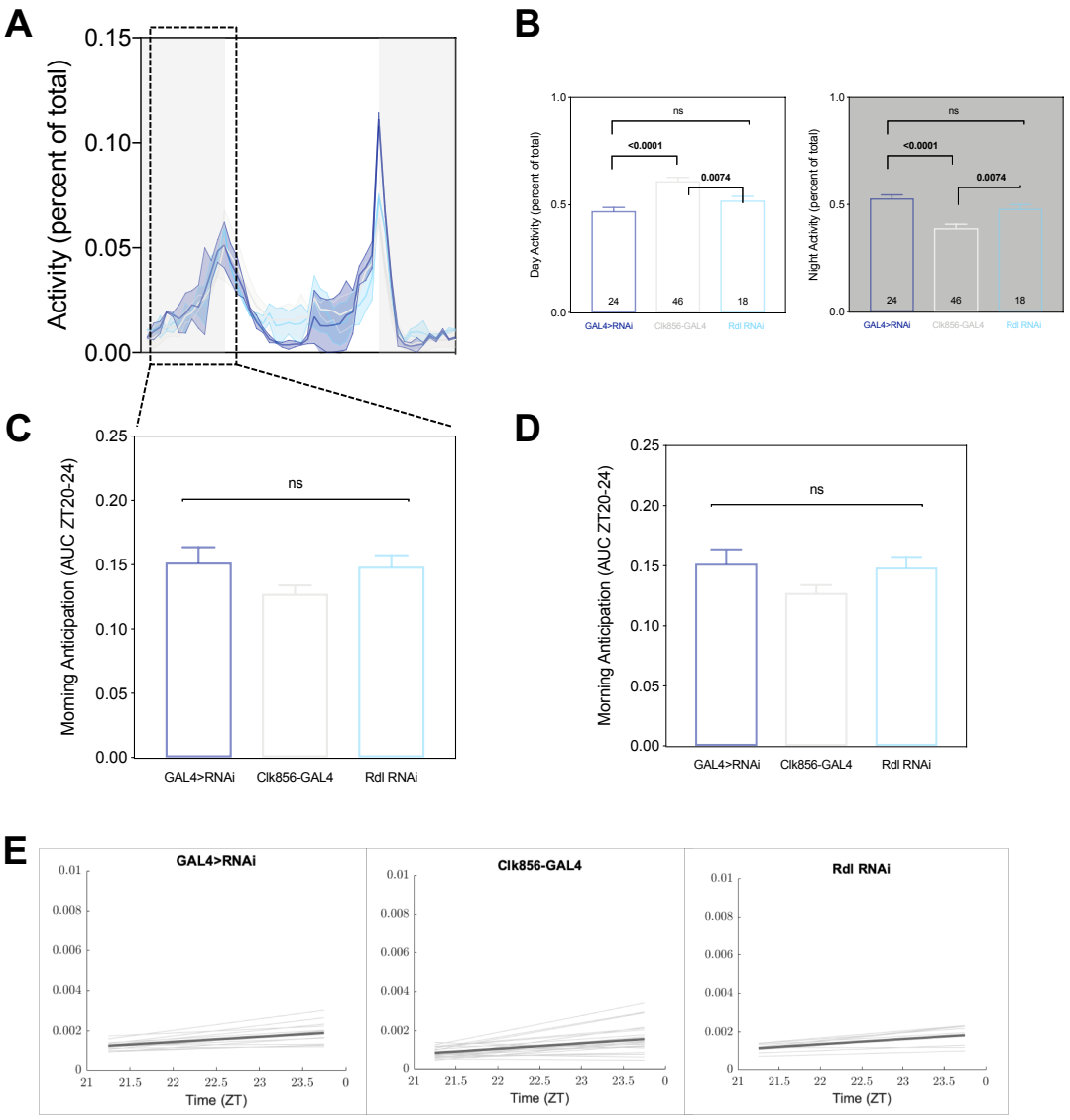

Figure 4.15. GABAergic signaling to the clock network promotes day activity during the day and night.

A-D. 2-5 day old male flies were entrained for two days to 12:12 LD cycles in constant temperature. All data in figure is sourced from the first 3 entrained days of 12:12 LD. A. Average normalized (IR beam crosses per bin/total beam crosses in period) daily activity for the first 3 entrained days of 12:12 LD of flies expressing *Rdl* RNAi under the control of *Clk856-GAL4* (dark blue), GAL4 control (grey) and RNAi control (light blue). Solid line represents activity mean averaged first by days, then by flies. SEM between experimental replicates is shaded above and below each mean line. B. Average normalized IR beam crosses (raw counts) in each 30min bin during the day (left) or night (right) portions of 3 days in 12:12 LD cycle. C. Average of 3 LD days normalized beam crosses in each 30min bin between ZT22 and ZT2. D. The mean of each genotypes' morning anticipation slope. Slopes are determined by projecting a best-fit line through each flies' 3 days average 1-min activity data in the 4 hours leading up to lights on (ZT21 to ZT0/24). E. Visual representation of evening anticipation slope. Light grey lines are individual fly slopes and dark lines are the mean slope for each genotype. Data in figure represents two experimental replicates. Error bars on histograms represent SEM between individual flies. All statistics are calculated using One-way ANOVA with Tukey's correction for multiple comparisons between all groups. Actual P-values are reported for values with significance less than 0.05. Values greater than 0.05 are reported as "ns" or non-significant. N for each group is reported in (B) : 24, GAL4>RNAi, 46, GAL4, 18, RNAi.

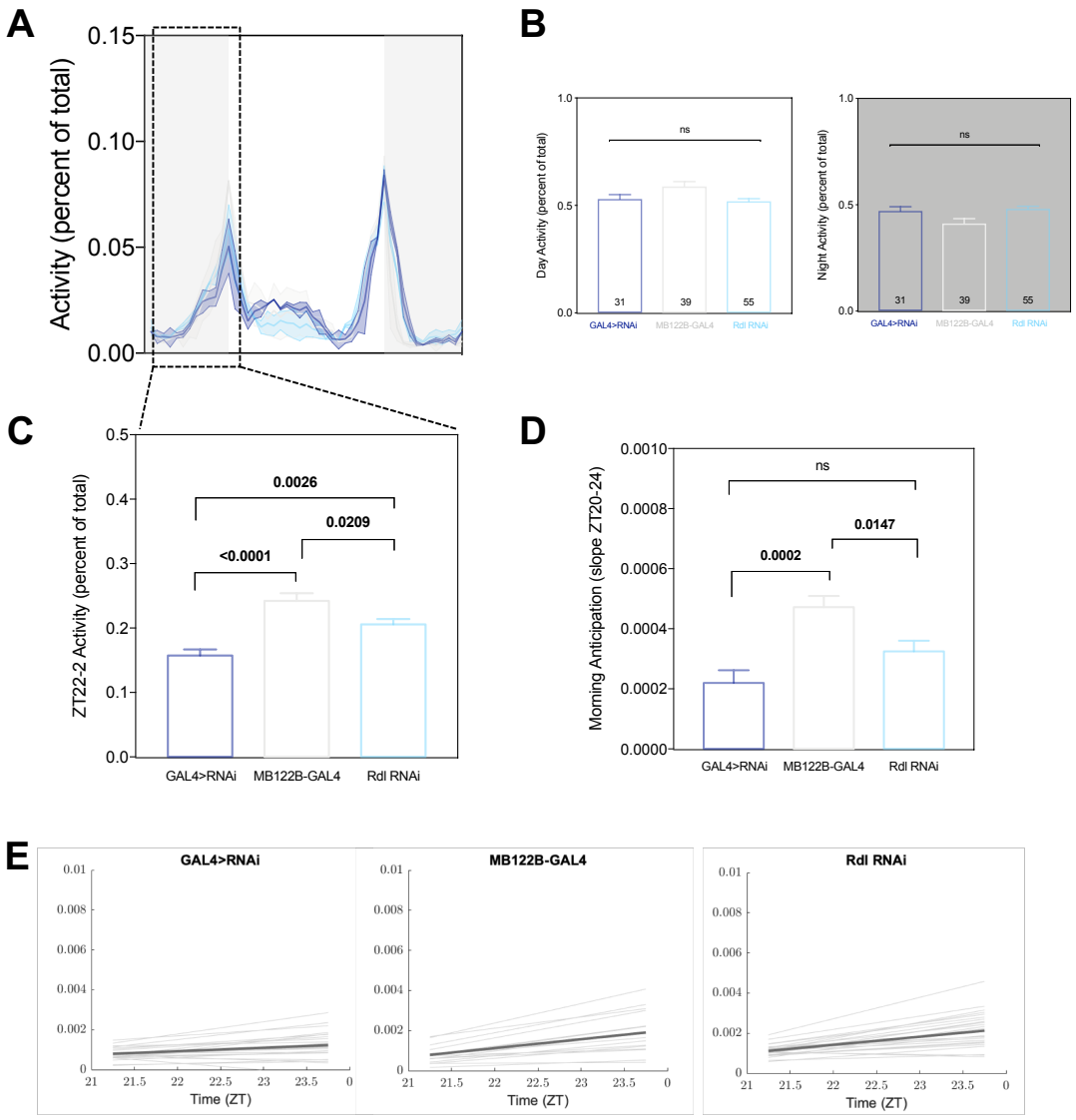

Figure 4.16. Receptivity in the LNds to GABAergic signals through Rdl promotes morning anticipatory behavior, and acute sensory activity response to night-day transition.

A-D. 2-5 day old male flies were entrained for two days to 12:12 LD cycles in constant temperature. All data in figure is sourced from the first 3 entrained days of 12:12 LD. A. Average normalized (IR beam crosses per bin/total beam crosses in period) daily activity for the first 3 entrained days of 12:12 LD of flies expressing *Rdl* RNAi under the control of *MB122B-GAL4* (dark blue), GAL4 control (grey) and RNAi control (light blue). Solid line represents activity mean averaged first by days, then by flies. SEM between experimental replicates is shaded above and below each mean line. B. Average normalized IR beam crosses (raw counts) in each 30min bin during the day (left) or night (right) portions of 3 days in 12:12 LD cycle. C. Average of 3 LD days normalized beam crosses in each 30min bin between ZT22 and ZT2. D. The mean of each genotypes' morning anticipation slope. Slopes are determined by projecting a best-fit line through each flies' 3 days average 1-min activity data in the 4 hours leading up to lights on (ZT21 to ZT0/24). E. Visual representation of evening anticipation slope. Light grey lines are individual fly slopes and dark lines are the mean slope for each genotype. Data in figure represents two experimental replicates. Error bars on histograms represent SEM between individual flies. All statistics are calculated using One-way ANOVA with Tukey's correction for multiple comparisons between all groups. Actual P-values are reported for values with significance less than 0.05. Values greater than 0.05 are reported as "ns" or non-significant. N for each group is reported in (B) : 31, GAL4>RNAi, 39, GAL4, 55, RNAi.

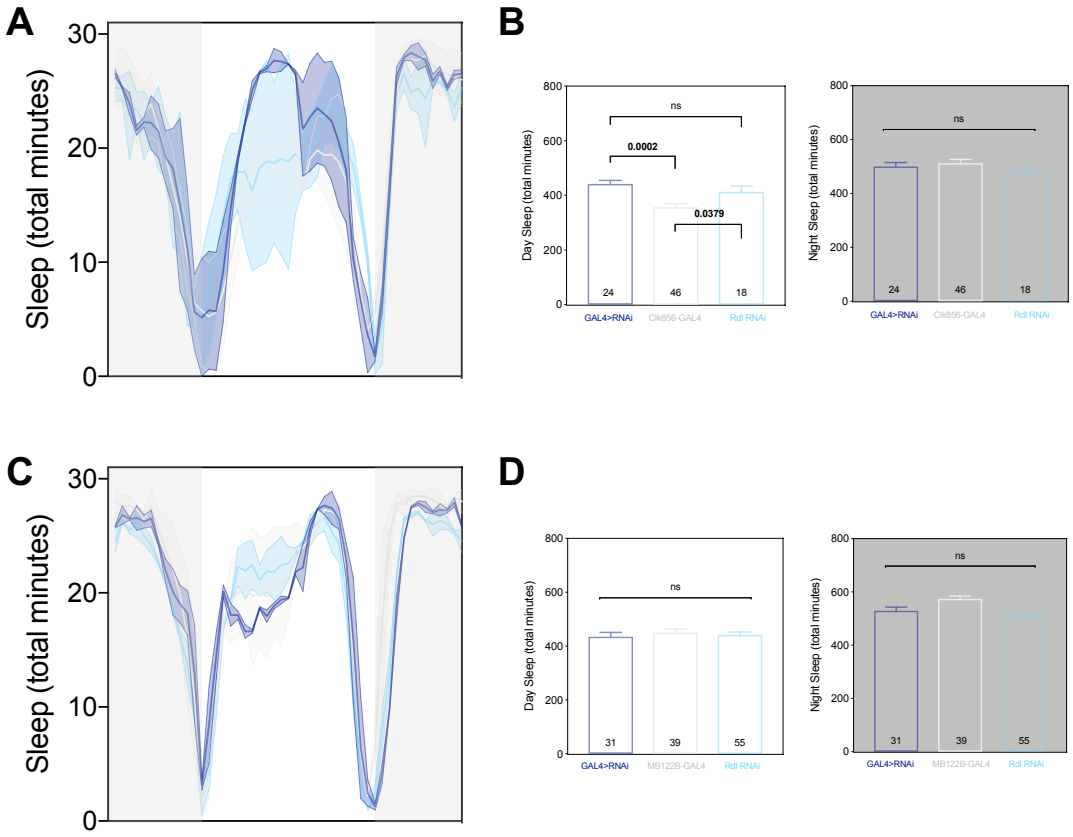

Figure 4.17. GABAergic signaling to the clock network through receptor subunit Rdl has marginal effects on day sleep, but not specifically through the CRY+ LNds.
A, C. Average sleep per 30-min bin for the first 3 entrained days of 12:12 LD of flies expressing *Rdl* RNAi under the control of *Clk856-GAL4* or *MB122B-GAL4* (dark blue), GAL4 controls (grey) and RNAi controls (light blue). Solid line represents sleep mean averaged first by days, then by flies. SEM between experimental replicates is shaded above and below each mean line. B, D. The average of 3 days sleep during the day or night portions of the 12:12 LD cycle. The effective maximum for each 12 hour portion for a single day is 720 minutes. C. The average of 3 days sleep in each 30min bin between ZT2 and ZT5. Figure data is sourced from two experimental replicates. Error bars on histograms represent SEM between individual flies. All statistics are calculated using One-way ANOVA with Tukey's correction for multiple comparisons between all groups. Actual P-values are reported for values with significance less than 0.05. Values greater than 0.05 are reported as "ns" or non-significant. N for each group is reported in (B) and (D). For *CLK856-GAL4* experiments: 24, GAL4>RNAi, 46, GAL4, 18, RNAi. For *MB122B-GAL4* experiments: 31, GAL4>RNAi, 39, GAL4, 55, RNAi.

References

Abruzzi, K.C., Zadina, A., Luo, W., Wiyanto, E., Rahman, R., Guo, F., Shafer, O., and Rosbash, M. (2017). RNA-seq analysis of *Drosophila* clock and non-clock neurons reveals neuron-specific cycling and novel candidate neuropeptides. PLoS Genet. 13.

Agosto, J., Choi, J.C., Parisky, K.M., Stilwell, G., Rosbash, M., and Griffith, L.C. (2008). Modulation of GABAA receptor desensitization uncouples sleep onset and maintenance in *Drosophila*. Nat. Neurosci. 11, 354–359.

Andretic, R., and Shaw, P.J. (2005). Essentials of sleep recordings in *Drosophila*: Moving beyond sleep time. Methods Enzymol.

Aton, S.J., Colwell, C.S., Harmar, A.J., Waschek, J., and Herzog, E.D. (2005). Vasoactive intestinal polypeptide mediates circadian rhythmicity and synchrony in mammalian clock neurons. Nat. Neurosci. 8, 476–483.

Aton, S.J., Huettner, J.E., Straume, M., and Herzog, E.D. (2006). GABA and Gi/o differentially control circadian rhythms and synchrony in clock neurons. Proc. Natl. Acad. Sci. U. S. A. 103, 19188–19193.

Bina, K.G., Rusak, B., and Semba, K. (1993). Localization of cholinergic neurons in the forebrain and brainstem that project to the suprachiasmatic nucleus of the hypothalamus in rat. J. Comp. Neurol.

Cao, G., and Nitabach, M.N. (2008). Circadian Control of Membrane Excitability in *Drosophila melanogaster* Lateral Ventral Clock Neurons. J. Neurosci.

Chung, B.Y., Kilman, V.L., Keath, J.R., Pitman, J.L., and Allada, R. (2009). The GABAA Receptor RDL Acts in Peptidergic PDF Neurons to Promote Sleep in *Drosophila*. Curr. Biol. 19, 386–390.

Colwell, C.S. (2011). Linking neural activity and molecular oscillations in the SCN. Nat. Rev. Neurosci.

Cusumano, P., Klarsfeld, A., Chélot, E., Picot, M., Richier, B., and Rouyer, F. (2009). PDF-modulated visual inputs and cryptochrome define diurnal behavior in *Drosophila*. Nat. Neurosci.

DeWoskin, D., Myung, J., Belle, M.D.C., Piggins, H.D., Takumi, T., and Forger, D.B. (2015). Distinct roles for GABA across multiple timescales in mammalian circadian timekeeping. Proc. Natl. Acad. Sci. 112, E3911–E3919.

Enoki, R., Oda, Y., Mieda, M., Ono, D., Honma, S., and Honma, K. (2017). Synchronous circadian voltage rhythms with asynchronous calcium rhythms in the suprachiasmatic nucleus. Proc. Natl. Acad. Sci. 114, E2476–E2485.

Flourakis, M., Kula-Eversole, E., Hutchison, A.L., Han, T.H., Aranda, K., Moose, D.L., White, K.P., Dinner, A.R., Lear, B.C., Ren, D., et al. (2015). A Conserved Bicycle Model for Circadian Clock Control of Membrane Excitability. Cell.

Freeman, G.M., Krock, R.M., Aton, S.J., Thaben, P., and Herzog, E.D. (2013). GABA networks destabilize genetic oscillations in the circadian pacemaker. Neuron 78, 799–806.

Gmeiner, F., Kolodziejczyk, A., Yoshii, T., Rieger, D., Nassel, D.R., and Helfrich-Forster, C. (2013). GABAB receptors play an essential role in maintaining sleep during the second half of the night in *Drosophila melanogaster*. J. Exp. Biol. 216, 3837–3843.

Golombek, D.A., and Rosenstein, R.E. (2010). Physiology of Circadian Entrainment. Physiol. Rev.

Grima, B., Chélot, E., Xia, R., and Rouyer, F. (2004). Morning and evening peaks of activity rely on different clock neurons of the *Drosophila* brain. Nature.

Gummadova, J.O., Coutts, G.A., and Glossop, N.R.J. (2009). Analysis of the *Drosophila* clock promoter reveals heterogeneity in expression between subgroups of central oscillator cells and identifies a novel enhancer region. J. Biol. Rhythms.

Guo, F., Yu, J., Jung, H.J., Abruzzi, K.C., Luo, W., Griffith, L.C., and Rosbash, M. (2016). Circadian neuron feedback controls the *Drosophila* sleep-activity profile. Nature.

Hamasaka, Y., Wegener, C., and Nässel, D.R. (2005). GABA modulates *Drosophila* circadian clock neurons via GABAB receptors and decreases in calcium. J. Neurobiol. 65, 225–240.

Hamasaka, Y., Rieger, D., Parmentier, M.L., Grau, Y., Helfrich-Förster, C., and Nässel, D.R. (2007). Glutamate and its metabotropic receptor in *Drosophila* clock neuron circuits. J. Comp. Neurol.

Helfrich-Förster, C. (2003). The neuroarchitecture of the circadian clock in the brain of *Drosophila melanogaster*. Microsc. Res. Tech.

Helfrich-Förster, C., Yoshii, T., Wülbeck, C., Grieshaber, E., Rieger, D., Bachleitner, W., Cusumano, P., and Rouyer, F. (2007). The lateral and dorsal neurons of *Drosophila melanogaster*: New insights about their morphology and function. In Cold Spring Harbor Symposia on Quantitative Biology.

Hendricks, J.C., and Sehgal, A. (2004). Why a fly? Using *Drosophila* to understand the genetics of circadian rhythms and sleep. Sleep.

Hendricks, J.C., Finn, S.M., Panckeri, K.A., Chavkin, J., Williams, J.A., Sehgal, A., and Pack, A.I. (2000). Rest in *Drosophila* is a sleep-like state. Neuron.

Herzog, E.D. (2007). Neurons and networks in daily rhythms. Nat. Rev. Neurosci. 8, 790 802.

Herzog, E.D., Hermanstyne, T., Smyllie, N.J., and Hastings, M.H. (2017). Regulating the suprachiasmatic nucleus (SCN) circadian clockwork: Interplay between cell autonomous and circuit-level mechanisms. Cold Spring Harb. Perspect. Biol.

Huber, R., Hill, S.L., Holladay, C., Biesiadecki, M., Tononi, G., and Cirelli, C. (2004). Sleep homeostasis in *Drosophila melanogaster*. Sleep.

Jones, A.K., Brown, L.A., and Sattelle, D.B. (2007). Insect nicotinic acetylcholine receptor gene families: From genetic model organism to vector, pest and beneficial species. In Invertebrate Neuroscience.

Kolodziejczyk, A., Sun, X., Meinertzhagen, I.A., and Nässel, D.R. (2008). Glutamate, GABA and acetylcholine signaling components in the lamina of the *Drosophila* visual system. PLoS One.

Lelito, K.R., and Shafer, O.T. (2012). Reciprocal cholinergic and GABAergic modulation of the small ventrolateral pacemaker neurons of *Drosophila*'s circadian clock neuron network. J. Neurophysiol.

Liang, X., Holy, T.E., Taghert, P.H., Lim, C., Allada, R., Partch, C.L., Green, C.B., Takahashi, J.S., Welsh, D.K., Takahashi, J.S., et al. (2016). Synchronous *Drosophila* circadian pacemakers display nonsynchronous Ca2+ rhythms in vivo. Science.

Liu, X., Krause, W.C., and Davis, R.L. (2007). GABAAReceptor RDL Inhibits *Drosophila* Olfactory Associative Learning. Neuron.

Muraro, N.I., and Ceriani, M.F. (2015). Acetylcholine from Visual Circuits Modulates the Activity of Arousal Neurons in *Drosophila*. J. Neurosci.

Nitabach, M.N. (2006). Electrical Hyperexcitation of Lateral Ventral Pacemaker Neurons Desynchronizes Downstream Circadian Oscillators in the Fly Circadian Circuit and Induces Multiple Behavioral Periods. J. Neurosci. 26, 479–489.

Nitabach, M.N., Blau, J., and Holmes, T.C. (2002). Electrical silencing of *Drosophila* pacemaker neurons stops the free-running circadian clock. Cell.

Nitabach, M.N., Sheeba, V., Vera, D.A., Blau, J., and Holmes, T.C. (2005). Membrane electrical excitability is necessary for the free-running larval *Drosophila* circadian clock. J. Neurobiol.

Parisky, K.M., Agosto, J., Pulver, S.R., Shang, Y., Kuklin, E., Hodge, J.J.L., Kang, K., Liu, X., Garrity, P.A., Rosbash, M., et al. (2008). PDF Cells Are a GABA-Responsive Wake-Promoting Component of the *Drosophila* Sleep Circuit. Neuron 60, 672 682.

Pfeiffer, B.D., Ngo, T.T.B., Hibbard, K.L., Murphy, C., Jenett, A., Truman, J.W., and Rubin, G.M. (2010). Refinement of tools for targeted gene expression in *Drosophila*. Genetics.

Restifo, L.L., and White, K. (1990). Molecular and genetic approaches to neurotransmitter and neuromodulator systems in *Drosophila*. Adv. In Insect Phys.

Rosato, E., and Kyriacou, C.P. (2006). Analysis of locomotor activity rhythms in *Drosophila*. Nat. Protoc.

S.M., A., J.M., A., Q., C., H., M., N., O., C., C., P.E., G., and J.V., S. (2013). Signals from the Brainstem Sleep/Wake Centers Regulate Behavioral Timing via the Circadian Clock. PLoS One.

Scammell, T.E., Arrigoni, E., and Lipton, J.O. (2017). Neural Circuitry of Wakefulness and Sleep. Neuron.

Schubert, F.K., Hagedorn, N., Yoshii, T., Helfrich-Förster, C., and Rieger, D. (2018). Neuroanatomical details of the lateral neurons of *Drosophila melanogaster* support their functional role in the circadian system. J. Comp. Neurol.

Stoleru, D., Peng, Y., Agosto, J., and Rosbash, M. (2004). Coupled oscillators control morning and evening locomotor behaviour of *Drosophila*. Nature.

Stoleru, D., Peng, Y., Nawathean, P., and Rosbash, M. (2005). A resetting signal between *Drosophila* pacemakers synchronizes morning and evening activity. Nature.

Stoleru, D., Nawathean, P., Fernández, M. de la P., Menet, J.S., Ceriani, M.F., and Rosbash, M. (2007). The *Drosophila* Circadian Network Is a Seasonal Timer. Cell.

Tataroglu, O., and Emery, P. (2014). Studying circadian rhythms in *Drosophila melanogaster*. Methods.

Tian, L., Hires, S.A., Mao, T., Huber, D., Chiappe, M.E., Chalasani, S.H., Petreanu, L., Akerboom, J., McKinney, S.A., Schreiter, E.R., et al. (2009). Imaging neural activity in worms, flies and mice with improved GCaMP calcium indicators. Nat. Methods.

Vansteensel, M.J., Michel, S., and Meijer, J.H. (2008). Organization of cell and tissue circadian pacemakers: A comparison among species. Brain Res. Rev. 58, 18–47.

Wang, T.A., Yu, Y. V., Govindaiah, G., Ye, X., Artinian, L., Coleman, T.P., Sweedler, J. V., Cox, C.L., and Gillette, M.U. (2012). Circadian rhythm of redox state regulates excitability in suprachiasmatic nucleus neurons. Science.

Welsh, D.K., Takahashi, J.S., and Kay, S.A. (2010). Suprachiasmatic Nucleus: Cell Autonomy and Network Properties. Annu. Rev. Physiol. 72, 551–577.

Wu, M., Robinson, J.E., and Joiner, W.J. (2014). SLEEPLESS is a bifunctional regulator of excitability and cholinergic synaptic transmission. Curr. Biol.

Yang, H.H.H., St-Pierre, F., Sun, X., Ding, X., Lin, M.Z.Z., and Clandinin, T.R.R. (2016). Subcellular Imaging of Voltage and Calcium Signals Reveals Neural Processing In Vivo. Cell.

Yang, J.-J., Wang, Y.-T., Cheng, P.-C., Kuo, Y.-J., and Huang, R.-C. (2010). Cholinergic modulation of neuronal excitability in the rat suprachiasmatic nucleus. J. Neurophysiol. 103, 1397–1409.

Yao, Z. (2016). Connectivity , Organization , and Network Coordination of the *Drosophila* Central Circadian Clock.

Yao, Z., and Shafer, O.T. (2014). The *Drosophila* circadian clock is a variably coupled network of multiple peptidergic units. Science.

Yao, Z., Macara, A.M., Lelito, K.R., Minosyan, T.Y., and Shafer, O.T. (2012). Analysis of functional neuronal connectivity in the *Drosophila* brain. J. Neurophysiol.

Yoshii, T., Wulbeck, C., Sehadova, H., Veleri, S., Bichler, D., Stanewsky, R., and Helfrich Forster, C. (2009). The Neuropeptide Pigment-Dispersing Factor Adjusts Period and Phase of *Drosophila*'s Clock. J. Neurosci. 29, 2597–2610.

Yoshii, T., Rieger, D., and Förster, C.H. (2012). Two clocks in the brain: An update of the morning and evening oscillator model in *Drosophila*. Prog. Brain Res.

Chapter 5. Concluding Remarks

My research aims to understand how organisms adapt to and synchronize with their environment. Circadian clocks evolved to serve this function; a sort of molecular "memory" that entrains to daily time cues to coordinate an organism's physiology and behavior rhythms. My thesis work characterizes the neurophysiological and behavioral functions of fast-neurotransmitters in a critical population of *Drosophila* circadian clock neurons, the LNds. The neuronal activity of the LNds promotes a consolidated bout of wakefulness at the end of the day (Grima et al., 2004; Stoleru et al., 2004). Therefore, they are a simple model to investigate the environmental and neurophysiological regulators of an organism's daily behavior. Using the genetically-encoded voltage sensor ASAP2f independently confirmed electrophysiological studies that found that the LNds receive excitatory cholinergic and inhibitory GABAergic signaling (Yang et al., 2016; Yao, 2016). My physiological studies demonstrate that the strength of transmitter inputs changes across the circadian cycle. GABAergic signaling is greater during the night during sleep, while cholinergic singling is greater during the day during wake. The daily rhythms in transmitter inputs are variably coupled to the endogenous molecular clock and environmental light inputs. I used genetic tools to manipulate ionotropic receptivity to GABA and acetylcholine, and behavior analysis to attribute these physiological inputs to aspects of activity, sleep and circadian behavior. Finally, I co-developed a software suite, PHASE, that in addition to classic measures of sleep and activity behavior, provides quantitative metrics of entrainment in DAM behavior data (Trikinetics, Waltham, MA).

Together, my biological findings suggest that the molecular clock and entraining light-inputs work cooperatively in circadian neurons to create daily rhythms in neurotransmitter receptivity that underlie circadian and sleep-wake behavior. The *Drosophila* circadian clock network is similar to the mammalian circadian system in the suprachiasmatic nuclei (SCN). Understanding the neurophysiological and molecular mechanisms that fly clock neurons use to receive and integrate entrainment cues has implications beyond the *Drosophila* field. This is especially true given the prevalence of human circadian disorders including insomnia, obesity and heart-disease caused by our modern environment bathed in artificial light, overabundant food, and round-the-clock work (Lunn et al., 2017). The impact of regular entraining time-cues, or the lack thereof as our modern case may be, on mental and physical states is an underappreciated and essential contributor to human health (McKenna et al., 2018). Below, I summarize the key findings and advancements of my work. I outline caveats and hypotheses that may be addressed with future physiological and behavioral experiments. Finally, I describe possible implications of my work in the context of mammalian systems and circadian entrainment.

Fast-neurotransmitters GABA and acetylcholine control the physiology of the LNds.

Electrophysiology is the gold-standard to precisely measure basal firing rate and changes in membrane potential with the injection of current or application of neurochemicals (Flourakis and Allada, 2015). However, electrophysiology in the fly brain, and particularly in deeper structures or small neurons is technically challenging and invasive. The LNds are such a case, and as a consequence remained one of the few clock neuron classes uncharacterized electrophysiologically until Zepeng Yao first

described the LNds' firing modalities and receptivity to fast-neurotransmitters GABA, glutamate and acetylcholine (Yao, 2016). His electrophysiological characterization was foundational for my thesis studies. Shortly after this electrophysiological undertaking, the genetically-encoded voltage indicator (GEVI) ASAP2f emerged as tool to record membrane voltage changes from multiple cells at a time in intact *Drosophila* brains (Yang et al., 2016). The ASAP2f construct was developed by fusing GFP to a membrane-bound, bidirectional voltage-sensitive domain. Upon membrane depolarization, ASAP2f fluorescence decreases (Yang et al., 2016). Conversely, re-polarization and hyperpolarization causes ASAP2f fluorescence increases (Yang et al., 2016). Genetically encoded sensors for neuronal activity like GCaMP and EPAC-cAMP are regularly used in the *Drosophila*, but GEVIs have never been used in the fly central brain, or in response to bath-applied neurotransmitter. In theory, ASAP2f is uniquely advantageous in that it is 1) a primary measurement of neuronal activity as opposed to secondary measures like Ca^{2+} or cAMP and 2) a bi-directional sensor with greater signal-to-noise for inhibitory, hyperpolarizing events (Chen et al., 2013; Tian et al., 2009; Yao et al., 2012). Until my studies, it was unknown whether ASAP2f would be a useful tool in the clock neuron network to infer membrane voltage *in vivo*. A major effort of my thesis work was to understand the limitations of the ASAP2f fluorescence construct, establish methods and quantitative metrics to extract and infer membrane voltage changes, and interpret their physiological relevance.

I used ASAP2f to record multiple LNds at the same time, in response to application of transmitters. I confirmed that GABA and acetylcholine have direct, dose-dependent hyperpolarizing and depolarizing actions, respectively in the LNds (Chapter 2). I found

that GABA signaling dominates at night, and nicotinic signaling dominates during the day (Chapter 2). I determined using a loss of function mutant for the critical molecular clock gene, *period* and experiments in constant conditions that the LNd's response to neurotransmitter inputs is coupled to a functional circadian clock and environmental light (Chapter 2). Rhythms in GABAergic receptivity persist in constant darkness, and the molecular clock controls both the magnitude of hyperpolarization and polarity of GABA responses. Conversely, rhythms in cholinergic receptivity are strongly dependent on environmental light and do not persist in constant darkness, however the molecular clock appears to modulate the magnitude of depolarization in light-entrained conditions (Chapter 2).

My studies suggest that the inhibitory and excitatory neurotransmitters GABA and acetylcholine may represent "night" and "day," respectively. In the LNds, these physiological rhythms are timed by the molecular clock and environmental cues. Their mutually exclusive distributions across the solar day suggest that GABA and acetylcholine may antagonize one another to properly synchronize wake behavior with daylight and cholinergic excitation, and sleep behavior with darkness and GABA inhibition. Work from our lab has established a physiological link between inhibitory and excitatory transmitters in the s- and l- LNvs whereby GABA decreases the magnitude of cholinergic excitation (Lelito and Shafer, 2012). In the mammalian SCN, GABA tunes the physiological response of circadian neurons to the peptide VIP (Aton et al., 2006; Liu and Reppert, 2000). SCN experiments and computer models suggest the balance of VIP receptivity and GABA inhibition underlie successful entrainment behavior to light in equinox, extremely short and long days (DeWoskin et al., 2015; Evans et al., 2013; Kingsbury et

al., 2016). The fly clock network, and the LNds, have likely developed mechanisms to precisely time the inhibition of excitatory responses. My findings in *period* mutant LNds support the idea that the molecular clock controls levels of GABAergic inhibitory receptivity across the solar day. Though it remains to be tested experimentally, GABA levels in *Drosophila* and mammals alike may control the strength of excitatory inputs particularly during the nighttime when sleep is the behavioral imperative, and facilitate consolidated bouts of sleep-wake behavior across entrainment paradigms.

The precise sources of these GABAergic and cholinergic inputs to the LNds or other clock network populations remain unmapped, but this is an essential effort for future work. Cells in the optic lamina and HB-eyelet that form direct synaptic connections with neurons in the clock network release acetylcholine; a functional analog of glutamate released from the light-sensitive cells in the retinohypothalamic tract of mammals (Golombek and Rosenstein, 2010; Muraro and Ceriani, 2015). The clock network itself also has sources of both transmitter types, and the extensive arborizations between populations indicate that these fast-neurotransmitters may be released at direct synaptic connections (Abruzzi et al., 2017; Aronstein and Ffrench-Constant, 1995; Johard et al., 2009; Schubert et al., 2018). My physiological studies do not address the heterogeneity of the LNds themselves, or the physiological properties of cells in other CCNN populations. The six cells that comprise the LNds are diverse in transmitter types, CRY expression and variably coupled to cells within the CCNN (Abruzzi et al., 2017; Yao and Shafer, 2014; Yao et al., 2016). Theoretically, ASAP2f can be expressed using GAL4s specific to clock neuron sub-populations (say, only the CRY+ LNds or small subsets of DN1s). Our understanding of the physiological properties of the CCNN would benefit

greatly from combining the ASAP2f construct with GAL4s that express in sparsely defined populations and genetic tools to manipulate neurochemical receptivity. I suspect we will find that each clock population's diverse receptivity to environmental cues and neurochemicals underlies flies' relatively broad entrainment range (Bywalez et al., 2012; Yoshii et al., 2009).

These studies may be limited by the abilities of the ASAP2f construct to detect small changes in membrane potential, the imaging acquisition speed and perfusion set-up, or insufficient quantitative methodology to extract true membrane voltage changes from noise. To minimize this latter challenge, I used a 6^{th}-order polynomial to filter raw fluorescence traces and preserve the overall signal's response area, but decrease large magnitude fluorescence changes due to the ASAP2f sensor "wobble" (GraphPad, Prism version 8.0.2 for Mac, GraphPad Software, San Diego, California USA). Using these filtered traces, I observed that ASAP2f fluorescence signals in wildtype LNds rarely deviate from baseline during the course of 200-second imaging time course in vehicle sessions. ASAP2f fluorescence signals reliably decrease with acetylcholine-mediated depolarization and increase with GABA-mediated hyperpolarization. At saturation levels, the effects of bath applied neurotransmitters are often distinguishable from vehicle controls by eye and quantitatively by measuring the mean total response area and mean maximum or minimum fluorescence change. However, I observed that at lower doses and in genetic (per^{01}) or experimental conditions (DD) where cells were not maintaining baseline membrane voltage or coherently responding to transmitter, it was exceedingly difficult to extract statistical significance from the mean of all imaged cells with these metrics. Therefore, I excluded non-responsive cells and sorted, compared responding

cells based on their depolarized or hyperpolarized modality. Comparing responsive cells within their modality between experiments made the effects of manipulations statistically more apparent. Given that ASAP2f functions bidirectionally, this analysis technique could be considered in situations where neurons exhibit highly variable, incoherent responses. Finally, it is important to note that manipulations to neurotransmitter receptivity may not be apparent if assessed by comparing fluorescence magnitude alone, or over the entire imaging time course. It may be useful to analyze particular imaging windows if qualitative differences in the *timing* of responses varies between experiments as consequence of receptors being occupied by endogenous transmitter, or decreased or increased in number with genetic manipulations.

My studies demonstrate that ASAP2f is advantageous relative to other *in vivo* methods to infer neural activity when the aim of the study is to assess increases and decreases in membrane voltage in intact circuits, or in small, inaccessible cells like the LNds. The ASAP2f construct is sensitive to the baseline membrane voltage of the imaged neurons; a particularly relevant point if the LNds exhibit circadian changes in membrane voltage that would change the effect of transmitter application. For example, if neurons are spontaneously firing at one time of day the additional application of an “excitatory” neurotransmitter may have little effect on the change in ASAP2f fluorescence. On the other hand, if a neuron’s membrane voltage is already near the equilibrium potential for chloride, application of GABA would be unlikely to make much of a difference in the perceived levels of hyperpolarization as assessed by ASAP2f fluorescence. Put simply, our observed depolarizations are not necessarily equal to excitation if they do not bring the neuron beyond threshold to firing, while hyperpolarizations are not necessarily equal

to inhibition if they do not prevent and suppress active neuronal firing. The interpretive power of future ASAP2f studies will be greatly enhanced by increasing the imaging rate to capture single action potentials and incorporation of a stable RFP fluorescence signal. These methods may enable us to discern whether changes, or lack thereof, in ASAP2f fluoresce reflect true instances of inhibition and excitation that vary heterogeneously between neurons or across the circadian period.

Behavioral functions of fast-neurotransmission in the LNds and the fly clock network.

The bimodal activity of male flies in entrained conditions is coordinated primarily by two clock network populations. While the neural activity of the PDF+ s- and l- LNvs coordinate morning wakefulness, the LNds coordinate evening wakefulness (Grima et al., 2004; Liang et al., 2016; Stoleru et al., 2004, 2005). My ASAP2f studies show that GABA and acetylcholine signals are received most strongly by the LNds during the night, and day respectively. Thus, I predicted that decreasing cholinergic excitation with *nAChR* RNAi would decrease evening wakefulness and increase sleep, while decreasing GABAergic inhibition with *Rdl* RNA might increase evening wakefulness and decrease sleep. In order to test this model, I combined ASAP2f imaging with genetic manipulations to neurotransmitter receptivity, and performed classic circadian behavioral studies to determine the contributions of nicotinic and GABAergic signaling to endogenous timekeeping, sleep and activity in the entire clock neuron network, or LNds alone. This work was aided by an exceptional colleague, TJ Waller, who during a short lab rotation screened (often two independent) RNAi knockdowns for each nAChR gene. Not only in male flies but also in virgin female flies, which notably had very different behavioral results (unpublished behavioral data). Of the flies' 10 nAChRs, we identified the alpha3 subunit

as the strongest contributor to circadian rhythmicity and periodicity, clock-wide in constant conditions (Jones et al., 2007). This is likely correct, as -a3 has strong genetic interactions with proteins involved in sleep-wake behavior in *Drosophila* (Wu et al., 2014). In our studies, flies without the *-a3* subunit expressed in all clock neurons are less than 40% rhythmic and are lengthened in periodicity in constant conditions after entrainment in equinox light (Chapter 4). This effect appears marginally dependent on the LNds, and is likely mediated by other clock classes (Chapter 4). However, *nAChRa3* expression across the clock network, and through the LNds specifically controls evening wakefulness and contributes to daytime sleep quantity (Chapter 4). My ASAP2f studies demonstrate 1) that RNAi knockdown of *nAChRa3* reduced the LNds physiological response to nicotine, and 2) that depolarization to the cholinergic agonist nicotine is greater during the day and coupled strongly to light inputs (Chapters 2 and 4). Together, these data suggest that nicotinic signaling, strongly linked to environmental light, forces the network to converge on a 24-hour behavioral rhythm in 12:12 entrainment conditions. And that through the LNds, cholinergic excitation facilitates evening activity prior to lights-off. These results were in accordance to my simple predictions given the causal role of the LNds' neural activity in evening behavior.

The clear circadian phenotypes of *nAChR* knockdown were in stark contrast to those of knocking down GABA-AR homolog, *Rdl*. *Rdl* RNAi expressed clock-wide or specifically in the LNds, has no effect on rhythmicity and periodicity in constant conditions (Chapter 4). The CCNN's network-wide receptivity to GABA and the physiological role of GABA-ARs for conducting inhibitory currents contradicts the lack of measurable circadian periodicity or rhythmicity phenotypes with *Rdl* knockdown and hypomorphs in my ASAP2f

work or the work of others (Abruzzi et al., 2017; Agosto et al., 2008; Aronstein and Ffrench-Constant, 1995; Chung et al., 2009; Parisky et al., 2008). I offer a few possible explanations for our observations additional to the conclusion that *Rdl* and ionotropic GABA signaling plays no role in endogenous rhythms. First, the exact composition of functional receptors remain unknown and other subunits may form functional receptors. In *Drosophila* and other insects there are two genes encoding GABA-AR subunits additional to *Rdl*: *Lcch3* and *Grd* (Dupuis et al., 2010). Metabotropic receptors for GABA, GABA-BRs are also expressed in the clock network and have roles in sleep and rhythmicity (Dahdal et al., 2010; Gmeiner et al., 2013; Hamasaka et al., 2005). In addition, GABA is not the only inhibitory neurotransmitter in the CCNN; glutamate is released by the DN1s and directly inhibits the s-LNvs and LNds (Guo et al., 2016; Hamasaka et al., 2007 and unpublished ASAP2f data). Nervous systems are incredibly plastic. It is possible that other GABA-AR subunits, metabotropic GABA-BRs, other inhibitory neurotransmitters or proteins controlling intrinsic membrane potential compensate for the loss of RDL. I suggest that future work use adult-specific manipulations of *Rdl* levels, validate the efficiency of RNAi and increase when needed with Dicer2, and knockdown GABA receptive ionotropic subunits simultaneously with metabotropic subunits, or in combination with other inhibitory neurotransmitters.

My behavioral studies did find that *Rdl* knockdown specifically in the LNds reduces the quantity of morning wakefulness in 12:12 LD conditions (Chapter 4). This is dissimilar to previous findings in the s- and l-LNvs, where manipulating *Rdl* levels only controlled sleep quantity and quality (Agosto et al., 2008; Chung et al., 2009; Parisky et al., 2008). These results were also surprising given my model's predictions and that the LNds'

neuronal activity controls evening activity in 12:12 LD entrained conditions, while the PDF+ LNvs control morning activity (Grima et al., 2004; Stoleru et al., 2004). These findings could be explained by reciprocal inhibition between the two primary lateral neuron classes: In the morning, GABAergic inhibition to the LNds may indirectly allow the LNvs to be excited and coordinate morning activity. In the evening, inhibition of the LNvs permits the LNds to be directly excited by cholinergic inputs that coordinate evening activity. Finally, it is worth noting that GABA has an well-documented role in entrainment to exotic light conditions in mammals (Evans et al., 2013). To my knowledge, no GABA manipulations have ever been performed outside of standard, equinox 12:12 LD conditions in flies. I anticipate more dramatic roles for GABA signaling when individual clock neuron populations are rearranging the networks' behavioral outputs to synchronize with new entrainment paradigms.

Defining circadian entrainment and sleep behavior.

Understanding entrainment- the modalities, ranges and intensities of time-giving cues over which an organism can adapt- is essential to understanding circadian systems (Roenneberg et al., 2003). Clock networks are adaptive, and I would argue this flexibility is responsible for the presence of life in almost every hospitable latitude and environment on earth. *Drosophila melanogaster* are built for a solar day with equinox light and temperature conditions. Yet, this equatorial species can coordinate behavior in short and long days, and to different period lengths within an approximately one-hour range (Green et al., 2015; Rieger et al., 2003; Schlichting et al., 2016). *Drosophila* have contributed fundamentally to our knowledge of the molecular underpinnings of circadian behavior. They have stereotyped behavior, mutants for each component of the molecular clock and

a genetically-accessible central clock neuron network similar to those in mammals. Tools (Trikinetics, DAM-system) and software (ClockLab, ActogramJ, ShinyR-DAM) to record and quantitate the behavioral consequences of manipulations are used near-universal among *Drosophila* circadian researchers (Trikinetics, Waltham, MA; Cichewicz and Hirsh, 2018; Rosato and Kyriacou, 2006; Schmid et al., 2011). However, unlike sleep, activity and circadian rhythmicity, entrainment lacks standardized, quantitative metrics. In collaboration with an incredibly talented and patient software developer Abbey Roelofs, I built PHASE to fill this gap (Chapter 3). PHASE performs Activity, Sleep, Entrainment analysis for individual flies and populations. PHASE uses an adjustable Savitzky-Golay filter to minimize signal-to-noise that may mask properties of entrainment, and mathematically define peak size and peak phase time relative to entrainment cues in smoothed activity or sleep data (Chapter 3). PHASE is able to perform these analyses in diverse entrainment paradigms, irrespective of day- or period-length. The *Drosophila* circadian network is far more complex than the dual-oscillator model predicts (Yoshii et al., 2012). I speculate that if the coming years are anything like my short tenure in the fly circadian field, experiments will demonstrate that each CCNN population is tuned to listen to a specific repertoire of entrainment cues. When leveraged with the fly's powerful genetic tools and striking similarity to mammalian circadian systems, PHASE's quantitative methodology may inform our understanding of the essential physiological and molecular mechanisms synchronizing circadian behavior and entrainment.

References

Abruzzi, K.C., Zadina, A., Luo, W., Wiyanto, E., Rahman, R., Guo, F., Shafer, O., and Rosbash, M. (2017). RNA-seq analysis of *Drosophila* clock and non-clock neurons reveals neuron-specific cycling and novel candidate neuropeptides. PLoS Genet. 13.

Agosto, J., Choi, J.C., Parisky, K.M., Stilwell, G., Rosbash, M., and Griffith, L.C. (2008). Modulation of GABAA receptor desensitization uncouples sleep onset and maintenance in *Drosophila*. Nat. Neurosci. 11, 354–359.

Aronstein, K., and Ffrench-Constant, R. (1995). Immunocytochemistry of a novel GABA receptor subunit Rdl in *Drosophila melanogaster*. Invertebr. Neurosci. 1, 25–31.

Aton, S.J., Huettner, J.E., Straume, M., and Herzog, E.D. (2006). GABA and Gi/o differentially control circadian rhythms and synchrony in clock neurons. Proc. Natl. Acad. Sci. U. S. A. 103, 19188–19193.

Bywalez, W., Menegazzi, P., Rieger, D., Schmid, B., Helfrich-Förster, C., and Yoshii, T. (2012). The dual-oscillator system of *Drosophila melanogaster* under natural-like temperature cycles. Chronobiol. Int.

Chen, T.W., Wardill, T.J., Sun, Y., Pulver, S.R., Renninger, S.L., Baohan, A., Schreiter, E.R., Kerr, R.A., Orger, M.B., Jayaraman, V., et al. (2013). Ultrasensitive fluorescent proteins for imaging neuronal activity. Nature.

Chung, B.Y., Kilman, V.L., Keath, J.R., Pitman, J.L., and Allada, R. (2009). The GABAA Receptor RDL Acts in Peptidergic PDF Neurons to Promote Sleep in *Drosophila*. Curr. Biol. 19, 386–390.

Cichewicz, K., and Hirsh, J. (2018). ShinyR-DAM: a program analyzing *Drosophila* activity, sleep and circadian rhythms. Commun. Biol.

Dahdal, D., Reeves, D.C., Ruben, M., Akabas, M.H., and Blau, J. (2010). *Drosophila* Pacemaker Neurons Require G Protein Signaling and GABAergic Inputs to Generate Twenty-Four Hour Behavioral Rhythms. Neuron.

DeWoskin, D., Myung, J., Belle, M.D.C., Piggins, H.D., Takumi, T., and Forger, D.B. (2015). Distinct roles for GABA across multiple timescales in mammalian circadian timekeeping. Proc. Natl. Acad. Sci. 112, E3911–E3919.Dupuis, J.P., Bazelot, M.,

Barbara, G.S., Paute, S., Gauthier, M., and Raymond-Delpech, V. (2010). Homomeric RDL and Heteromeric RDL/LCCH3 GABA Receptors in the Honeybee Antennal Lobes: Two Candidates for Inhibitory Transmission in Olfactory Processing. J. Neurophysiol.

Evans, J.A., Leise, T.L., Castanon-Cervantes, O., and Davidson, A.J. (2013). Dynamic Interactions Mediated by Nonredundant Signaling Mechanisms Couple Circadian Clock Neurons. Neuron 80, 973–983.

Flourakis, M., and Allada, R. (2015). Patch-clamp electrophysiology in *Drosophila* circadian pacemaker neurons. Methods Enzymol.

Gmeiner, F., Kolodziejczyk, A., Yoshii, T., Rieger, D., Nassel, D.R., and Helfrich-Forster, C. (2013). GABAB receptors play an essential role in maintaining sleep during the second half of the night in *Drosophila melanogaster*. J. Exp. Biol. 216, 3837–3843.

Golombek, D.A., and Rosenstein, R.E. (2010). Physiology of Circadian Entrainment. Physiol. Rev.

Green, E.W., O'Callaghan, E.K., Hansen, C.N., Bastianello, S., Bhutani, S., Vanin, S., Armstrong, J.D., Costa, R., and Kyriacou, C.P. (2015). *Drosophila* circadian rhythms in seminatural environments: Summer afternoon component is not an artifact and requires TrpA1 channels. Proc. Natl. Acad. Sci.

Grima, B., Chélot, E., Xia, R., and Rouyer, F. (2004). Morning and evening peaks of activity rely on different clock neurons of the *Drosophila* brain. Nature.

Guo, F., Yu, J., Jung, H.J., Abruzzi, K.C., Luo, W., Griffith, L.C., and Rosbash, M. (2016). Circadian neuron feedback controls the *Drosophila* sleep-activity profile. Nature.

Hamasaka, Y., Wegener, C., and Nässel, D.R. (2005). GABA modulates *Drosophila* circadian clock neurons via GABAB receptors and decreases in calcium. J. Neurobiol. 65, 225–240.

Hamasaka, Y., Rieger, D., Parmentier, M.L., Grau, Y., Helfrich-Förster, C., and Nässel, D.R. (2007). Glutamate and its metabotropic receptor in *Drosophila* clock neuron circuits. J. Comp. Neurol.

Johard, H.A.D., Yoishii, T., Dircksen, H., Cusumano, P., Rouyer, F., Helfrich-Förster, C., and Nässel, D.R. (2009). Peptidergic clock neurons in *Drosophila*: Ion transport peptide and short neuropeptide F in subsets of dorsal and ventral lateral neurons. J. Comp. Neurol.

Jones, A.K., Brown, L.A., and Sattelle, D.B. (2007). Insect nicotinic acetylcholine receptor gene families: From genetic model organism to vector, pest and beneficial species. In Invertebrate Neuroscience.

Kingsbury, N.J., Taylor, S.R., and Henson, M.A. (2016). Inhibitory and excitatory networks balance cell coupling in the suprachiasmatic nucleus: A modeling approach. J. Theor. Biol. 397, 135–144.

Lelito, K.R., and Shafer, O.T. (2012). Reciprocal cholinergic and GABAergic modulation of the small ventrolateral pacemaker neurons of *Drosophila*'s circadian clock neuron network. J. Neurophysiol.

Liu, C., and Reppert, S.M. (2000). GABA synchronizes clock cells within the suprachiasmatic circadian clock. Neuron 25, 123–128.

Lunn, R.M., Blask, D.E., Coogan, A.N., Figueiro, M.G., Gorman, M.R., Hall, J.E., Hansen, J., Nelson, R.J., Panda, S., Smolensky, M.H., et al. (2017). Health consequences of electric lighting practices in the modern world: A report on the National Toxicology Program's workshop on shift work at night, artificial light at night, and circadian disruption. Sci. Total Environ.

McKenna, H., van der Horst, G.T.J., Reiss, I., and Martin, D. (2018). Clinical chronobiology: A timely consideration in critical care medicine. Crit. Care.

Muraro, N.I., and Ceriani, M.F. (2015). Acetylcholine from Visual Circuits Modulates the Activity of Arousal Neurons in *Drosophila*. J. Neurosci.

Parisky, K.M., Agosto, J., Pulver, S.R., Shang, Y., Kuklin, E., Hodge, J.J.L., Kang, K., Liu, X., Garrity, P.A., Rosbash, M., et al. (2008). PDF Cells Are a GABA-Responsive Wake-Promoting Component of the *Drosophila* Sleep Circuit. Neuron 60, 672 682.

Rieger, D., Stanewsky, R., and Helfrich-Förster, C. (2003). Cryptochrome, compound eyes, Hofbauer-Buchner eyelets, and ocelli play different roles in the entrainment and masking pathway of the locomotor activity rhythm in the fruit fly *Drosophila melanogaster*. J. Biol. Rhythms.

Roenneberg, T., Daan, S., and Merrow, M. (2003). The art of entrainment. J. Biol. Rhythms.

Rosato, E., and Kyriacou, C.P. (2006). Analysis of locomotor activity rhythms in *Drosophila*. Nat. Protoc.

Schlichting, M., Menegazzi, P., Lelito, K.R., Yao, Z., Buhl, E., Dalla Benetta, E., Bahle, A., Denike, J., Hodge, J.J., Helfrich-Forster, C., et al. (2016). A Neural Network

Underlying Circadian Entrainment and Photoperiodic Adjustment of Sleep and Activity in *Drosophila*. J. Neurosci.
Schmid, B., Helfrich-Förster, C., and Yoshii, T. (2011). J Biol Rhythms. A New ImageJ Plug-in "ActogramJ" Chronobiol. Anal.
Schubert, F.K., Hagedorn, N., Yoshii, T., Helfrich-Förster, C., and Rieger, D. (2018). Neuroanatomical details of the lateral neurons of *Drosophila melanogaster* support their functional role in the circadian system. J. Comp. Neurol.
Stoleru, D., Peng, Y., Agosto, J., and Rosbash, M. (2004). Coupled oscillators control morning and evening locomotor behaviour of *Drosophila*. Nature.
Tian, L., Hires, S.A., Mao, T., Huber, D., Chiappe, M.E., Chalasani, S.H., Petreanu, L., Akerboom, J., McKinney, S.A., Schreiter, E.R., et al. (2009). Imaging neural activity in worms, flies and mice with improved GCaMP calcium indicators. Nat. Methods.
Wu, M., Robinson, J.E., and Joiner, W.J. (2014). SLEEPLESS is a bifunctional regulator of excitability and cholinergic synaptic transmission. Curr. Biol.
Yadlapalli, S., Jiang, C., Bahle, A., Reddy, P., Meyhofer, E., and Shafer, O.T. (2018). Circadian clock neurons constantly monitor environmental temperature to set sleep timing. Nature.
Yang, H.H.H., St-Pierre, F., Sun, X., Ding, X., Lin, M.Z.Z., and Clandinin, T.R.R. (2016). Subcellular Imaging of Voltage and Calcium Signals Reveals Neural Processing In Vivo. Cell.
Yao, Z. (2016). Connectivity , Organization , and Network Coordination of the *Drosophila* Central Circadian Clock.
Yao, Z., and Shafer, O.T. (2014). The *Drosophila* circadian clock is a variably coupled network of multiple peptidergic units. Science.
Yao, Z., Macara, A.M., Lelito, K.R., Minosyan, T.Y., and Shafer, O.T. (2012). Analysis of functional neuronal connectivity in the *Drosophila* brain. J. Neurophysiol.
Yao, Z., Bennett, A.J., Clem, J.L., and Shafer, O.T. (2016). The *Drosophila* Clock Neuron Network Features Diverse Coupling Modes and Requires Network-wide Coherence for Robust Circadian Rhythms. Cell Rep.
Yoshii, T., Wulbeck, C., Sehadova, H., Veleri, S., Bichler, D., Stanewsky, R., and Helfrich Forster, C. (2009). The Neuropeptide Pigment-Dispersing Factor Adjusts Period and Phase of *Drosophila*'s Clock. J. Neurosci. 29, 2597–2610.
Yoshii, T., Rieger, D., and Förster, C.H. (2012). Two clocks in the brain: An update of the morning and evening oscillator model in *Drosophila*. Prog. Brain Res.

Appendix.

Drosophila Activity, Sleep and Entrainment Behavior Analysis Using MATLAB Program PHASE

Jenna L Persons[1*], Abbey Roelofs[2*], and Orie T Shafer[1]

[1]Department of Molecular, Cellular, and Developmental Biology, University of Michigan, Ann Arbor, MI 48109, [2]Department of Information Technology, Advocacy and Research Support, University of Michigan, Ann Arbor, MI 48109

Author Contributions

JLP, AR, OTS, drafting and revising the manuscript.

Preface

This manual is designed to guide users of PHASE in the analysis of *Drosophila* activity, sleep and circadian entrainment behavior using data collected from the *Drosophila* Activity Monitor (DAM) system (TriKinetics Inc, Waltham, MA). Section 1 describes the PHASE software and accepted data formats. Section 4 describes the Savitzky-Golay filtering used in Phase Analysis, and Anticipation or Latency Analysis. Sections 2, 3, 5, and 6 outline each element of PHASE's visible user-interface with a *Description*, a step-by-step *Protocol*, and a guide to calculations used in *Excel Outputs*, and data

representation in *Graphs*. PHASE may also be a useful application outside of the *Drosophila* circadian field, provided primary behavior data is in a format read and processed by DAMFileScan into 1-minute bins.

Section 1. PHASE Software

1.1. Software Accessibility

PHASE functions on both Mac and PC. PHASE for MATLAB versions R2017b or later (PHASE.mlappinstall) and the folder containing the standalone versions for Mac and PC (PHASE.installer.zip) may be downloaded from the software Google Drive. The full version of PHASE for MATLAB will require the additional toolbox to create Excel workbooks (xlwrite.mltbx) also available for download on the Google Drive. The standalone version requires MATLAB Runtime versions R2017b or later which is freely available for download at the MATLAB website. The original manuscript using PHASE's functions to describe wildtype and circadian mutant *Drosophila* activity and sleep behavior is available on the Google Drive. Requests for software updates and code modifications may be made directly to the corresponding author.

1.2. Data Processing Protocol

1. Use DAMFileScan (Trikinetics Inc, Waltham, MA) to process DAM monitor data into 1-minute bins, in channel (individual fly) counts for the duration of the experiment.

2. Place all data from a single experiment into a folder.

    a. All DAM-processed data must have the same file name, and same experiment start and end bins.

b. Experiments originating from different dates or with different file names must be processed by PHASE from separate data folders.

3. Ensure that no other file structures are in this folder as PHASE will not be able to read the first experiment start bin.

a. This includes all folders generated by PHASE. Create a new folder for PHASE's Excel and graph outputs.

4. Dead flies may be deleted directly in the PHASE interface.

a. Deleting dead flies prior to data processing by PHASE, and forgetting to exclude them from channels selected for analysis may result in errors as the program tries to locate missing monitor files within the selected folder.

Section 2. Data Settings

2.1. Description

"Data Settings" is required to upload and define experimental parameters for analysis using "Activity or Sleep," "Phase Analysis," or "Anticipation or Latency" functions.

2.2. Protocol

1. Start MATLAB, and open "PHASE" in Apps or open the standalone version directly.

2. Select Data Folder containing DAMFileScan processed 1-minute data using "…"

a. Run Name, Exp. Start Date, Exp. Start Time should autofill with the very first bin collected.

b. Failure to autofill results if there are 1) other files in the Data Folder or 2) if there are monitor files with multiple start bin times/dates, or 3) multiple file names. Ensure that only monitor files processed by DAMFileScan with the same set of continuous bins, and same name occupy the Data Folder.

3. Under “Data Settings” highlight the channels/individual flies (second box, channels 1-32) to be processed from the auto-loaded monitors (first box, monitors 1-120).

a. Use the arrow to push the selected monitor files to the analysis box (third box).

b. Use the red “X” to delete all selected monitor files from the analysis box.

c. Exclude dead flies from analysis at this step. Individual channels/flies may be deleted from the analysis box by selecting a single channel and pressing the keyboard delete button.

4. Change the autofilled “Exp. Start Date” from calendar in “…” to select the first date of analysis.

a. “Exp. Start Date” autofills with first bin in monitor file, thus, select the date to start data analysis. This is typically post entrainment, usually 1-2 days after the autofilled date.

5. Change autofilled “Exp. Start Time” to the first 24-hour time (HH:MM) to start analysis.

a. For example, to start analyses at ZT0 where a Zeitgeber turned on at 9AM, enter “09:00”.

6. Change “Period Length”, “Zeitgeber On”, and “Hours of Zeitgeber” as needed.

a. Autofills are “24”, “0” and “12”, respectively. Note that “Day” statistics are derived from the hours between “Zeitgeber On” and off, “Night” statistics are derived from the remaining hours.

b. Adjust these parameters to quantify sleep or activity during a particular window. For example, to quantify behavior only between ZT3-8, change the “Zeitgeber On” to “3” and enter “5” for “Hours of Zeitgeber”. All “Day” sleep and activity statistics in Excel outputs generated by PHASE will result from the ZT3-8 window specified.

Section 3. Activity or Sleep Analysis

3.1. Description

"Activity or Sleep Analysis" analyzes 1-minute binned data with respect to parameters described in "Data Settings" to define and graphically represent activity and sleep measures for individual flies. "Sleep" is defined as any 1-minute data collection bins that were part of a 5-minute (or more) series of bins without activity (IR beam crosses) (Hendricks and Sehgal, 2004; Huber et al., 2004). Sleep bins are subsequently marked with a 1, and all other bins marked with a zero.

The activity in each user-specified bin may be 1) "Averaged" by the "Bin Size" or 2) "Normalized" to the total activity (total IR beam crosses) in a day or average of days. The latter function is the standard for representing fly circadian behavior data. Normalizing by total activity divides each bin's total IR beam crosses by the total IR beam crosses in a day (or average of selected days). Normalization preserves the temporal (X-axis) qualities of activity data, because each bin is a percentage (in decimal form from 0 to 1) of the day's total IR beam crosses. Averaging by bin size divides each bin's total IR beam crosses by the user's specified "Bin Size." Averaging preserves both temporal (X-axis) and magnitude (Y-axis) changes in activity data and is useful for comparing not only when, but how much flies are active. PHASE offers both options, and users should select the activity analysis that suits their needs. For example, while total activity normalization is most suited for Activity Anticipation (in minutes from a given ZT), averaging by bin size may be best for comparing true measures of overall activity and peak areas in "Phase Analysis."

3.2. Protocol

1. Check the “Include Activity/Sleep Analysis” box.

2. Change “Bin Size” from autofilled “30min,” as needed. “Bin Size” may be any whole number no smaller than 1-minute. Data is grouped into bins based on the specified “Bin Size,” and then bins are averaged across days or flies.

    a. “Bin Size” changes the graphical presentation of data, any averaging by “Bin Size” that takes place in “Average Activity Analysis”, and the “Bin Size” in which IR counts are collected when “Total Activity” normalization is selected. It will not change “Sleep Analysis” or the raw activity counts/IR beam crosses. (see 3.1 Description, bolded statements)

3. Select “Days to Use”. Separate days by a comma.

    a. Day “1” begins at the “Exp. Start Time” for the indicated “Day Length” with “Day” beginning at “Zeitgeber On” and “Night” beginning after the given “Hours of Zeitgeber” in “Data Settings”. Day “2” begins the indicated “Day Length” after day “1”.

    b. “Days to Use” may be consecutive (1 ,2, 3), non-consecutive (1, 2, 3, 10), or a single day (2).

4. Specify the “Averaging” type for graphically representing behavior data of flies in the analysis box (third box) in “Data Settings”.

    a. “Flies” averages behavior of all flies in analysis box for the indicated “Days to Use” and provides a single graph with each day of data displayed consecutively

    b. “Days” averages indicated “Days to Use” for each individual fly in analysis box. Results in a single day-averaged plot for each fly in “Data Settings.”

c. “Both” results in a single plot that first averages individual flies’ behavior for each day included in “Days to Use,” then averages all days together.

d. “No Averaging” creates individual fly graphs and displays the “Days to Use” consecutively.

2. Select the “Plot Style”. All styles will center “Zeitgeber On” hours between Zeitgeber Off hours (shaded bars or regions) at the left and right of the graph. The exceptions are 1) “No Averaging” or 2) “Flies” where multiple days are selected, which will display each day consecutively beginning with the first days’ Zeitgeber On to last days Zeitgeber Off.

a. “Bars” creates a traditional bar graph displaying binned activity or sleep data with standard error of mean (SEM) error bars.

b. “Lines” creates a line graph with SEM shaded above and below the mean line.

c. “Both” creates plots with both graph styles.

d. When “Averaging” by “Both” days and flies is selected, averaging is done first by flies and then (in a separate step) by days. The SEM is calculated on the second step only, that is, it's the standard error across days of the averaged fly data.

5. Enter the “Output File Name”. “Output File Name” automatically uploads to graph titles.

6. Specify an “Output Folder” with “…”

a. To avoid errors in uploading data in to the Activity Monitor, create a new folder exclusively to export graphs and Excel outputs.

7. For sleep analysis, click “Sleep Analysis” button.

8. For activity analysis, click either “Averaged Activity Analysis” or “Normalized Activity Analysis”

a. Each bin in “Averaged Activity Analysis” is equal to the (Bin’s Total IR Crosses/”Bin Size”). Y-axis values will not distort the original magnitude of activity.

b. Each bin in “Normalized Activity Analysis” is equal to the (Bin’s Total IR Crosses/Total IR Crosses). Therefore, Y-axis values will only range from 0 to 1 since each bin represents a percent of total IR activity.

3.3. Activity Analysis Excel Outputs

Exports from “Normalized” or “Averaged” Activity analysis will be summarized in the Excel file “ActivityAnalysis_OutputFileName_YYYMMDD_HHMM.” Values are summed (sheets titled “Summed”) or averaged (sheets titled “DayAve”) activity from all indicated days in “Days to Use”. Following the “Settings” sheet, values are broken down for each individual day indicated in “Days to Use.”

Statistics (Raw) and Statistics

Descriptions below are for the "Statistics (Raw)" sheets where the values are actual binned IR beam crosses. For “Statistics” sheets, the counts of binned IR beam crosses are either 1) divided by the “Bin Size” in “Averaged Activity Analysis” or 2) divided by the total activity in “Normalized Activity Analysis”. All calculations for “Statistics” are as described below but represent values averaged by “Bin Size” (Bin’s Total IR Crosses/”Bin Size”) or normalized to total activity (Bin’s Total IR Crosses/Total IR Crosses) instead of Raw IR counts. Columns:

A. Board. Monitor number (1-120).
B. Fly. Channel number (1-32).
C. TotalCounts. The sum of all values in the data series for the selected days (first four sheets) or indicated day (subsequent sheets) in “Days to Use”.

D. AverageCounts. The “TotalCounts” divided by the total number of data collection bins. For example, a 30-minute “Bin Size” over a 24-hour “Day Length” would divide all “TotalCounts” values by 48.
E. DayTotalCounts. The total IR beam crosses that took place during “Zeitgeber On” hours.
F. AverageDayCounts. The “DayTotalCounts” divided by the total number of data collection bins in “Zeitgeber On” hours.
G. NightTotalCounts. The total IR beam crosses that took place outside of “Zeitgeber On” hours.
H. AverageNightCounts. The “NightTotalCounts” divided by the total number of data collection bins outside of “Zeitgeber On” hours.

BinnedData (Raw) and BinnedData

BinnedData (Raw) and BinnedData are values in the same format as MATLAB graph exports. They are centered around “Zeitgeber On” hours. Therefore, the first, far left bin in Column A is not ZT0 unless consecutive days of data are indicated in “Averaging” by “Flies” or “No Averaging”. Descriptions below are for the "BinnedData (Raw)" sheets where the values are each bin’s actual IR beam crosses. All calculations in “BinnedData” sheets represent activity averaged (each bin’s IR beam crosses divided by “Bin Size”) or normalized (each bin’s IR beam crosses divided by total IR beam crosses) instead of Raw IR counts. Columns:

A. Bin. The first bin represents the first, leftmost bin on the graph. Values are centered on “Zeitgeber On” hours. Therefore, the first bin in Column A is in middle of the Zeitgeber Off hours.

B. “MxxxCxx”. The individual fly represented by its monitor number (“Mxxx”) and channel number (“Cxx”).

3.4. Sleep Analysis Excel Outputs

Sleep Analysis quantifications are summarized in the Excel file “SleepAnalysis_OutputFileName_YYYMMDD_HHMM.” Values are summed (sheets titled “Summed”) or averaged (sheets titled “DayAve”) from all indicated days in “Days to Use”. Following the “Settings” sheet, sleep quantifications from each individual day indicated in “Days to Use” are summarized.

Statistics (Raw)

Statistics below represent minutes of sleep. “Sleep” is defined as any 1-minute data collection bins that were part of a 5-minute (or more) series of bins without activity (IR beam crosses). Sleep bins are subsequently marked with a 1, and all other bins marked with a zero. Values are either 1 (sleep) or 0 (not sleep) for each bin- that is, they don't indicate actual minutes. A single bout of sleep has an effective minimum of 5-minutes.

A. Board. Monitor number (1-120).
B. Fly. Channel number (1-32).
C. TotalMinutes. The sum of all sleep values in the data series for the “Days to Use” multiplied by the data collection bin size.
D. AverageMinutes. The “TotalMinutes” divided by the total number of data collection bins.
E. TotalBouts. The total number of bouts of sleep. A bout is defined as a series of non-zero values of any length. Note that because each data bin has been marked

as sleep or not sleep and since only bins within a minimum 5-minute series are marked sleep, there's an effective minimum of 5 minutes for a bout.

F. AverageBoutDuration. The sum of the bout durations in minutes divided by the total number of bouts.
G. DayTotal. Total minutes of sleep during “Zeitgeber On” hours.
H. AverageDayMinutes. The “DayTotal” divided by the total number of data collection bins in “Zeitgeber On” hours.
I. DayBouts. The total number of bouts beginning during “Zeitgeber On” hours.
J. AverageDayBoutDuration. The total minutes of sleep in bouts that began during “Zeitgeber On” hours divided by the total number of bouts that during the same time.
K. NightTotal. Total minutes of sleep outside “Zeitgeber On” hours.
L. AverageNightMinutes. The “NightTotal” divided by the total number of data collection bins outside of “Zeitgeber On” hours.
M. NightBouts. The total number of bouts beginning after “Zeitgeber On” hours.
N. AverageNightBoutDuration. The total minutes of sleep in bouts that began after “Zeitgeber On” hours divided by the total number of bouts that during the same time.

BinnedData (Raw)

BinnedData (Raw) values are in the same format as MATLAB graph exports. They are centered around “Zeitgeber On” hours. Therefore, the first, far left bin in Column A is not ZT0 except where multiple days of sleep are displayed consecutively in “Averaging” by “Flies” or “No Averaging”. "BinnedData (Raw)" values represent minutes of sleep per

specified bin size. “Sleep” is any 1-minute bin part of a 5-minute (or more) series of bins without IR beam crosses. These bins are marked with a 1 to indicate sleep. All other bins are marked as a zero. Minutes of sleep are then summed into the indicated “Bin Size.”

A. Bin. The first bin represents the first, leftmost bin on the graph. Values are centered on “Zeitgeber On” hours. Therefore, the first bin in Column A is in middle of the Zeitgeber Off hours.
B. “MxxxCxx”. The individual fly represented by its monitor number (“Mxxx”) and channel number (“Cxx”).

3.5. Graphs

Graphs represent activity or sleep data collected in the “Bin Size” specified for each individual fly included in “Data Settings”. Activity graphs’ Y-values represent either activity data “Averaged” by the “Bin Size” or “Normalized” to total activity. Zeitgeber On hours (“Day”) are centered between Zeitgeber Off hours (“Night”) at the left and right of the graph except where multiple days of sleep are displayed consecutively in “Averaging” by “Flies” or “No Averaging”. Bar and line graphs represent Zeitgeber Off hours with darker bars or shaded background regions, respectively. Bar graphs display SEM as error bars above the mean activity/sleep bar. Line graphs shade the SEM area above and below a darker, mean activity/sleep line. When “Averaging” by “Both” days and flies is selected, averaging is done first by flies and then (in a separate step) by days. The SEM is calculated on the second step only, that is, it's the standard error across days of the averaged fly data.

Section 4. Savitzky-Golay Filtering

4.1. Description

PHASE uses MATLAB function *sgolay* from the Signal Processing Toolbox to filter 1-minute activity or sleep data with a Savitzky-Golay FIR smoothing filter of a given "Filter Order" and "Filter Frame Length." Savitzky-Golay filtering is optimal for smoothing data with a large frequency span (such as 1-minute activity data); reducing signal-to-noise while preserving the original shape of signals that are often distorted using standard averaging filters (Orfanidis, 1995). *sgolay* replaces successive central points in frames (minutes of behavior within the "Filter Frame Length") with the weighted average of all measures within the frame. The weighted coefficients are obtained by fitting all frame values to a polynomial of a given degree ("Filter Order") using the linear least squares method. PHASE uses the *sgolay* smoothed data to derive maximum and minimum activity and sleep bins within a given window (minutes) from an indicated ZT for "Anticipation or Latency" Analyses. "Phase Analysis" also applies the *sgolay* filter to an entire day, or average of days of activity or sleep behavior, and unbiasedly defines peak maximums, ZTs, and peak areas in the smoothed data.

4.2. Protocol

PHASE applies a low-order polynomial function specified by the "Filter Order" across an odd-number of minutes of activity or sleep behavior within the "Filter Frame Length". The "Filter Order" and "Filter Frame Length" is user-specified in Phase Analysis, and Activity or Latency Analysis. Therefore, it is imperative that users find the best representation of activity and sleep data that minimizes noise and signal distortion and maximizes signal. This is an iterative process until the final polynomial order and frame length are defined. To best utilize PHASE's smoothing functions, users may begin by generating activity or sleep graphs using the autofilled parameters for "Filter Order" and

“Filter Frame Length.” After visual inspection, users should apply the following principles of Savitzky-Golay filtering in order to more accurately represent their data and avoid generating errors in PHASE.

A. The polynomial degree in “Filter Order” must not exceed the minutes defined by “Filter Frame Length”.
B. The “Filter Frame Length” must be an odd-number. Savitzky-Golay methodology assumes that the data within the specified frame are equidistant. Symmetry requires the window to contain an odd number of points in order to replace a central point by the best representation of all values within the frame.
C. Signal-to-noise generally increases as the polynomial degree decreases. A higher “Filter Order” will best preserve narrow feature height and width but perform less well on broad peaks. A lower “Filter Order” conversely, will smooth broad features, at the expense of minimizing narrow features.
D. Signal-to-noise increases as “Filter Frame Length” increases as there are more data points over which to derive the weighted average of the center point. Increased frame length also increases original signal distortion, however.
E. The ratio between the “Filter Order” and “Filter Frame Length” controls original data distortion. Smoothing generally increases as the ratio between the two values increases.

Section 5. Phase Analysis

5.1. Description

“Phase Analysis” applies a Savitzky-Golay filter of a given polynomial “Filter Order” within a “Filter Frame Length” to raw IR beam activity data or sleep data, where “sleep”

is any 1-minute data collection bin that was part of a 5-minute (or more) series of bins without activity (IR beam crosses). Where multiple days are specified in “Days to Use” averaging takes place prior to filter application.

PHASE uses the MATLAB function *findpeaks* to find local maxima within the “Minimum Distance” of filtered data. The “Minimum Distance” restricts the *findpeaks* function to an acceptable peak-to-peak distance (in minutes), effectively ignoring any peaks which are close together. Smaller minimum distances will allow PHASE to find many, small peaks. Larger minimum distances will favor larger, broader peak features. PHASE determines the peak’s maximum 1-minute bin within the filtered data and the peak’s ZT relative to “Data Settings”. PHASE uses *findpeaks* to determine the peak height/prominence (in minutes of sleep or IR beam counts) and the width/half-prominence (in minutes) and uses these values to calculate the peak area. PHASE can find, quantify and visualize all peaks within smoothed behavior data. However, users may also search for peaks closest to given ZT, or set of ZT(s) inputted in “ZT(s) to Search for Peaks.”

Phase Analysis for “Activity” may be calculated using the actual 1-minute IR activity data (“Averaged Activity Analysis”), or data normalized to the total activity (“Normalized Activity Analysis”) where each 1-minute bin is a percentage of the total activity. Phase Analysis for “Sleep” utilizes the raw 1-minute sleep data.

5.2. Protocol

1. Check “Include Phase Analysis” in “Phase Analysis” tab.

    a. If using the autofilled settings, skip to 6.

2. Specify the “Filter Order” and “Filter Frame Length”.

    a. The filter frame length must be an odd number.

3. Indicate the “Minimum Distance Between Peaks” in minutes.

4. Input the day (1) or days (1, 2, 3) to analyze in “Days to Use”.

5. Enter relevant ZT(s) to search for peaks in “ZT(s) to Search for Peaks”. Separate multiple ZT(s) by a comma (ex. 0,12)

    a. If no entry is made in to this box, PHASE will find and describe all smoothed peaks for every fly.

6. Create an “Output File Name.”

7. Select an “Output Folder” separate from the folder containing monitor files.

8. Click the “Sleep Analysis” button if analyzing sleep.

9. If analyzing activity, click either the “Normalized” or “Averaged Activity Analysis” buttons.

5.3. Excel Outputs

When no ZT(s) are indicated to direct peak calling in PHASE, “Activity/SleepPhase_OutputFileName_YYYYMMDD_HHMM” ranks each individual fly’s set of peaks by decreasing ZT and gives the “Peak Time (ZT),” “Peak Height,” and “Peak Area” for each peak identified by *findpeaks*. When ZT(s) are specified in “ZT(s) to Search for Peaks,” the Excel output separates each ZT into individual sheets and gives the “Peak Time (ZT),” “Height,” and “Area” for smoothed peaks closest to the indicated ZT.

A. “MxxCxx”. The individual fly represented by its monitor number (“Mxxx”) and channel number (“Cxx”).
B. Peak Time (ZT). The peak maximum’s 1-minute filtered data bin converted to ZT relative to “Data Settings”

C. Peak Height. The peak height in IR beam crosses (activity) or minutes of sleep (sleep)

D. Peak Area. The “Peak Height” multiplied by the peak width (in minutes).

5.4. Graphs

Graphs represent 1-minute binned activity, normalized activity, or sleep data for each individual fly included in “Data Settings” for the day or average of days indicated in “Days to Use.” Phase Analysis uses *findpeaks* to analyze 1-minute binned activity and sleep data, therefore raw activity and sleep data best represent the data processed by the Savitzky-Golay filter. The blue line represents the filtered data curve of the 1-minute data. Graphs shade each peak area in blue and label the peak maximum with a blue carrot and the ZT.

Section 6. Anticipation or Latency Analysis

6.1. Description

“Anticipation or Latency Analysis” applies a Savitzky-Golay filter of the given polynomial “Filter Order” within a “Filter Frame Length” to raw IR beam activity data or sleep data, where “sleep” is any 1-minute data collection bin that was part of a 5-minute (or more) series of bins without activity (IR beam crosses). Where multiple days are specified in “Days to Use” averaging takes place prior to filter application.

PHASE analyzes each indicated ZT for each fly with reference to the “Window Length” (minutes). Activity “Anticipation” functions move negatively along the x-axis (time) from a ZT to grab the maxima/greatest activity and then the minimum/least activity from filtered data. Sleep “Latency” functions move positively along the x-axis (time) from a ZT to derive the first minima/least amount of sleep and the maxima/greatest amount of sleep

from filtered data. PHASE determines the duration in minutes between defined maximums and minimums and the area under the smoothed curve (AUC). “Index” (AUC) and “Anticipation” or “Latency” (duration) calculations exclude the “startle effect” by gathering maxima and minima from the first bin after or before a given ZT, respectively. PHASE also finds the slope (“Intensity”) of a linear regression fitted to unsmoothed 1-minute activity or sleep data for each ZT within the “Window Length” indicated. Where multiple days are specified in “Days to Use” averaging takes place prior to fitting the linear regression. Activity Anticipation, and Activity Slope (“Intensity”) may be calculated using the actual 1-minute IR activity data (“Average Activity Analysis”), or data normalized to the total activity (“Normalized Activity Analysis”) where each 1-minute bin is a percentage of the total activity.

6.2. Protocol

1. Check “Include Latency or Anticipation Analysis”.
    a. If using the autofilled settings, skip to 6.
2. Specify the Savitzky-Golay “Filter Order” and “Filter Frame Length”.
    a. The filter frame length must be an odd number.
3. Enter the “ZT” or ZTs to analyze separated by a comma for multiple ZTs (ex. 0,12).
4. Indicate the “Window Length” in minutes.
    a. Window lengths must not be so large that ZTs overlap.
5. Input the day (1) or days (1, 2, 3) to analyze in “Days to Use”.
6. Create an “Output File Name.”
7. Select an “Output Folder” separate from the folder containing monitor files.
8. Click the “Sleep Analysis” or “Activity Analysis” buttons.

a. If “Activity Analysis”, indicate whether activity data should be normalized to total activity (“Normalized Activity Analysis”) or raw (“Average Activity Analysis”).

6.3. Excel Outputs

“ActivityAnticipation/SleepLatency_OutputFileName_YYYYMMDD_HHMM” separates each ZT indicated in “ZT” by sheet and gives the Index, Duration (filtered data) and Slope (unsmoothed data) for each fly included in “Data Settings.”

A. Max Activity/Sleep Time (ZT). The maximum activity or sleep bin of the filtered data.
B. Min Activity/Sleep Time (ZT). The minimum activity or sleep bin of the filtered data.
C. Anticipation/Latency (minutes). The duration between maxima and minima.
D. Index (AUC)- the area under the curve (AUC) for filtered activity or sleep data between the maxima and minima.
E. Slope. The slope of a linear regression fitted to unsmoothed raw activity data (“Averaged Activity Analysis”), activity data normalized to total activity (“Normalized Activity Analysis”), or sleep data (“Sleep Analysis”) within the given window from a ZT. When normalization is indicated, the slopes are taken from the unsmoothed, normalized data where each 1-minute bin is a percentage (0 to 1) of the total activity.

6.4. Graphs

Index and Duration

Graphs represent 1-minute binned raw activity data (when “Averaged Activity Analysis” is selected), normalized activity data (“Normalized Activity Analysis), or sleep data for each individual fly included in “Data Settings” for the day or average of days indicated in “Days

to Use." Note that Anticipation or Latency Analysis analyzes 1-minute binned activity and sleep data, therefore graphs with un-binned data best represent the trends captured by the Savitzky-Golay filter. Each region included in the analysis is shaded in light grey. The blue line represents the filtered data curve. Blue carrots indicate the filtered activity or sleep maximum and minimum bins determined by PHASE within the "Window Length" from each ZT. The duration (minutes) between each maximum and minimum is annotated for each region above the blue carrot.

Intensity (Slope)

Graphs represent slopes calculated from unsmoothed 1-minute raw activity data ("Averaged Activity Analysis"), normalized activity data ("Normalized Activity Analysis", or sleep data within the analysis window of a given ZT for all flies included in "Data Settings". As sleep values range from 1 or 0 for a given bin, these values are far more discreet than raw activity values (presented as unsmoothed IR beam crosses.) For example, given the 0-or-1 sleep values, for three days of activity there are only four possible average values: 0, 1/3, 2/3, or 1 depending how many of those days the fly was asleep during each interval. Each ZT included in the "Anticipation or Latency Analysis" is plotted individually. The linear regression/slope for individual flies is in light grey. The average linear regression/slope for all flies included in analysis is in dark grey.

References

Hendricks, J. C., & Sehgal, A. (2004). Why a fly? Using *Drosophila* to understand the genetics of circadian rhythms and sleep. Sleep. https://doi.org/10.1093/sleep/27.2.334

Huber, R., Hill, S. L., Holladay, C., Biesiadecki, M., Tononi, G., & Cirelli, C. (2004). Sleep homeostasis in *Drosophila melanogaster*. Sleep. https://doi.org/10.1093/sleep/27.4.628

Orfanidis, S. J. (1995). Introduction to Signal Processing. In Introduction to Signal Processing. https://doi.org/10.1109/TCOM.1972.1091274